Microglia as therapeutic targets in retinal degeneration: role of translocator protein (18 κDa) (TSPO) and minocycline

Inaugural Dissertation

zur

Erlangung des Doktorgrades

Dr. nat. med.

der Medizinischen Fakultät

und

der Mathematisch-Naturwissenschaftlichen Fakultät

der Universität zu Köln

vorgelegt von

Rebecca Scholz

aus Neuss

Köln, 2016

Berichterstatter/Berichterstatterin:	Prof. Dr. Rudolf Wiesner
	Prof. Dr. Ines Neundorf
Tag der letzten mündlichen Prüfung:	12.07.2016

Table of contents

1 Summary

Microglia are the resident immune cells of the central nervous system (CNS) and play an important role in innate immune defense as well as tissue homeostasis. Chronic microglial reactivity, microgliosis, is a general hallmark of inflammatory and degenerative diseases that affect the CNS, including the retina. There is increasing evidence that chronic microgliosis is more than just a bystander effect, but rather actively contributes to progression of degeneration through processes such as toxic nitric oxide (NO) production and even phagocytosis of stressed but viable photoreceptors. Therefore immunmodulation of microglia presents a possible therapeutic strategy for retinal degenerations. Notably, the expression of the mitochondrial translocator protein 18 (κDa) (TSPO) is highly elevated in reactive microglia as seen in several neuroinflammatory diseases such as Alzheimer's disease, Parkinson's disease and multiple sclerosis. Therefore it is used as a gliosis biomarker in the brain. Moreover TSPO ligands show potent effects in resolving neuroinflammatory brain disorders. However, TSPO expression in the eye had not been investigated before. Further, it was unknown whether TSPO ligands' potent immunomodulatory effects could be used to treat retinal degenerations.

To fill this gap, the study aimed to analyze whether TSPO is also a potential biomarker for degenerative processes in the retina. Moreover the thesis attempted to determine whether a specific TSPO ligand, XBD173, might modulate microglial reactivity and is a potent therapeutic, to treat retinal degenerative diseases.

The findings revealed that TSPO is strongly upregulated in microglial cells of retinoschisin-deficient ($RS1^{-/y}$) mice, a model of inherited retinal degeneration and in a murine light damage model. A co-localization of TSPO and microglia was furthermore detectable in human retinal sections, indicating a potential role for TSPO as a biomarker for retinal degenerations. *In vitro* assays showed that the TSPO ligand XBD173 effectively inhibited features of microglial activation such as morphological transformation into reactive phagocytes and enhanced expression of pro-inflammatory cytokines. XBD173 also reduced microglial migration and proliferation and reduced their neurotoxic potential on photoreceptor cells. In two independent mouse models of light-induced retinal degeneration, the treatment with XBD173 reduced accumulation of amoeboid, reactive microglia in the outer retina

and attenuated degenerative processes, indicated by a nearly preserved photoreceptor layer.

A further question addressed in this thesis was whether minocycline, an antibiotic with additional anti-inflammatory properties is able to reduce microglial neurotoxicity and to protect the retina from degeneration.

Minocycline administration dampened microglial pro-inflammatory gene expression, NO production and neurotoxicity on photoreceptors. Interestingly, in addition to its immunomodulatory effect, minocycline also increased the viability of photoreceptors in a direct manner. In the light damage model, minocycline administration counteracted microglial activation and blocked retinal degeneration.

Taken together these results identified TSPO as a biomarker for microglial reactivity and as therapeutic target in the retina. Targeting TSPO with XBD173 was able to reverse microglial reactivity and could prevent degenerative processes in the retina. In addition, the study showed that the antibiotic minocycline effectively counterregulates microgliosis and light-induced retinal degeneration. Considering that microgliosis is a major contributing factor for retinal degenerative disorders, this thesis supports the concept of a microglia-directed therapy to treat retinal degeneration.

2 Zusammenfassung

Mikrogliazellen sind die Gewebsmakrophagen des zentralen Nervensystems (ZNS). Sie spielen eine wichtige Rolle bei der Immunabwehr sowie der Aufrechterhaltung der Gewebshomöostase. Chronische Mikrogliaaktivierung, Mikrogliose, gilt als generelles Kennzeichen von degenerativen und entzündlichen Erkrankungen des ZNS, inklusive der Retina. Eine zunehmende Anzahl von Studien belegt, dass persistierende Mikrogliareaktivität nicht nur eine Folgeerscheinung degenerativer Erkrankungen, sondern aktiv am Voranschreiten solcher Prozesse beteiligt sein kann, beispielsweise durch Produktion reaktiver Sauerstoffspezies oder sogar Phagozytose gestresster, aber lebender Photorezeptoren. Mikroglia-gerichtete Therapien könnten daher ein Behandlungskonzept für retinale Degenerationen darstellen. Bei neurodegenerativen Erkrankungen wie Alzheimer, Parkinson oder Multipler Sklerose wurde festgestellt, dass reaktive Mikrogliazellen eine erhöhte Expression des mitochondrialen Translokatorproteins (18κDa) (TSPO) aufweisen. Deshalb wird TSPO als Gliosemarker im Gehirn verwendet. Spezifische TSPO-Liganden zeigten außerdem Wirksamkeit bei der Behandlung von neuroinflammatorischen Erkrankungen des ZNS. Ob TSPO auch im Auge exprimiert wird und ob TSPO-Liganden möglicherweise zur Therapie von retinalen Degenerationen geeignet sind, ist bisher noch nicht untersucht worden.

Neben der Überprüfung, ob TSPO auch als Biomarker für degenerative Veränderungen der Netzhaut verwendet werden kann, wurde in dieser Arbeit untersucht, inwiefern der spezifische TSPO-Ligand, XBD173, Mikroglia Reaktivität modulieren kann und sich zur Therapie von retinalen Degenerationen eignet.

Sowohl Untersuchungen an Retinoschisin-defizienten Mäusen, einem Modell für erbliche Netzhautdegeneration, als auch in einem Licht-Schadensmodell zeigten eine Hochregulation von TSPO in Mikrogliazellen. Eine Kolokalisation von TSPO und Mikrogliazellen war außerdem in humanen Retinapräparaten erkennbar und verdeutlicht die potentielle Eignung als Biomarker für retinale Erkrankungen. I*n vitro* Analysen zeigten, dass XBD173 Zeichen von Mikrogliareaktivität wie erhöhte Expression inflammatorischer Marker, Migration, Proliferation und die morphologische Transition zu reaktiven Phagozyten reduziert sowie das neurotoxische Potential von Mikrogliazellen verringert. In zwei unabhängigen murinen Modellen für Licht-induzierte Degeneration, reduzierte die Behandlung mit

XBD173 die Akkumulation amoeboider, reaktiver Mikrogliazellen in der äußeren Netzhaut und schützte die Retina vor degenerativen Prozessen, erkennbar durch den Erhalt der Photorezeptorschicht.

Ein weiteres Ziel dieser Arbeit war zu untersuchen, ob Minocyclin, ein Antibiotikum mit zusätzlichen anti-inflammatorischen Eigenschaften, Mikroglia Reaktivität modulieren und die Retina vor degenerativen Prozessen schützen kann.

Stimulation von Mikrogliazellen mit Minocycline verringerte die Expression von Entzündungsmarkern, die Produktion von toxischem Stickstoffmonoxid und die Neurotoxizität von Mikrogliazellen gegenüber Photorezeptoren. Interessanterweise war zusätzlich zu der immunmodulativen Wirkung war auch ein direkter protektiver Effekt auf Photorezeptoren festzustellen. Behandlung mit Minocyclin bei Licht-induzierter Degeneration wirkte pro-inflammatorischer Mikroglia-Aktivierung entgegen und schützte die Retina vor Degeneration.

Die Ergebnisse zeigen, dass sich TSPO als Biomarker für Mikroglia-Reaktivität und therapeutisches Target bei retinalen Degenerationen eignet. TSPO gerichtete Therapie mit XBD173 reduzierte Mikroglia-Reaktivität und verhinderte degenerative Prozesse in der Retina. Zusätzlich zeigt die vorliegende Arbeit, dass das Antibiotikum Minocyclin, Mikrogliose entgegenwirkt und die Retina vor Licht-induzierter Degeneration schützt. Unter der Annahme, dass chronische Mikrogliose maßgeblich den Verlauf von degenerativen Prozessen beeinflussen kann, stellen Mikroglia-gerichtete Therapieansätze ein erfolgsversprechendes Konzept zur Behandlung von retinalen Degenerationen dar.

3 Introduction

3.1 Structure and function of the retina

The gross morphological structure of the human eye consists of three different layers (shown as sagittal section of the adult human eye Fig. 1, A). The external layer consists of the sclera and the cornea. The intermediate layer is generally further divided into an anterior part, which includes iris and ciliary body and a posterior part, the choroid. The retina belonging to the CNS is designated as inner layer. The chambers that occur between these layers are the anterior chamber (between iris and cornea) and the vitreous humor (between lens and retina). Both are filled with differently viscous fluids (Kolb, 2005).

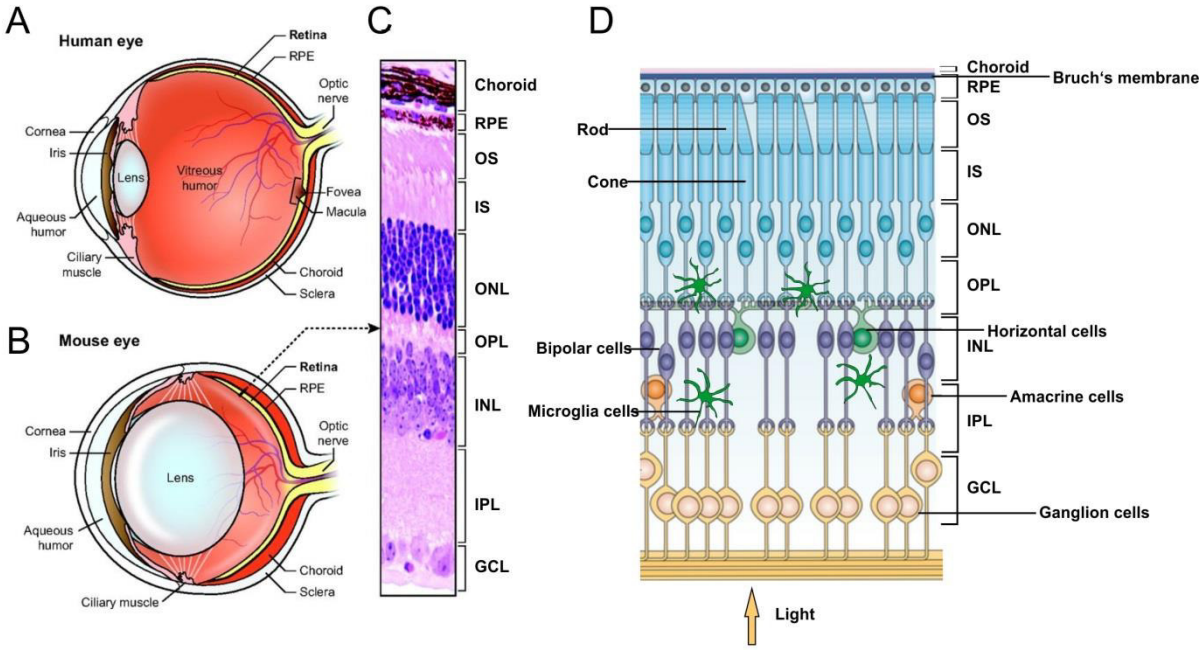

Figure 1: Schematic overview of the mammalian eye and its retinal structure. (A) Cross section of the human eye. The retina is located at the posterior part of the eye and is loosely stocked to the retinal pigment epithelium (RPE) **(B)** Cross section of the murine eye. **(C)** H&E stained murine retinal cross section showing the different retinal layers. **(D)** Schematic overview of the different retinal layers, including respective cell types. (GCL) ganglion cell layer, (IPL) inner plexiform layer, (INL) inner nuclear layer, (OPL) outer plexiform layer, (ONL) outer nuclear layer, (IS) inner segments, (OS) outer segments (A-C) modified from (Veleri et al., 2015) D modified from (Kimbrel and Lanza, 2015)

During embryogenesis, the retina derives from the neural tube (Lamb et al., 2007). As sensory part of the eye, the retina absorbs light and converts it into electrical signals that are transferred to the brain and are decoded to gain visual information. The retina consists of different neuronal cell types that roughly divide the retina into

three cellular layers, the ganglion cell layer (GCL), the inner nuclear layer (INL) and the outer nuclear layer (ONL) which are separated from each other by two synaptic layers, the inner plexiform layer (IPL) and the outer plexiform layer (OPL)) (Fig. 1 C, D). The retinal pigment epithelium (RPE) lies juxtaposed to the apical side of the photoreceptors and is essential to support the retina (Sung and Chuang, 2010). Beside the absorption of light the RPE phagocytoses sheded membrane discs of the photoreceptors that are damaged due to photo-oxidative stress. This is a daily occurring process that leads to a complete membrane disc renewal in about 10-15 days. Furthermore the RPE is co-responsible for the recycling of rhodopsin after bleaching, a process called visual cycle and supports the retina with nutrients (Travis et al., 2007). Additionally the RPE is part of the blood-retina barrier (BRB) and controls the transport of molecules between choroidal blood flow and retina (Campbell and Humphries, 2012, Strauss, 2005, Young, 1967).

After passing the different retinal layers light is absorbed by the photoreceptors that are located at the outer side of the retina. In the human retina, photoreceptors can be divided into two subtypes: rods (~120 million cells), which are responsible for dim light vision and cones (~6 million cells), which mediate color vision under brighter light conditions (Bommas-Ebert et al., 2006). Dependent of its spectral sensitivity three cone types with different opsins can be distinguished in primates: L- (long, 564nm), M- (medium, 533 nm) and S- (short, 437nm) wavelength cones (Bowmaker and Dartnall, 1980). In the human retina, a certain spot called fovea (~1,5 mm^2) consists only of cones and has the highest visual acuity. The area (~3 mm^2) around the fovea, recognizable by its yellow screening pigments (zeaxanthin and lutein), is named macula. (Veleri et al., 2015, Morrow et al., 1998, Balashov and Bernstein, 1998). The absorption of a photon by the chromophore 11-cis retinal within the photoreceptors, leads to isomerization to all-trans retinal and initiates the process of phototransduction, which is a cascade of biochemical events resulting in closure of ion channels, photoreceptor hyperpolarization and signal transmission to second order neurons, such as bipolar, horizontal and amacrine cells that form the inner nuclear layer (INL) (Travis et al., 2007, Sung and Chuang, 2010, Yau and Hardie, 2009). Neurons of the INL are interconnected to each other, which allows reciprocal excitation or inhibition and serves as contrast intensification (Bommas-Ebert et al., 2006). After processing of the signal by the different cell types of the INL, the signal is forwarded to the ganglion cells, whose axons form the optic nerve and transmit the

converted light signals to the brain (Sung and Chuang, 2010). Furthermore three glial cell types are found in the retina: Müller cells, microglia and astrocytes (Bringmann et al., 2006). Microglia are the immune cells of the eye which are under homeostatic conditions located in the plexiform layers (Kettenmann et al., 2011). Müller cells span the entire retina and are important for the maintenance of retinal homeostasis (Bringmann et al., 2006).

Although the murine eye is structurally very similar to the human eye, some differences remain: the lens of the mouse eye is much bigger in proportion to the rest of the eye (Fig. 1, B) (Veleri et al., 2015). Furthermore mice, as nocturnal animals, rely predominantly on rod-mediated vision and in contrast to humans possess only two different types of cones, M- and S-cones (dichromatic vision) and no macula or fovea (Morrow et al., 1998).

3.2 Inherited retinal degenerative diseases

Loss of visual function means a severe loss of life quality for the affected individuals. Major causes for blindness are neurodegenerative retinal diseases that lead to dysfunction or death of photoreceptors (Veleri et al., 2015). In general, retinal degenerations can be divided into monogenic or multifactorial (complex) disorders (Berger et al., 2010). A relatively common form of monogenic retinal degeneration affecting 1 in 4000 individuals, is retinitis pigmentosa (RP) (Ferrari et al., 2011). Within the group of multifactorial retinopathies, age-related macular degeneration (AMD) is the leading cause of blindness in elderly populations in developed countries (The Eye Diseases Prevalence Research Group, 2004) (Coleman et al., 2008). Genetic susceptibility factors such as variants in complement factor H (CFH) and age-related maculopathy susceptibility 2 (ARMS2) genes, risk factors such as smoking, diet and higher age are associated with the development of this late-onset disease (Swaroop et al., 2009, Cooke Bailey et al., 2013, Jager et al., 2008). Improvement of molecular techniques such as next generation sequencing and large scale genotyping allowed the identification of many disease-causing genes. Nowadays more than 250 causal genes are known for this heterogeneous group of retinal diseases (RetNet:https://sph.uth.edu/retnet/). Despite this knowledge, there is a need to develop novel therapeutic strategies for retinal degenerations.

Because of limitations to study disease mechanisms in patients, mouse models provide a valuable tool to analyze disease pathology and to validate novel therapeutic strategies (Veleri et al., 2015). Despite the fact that the mouse eye is not completely identical to the human eye, mouse models allow to study important features of retinal degeneration such as immune activation or photoreceptor apoptosis. Several genetic as well as experimental models are available including those that mimick the damaging features of bright light. These models vary basically in the onset and severity of degeneration and discriminate underlying causes such as defects in cilia or RPE function, phototransduction and synaptic transmission (Veleri et al., 2015, Wenzel et al., 2005, Morrow et al., 1998). A common feature of retinal degenerative diseases, which is also detectable in most mouse models, is microglial activation. There is now ample evidence that chronic microglial activation is more than a bystander effect of such pathologies, but rather actively contributes to progression of retinal degeneration (Karlstetter et al., 2015, Chen and Xu, 2015, Gupta et al., 2003). For instance, it was reported that reactive microglial cells are able to produce cytotoxic oxygen radicals such as NO and may even phagocytose stressed, but viable photoreceptors (Zhao et al., 2015, Yang et al., 2007a). For the therapeutic intervention studies in this thesis, we have chosen the acute white light-induced degeneration paradigm, which models both disease characteristics, the fast degeneration of photoreceptors and activation of microglial cells (Zhang et al., 2004) (Joly et al., 2009, Ng and Streilein, 2001).

3.2.1 Light damage as retinal degeneration model

Light-induced retinal degeneration represents an inducible model to study mechanisms of neuronal cell death and to test immune-directed treatment strategies simultaneously. Besides that, light is also a promoting factor in human retinal degenerations and is therefore not just an artificial stimulus (Cruickshanks et al., 1993, Swaroop et al., 2009, Wenzel et al., 2005). The advantage over genetically modified mouse strains is that the start of degeneration can be well defined. It has a relatively synchronized wave of cell death and progresses relatively fast. These features allow to better analyze biochemical processes leading to photoreceptor degeneration and proper timing of intervention approaches (Grimm and Reme, 2013). Different light exposure settings can be distinguished: short-term exposure to

bright white light, long-term exposure to low levels of white light and exposure to monochromatic light of a specific wavelength (Grimm and Reme, 2013). The damaging potential of light critically depends on its wavelength. Short wavelength blue light has a higher damaging potential than long-wavelength green light. This is due to a process called photo-reversal, the regeneration of rhodopsin from bleaching intermediates that results in a higher absorption of photons in a certain time span (Grimm et al., 2001). In addition, there are also indications that the different light-damage setups vary in mechanisms of cell death, and caspases involved in cell death induction are differentially expressed (Wenzel et al., 2005). Responsible for the induction of light-induced degeneration is the excessive and ongoing bleaching of rhodopsin. This leads to the production and accumulation of retinoid metabolites and other toxic byproducts that initiate a cascade of death signals, subsequently resulting in photoreceptor cell death (Wenzel et al., 2005). Crucial for this process is a functional visual cycle as RPE 65 deficiency, an enzyme involved in the rhodopsin recycling process, protects from light-induced degeneration (Grimm et al., 2000). Furthermore, the RPE65 $_{Leu450Met}$ variation, in which leucine is substituted by methionine, slows down the visual cycle and thereby decreases the light damage susceptibility (Wenzel et al., 2001b). Other factors that can influence light damage susceptibility are increased levels of corticosteroids, which suppress AP-1-induced cell death and circadian dependent effects (Wenzel et al., 2001a, Organisciak et al., 2000).

3.3 Microglia

3.3.1 Microglial reactivity markers

Microglia cells represent the resident immune cells of the CNS, including the retina (Kettenmann et al., 2011). They were first described by the Spanish histopathologist Pio Del Rio Hortega back in the 1920s. The invention of the silver carbonate staining procedures enabled Hortega, to identify and distinguish microglia from neurons, astrocytes and oligodendendroglia by morphological criteria (Rio-Hortega, 1939, Perez-Cerda et al., 2015). Nowadays, several macrophage-related surface and intracellular markers are known and used to study the role of microglia in health and disease. These markers include F4/80 (β-glucan receptor dectin-1), CD68

(macrosialin), CD11b/CD18 (also called complement factor 3 (CR3), Mac1) and ionized calcium-binding adapter molecule 1 (iba1), which is currently the most reliable and widely used marker in humans and mice (Hume et al., 1983, Xu et al., 2007, Ito et al., 1998, Karlstetter et al., 2015). Other known markers are CD16, CD169 (siglec-1), CD 206 and MHC II. A few of these markers were shown to increase with microglial reactivity. This was observed for iba1 and CD11b. As microglial reactivity is often associated with neurodegeneration, the identification of activity markers is important as it complements the known morphological criteria of ramified versus amoeboid cell shape. Unfortunately, none of the introduced markers is exclusively expressed on microglia so that resident microglia can be hardly separated from CNS-recruited monocytes (Kettenmann et al., 2011). Another method to specifically label microglia is the use of genetically modified animals that express enhanced green fluorescent protein (EGFP) under the control of a microglia/macrophage specific gene promoter factor such as CX3CR1 (fraktalkine receptor) (Xu et al., 2007, Kezic and McMenamin, 2008).

3.3.2 Origin and self-renewal of microglia cells

The origin and renewal of microglial cells has been discussed controversially over the last twenty years. Adoptive transfer experiments with bone marrow (BM) cells from EGFP+ transgenic donors transferred into full body-irradiated adult wild-type mice, initially indicated that microglial cells originate and renew from BM precursors, because EGFP+ BM cells were detectable in the retina of wildtype recipients a few weeks after transfer (Xu et al., 2007, Kezic and McMenamin, 2008). But criticism was raised that whole body irradiation and the transfusion of BM do not reflect normal physiological conditions, because they may lead to the breakdown of the blood-brain-barrier (BBB) and the blood-retina-barrier (BRB) and bring progenitors into the circulation which would normally rest in the BM (Li et al., 2004, Ajami et al., 2007). In contrast to adoptive transfer studies, parabiosis experiments, in which the blood-flow of wildtype and GFP+ transgenic mice were connected, showed that cells from the circulation are not recruited to the retina, neither in healthy nor in disease conditions (Ajami et al., 2007). This and other findings strongly suggest that microglial cells are not recruited from the circulation under physiological conditions and that observed microglial replacement in older studies was very likely caused by the experimental

procedure of irradiation and bone marrow transplantation (Mildner et al., 2007, Ransohoff, 2007, Kierdorf et al., 2013b, Alliot et al., 1999). Furthermore, different fate mapping approaches independently reveal that microglia cells are ontogenetically distinguishable from hematopoietic cells and derive from the yolk-sac during early embryonic development (Ginhoux et al., 2010, Schulz et al., 2012, Kierdorf et al., 2013a).

3.3.3 Microglial function in the developing and adult retina

During retinal development, before the complex structure of the retina is fully differentiated, a burst of developmental apoptosis can be observed in neurons located in the GCL and in the IPL (Hume et al., 1983). The phenomenon of developmental apoptosis is detectable in the entire CNS and different studies proof that microglia cells actively contribute to that process (Bessis et al., 2007). Microglia cells seem to orchestrate apoptosis by the production of several molecules, like tumor necrosis factor-α (TNF-α), nerve growth factor (NGF) and nitric oxide (NO). However, they are also important for phagocytosis of occurring cellular debris (Sedel et al., 2004, Frade and Barde, 1998, Chao et al., 1992, Hume et al., 1983). Although the underlying reasons of developmental apoptosis are not completely understood, the chronology showing developmental apoptosis preceding synaptogenesis, indicates a possible correlation between both processes (Bessis et al., 2007). This is further sustained by studies that propose microglia cell involvement in synaptogenesis. The deletion of the microglial specific protein KARAP/DAP 12 as well as the blockage of complement receptor 3 CR3/C3 signaling negatively influenced synaptic function and the process of synaptic pruning and also reduced the connectivity between neurons (Roumier et al., 2004, Schafer et al., 2012). These studies implicate that microglia can control neuronal function by orchestrating synaptogenesis and apoptosis, starting early during retinal development.

In the healthy adult retina microglia cells are mainly located in the plexiform layers, where they build up a not overlapping meshwork that spans the entire retina (Lee et al., 2008). Under physiological conditions microglia have a ramified morphology with a small somata and wide ranging, fine processes (Figure 2, A). Normal microglial appearance is often denoted as “resting state”, but their processes are highly motile and permanently scan their microenvironment to clear it from metabolic products or

tissue debris and to detect pathological changes. They also directly contact other cells such as astrocytes, neurons and blood vessels. Furthermore, microglial protrusions undergo a permanent reconstruction process. The permanent monitoring and the expression of several surface receptors, such as purino-and fractalkine receptors, receptors for complement factors, immunoglobulins, adhesion molecules and chemokines enable microglia to sense and react quickly to potential danger signals (Nimmerjahn et al., 2005, Karlstetter et al., 2015, Langmann, 2007, Kettenmann et al., 2011). Such activation goes along with an extensive change in morphology, gene expression and function (Figure 2, B) (Kettenmann et al., 2011).

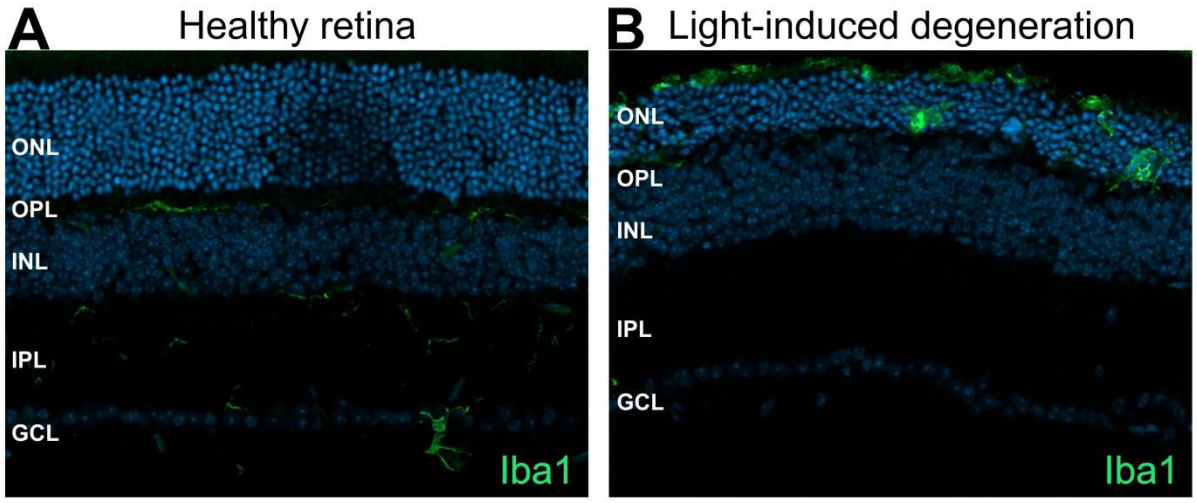

Figure 2: Microglial retinal location and appearance during health and disease. (A) In the healthy retina Iba1 positive ramified microglial cells are located in the plexiform layers. **(B**) After exposure to bright white light microglial cells migrate to the degenerating outer retina and the amoeboid shape points towards a much more activated state. (ONL) outer nuclear layer, (OPL) outer plexiform layer, (INL) inner nuclear layer, (IPL) inner plexiform layer, (GCL) ganglion cell layer.

In general reactive microglia cells have a more amoeboid shape, with less branches and thicker processes. But there are many different intermediate forms described, ranging from highly ramified to more or less round cells completely lacking processes (Figure 3) (Karperien et al., 2013). In addition to these morphological changes, microglia cells can become motile and migrate into damaged areas following chemotactic signals from neurons, astrocytes and endothelial cells.

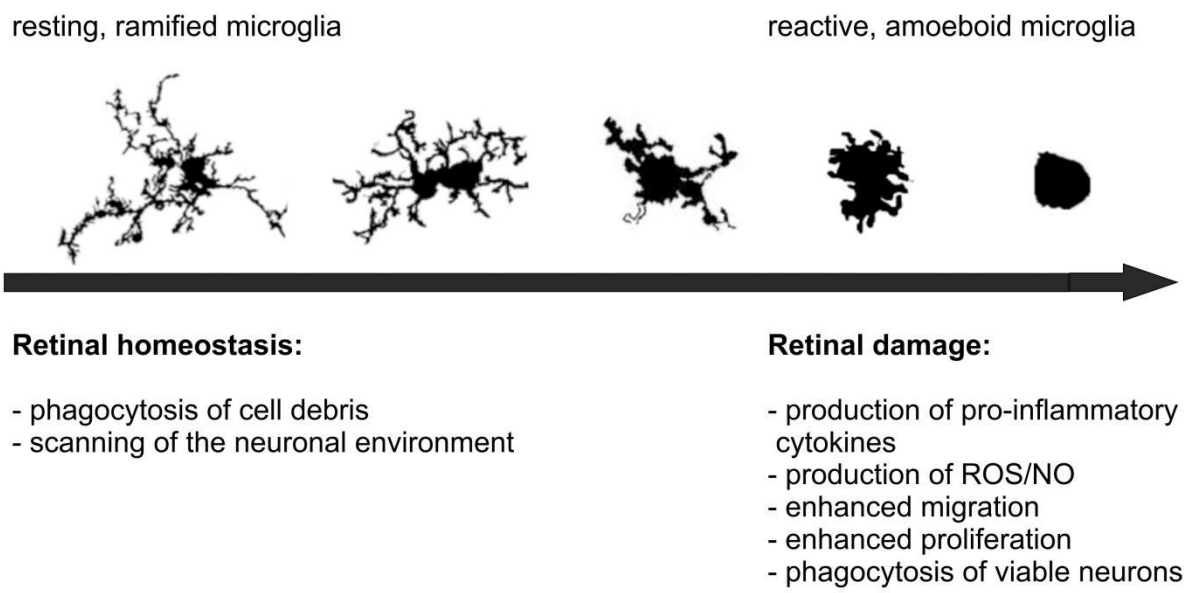

Figure 3: Microglial morphological plasticity. Under homeostatic conditions microglial cells have a small cell body and scan their environment with their long-branched protrusions. Microglia are able to sense subtle degenerative changes and respond quickly. Activation of microglial goes a long with a morphological transformation from a ramified to a much more amoeboid shape. Drawings modified from Karperien et al. 2013.

The phenotypical changes are accompanied by several functional changes. Enhanced phagocytic activity is observed, release of several neurotropic factors, chemokines or molecules like NO, upregulation of intracellular cytokines, expression of several surface markers, which are important for cell-cell interaction and enhanced proliferation (Hanisch and Kettenmann, 2007, Kettenmann et al., 2011).

Microglial cells are located in a highly specialized tissue, where immune reactions including chronic activation and recruitment of other immune cells such as T-cells would have detrimental effects. So there are many control mechanisms available to surveil microglial reactivity. These mechanisms constitute to the immune privilege of the eye and the CNS to prevent overwhelming and damaging immune reactions (Carson et al., 2006, Zhou and Caspi, 2010). Several retinal cell types are essentially involved in the control of microglial reactivity either by direct interaction or by the production of different soluble factors. For instance, healthy neurons express CD200 (OX2), a membrane glycoprotein that represents an inhibitory signal for microglia. CD200 deficiency or the missing interaction of CD200 and its receptor leads to an activation of microglial cells and promotes the susceptibility to autoimmune and degenerative pathologies of the CNS in animal models (Hoek et al., 2000, Wang et

al., 2007, Chitnis et al., 2007, Dick, 2003). Fractalkine (CX3CL1) is a further regulatory molecule produced by neurons and endothelial cells. In the CNS only microglia cells express the respective receptor for fractalkine and its deficiency can increase microglial neurotoxicity in models for Parkinson's disease, amyotrophic lateral sclerosis (ALS) and Alzheimer's disease (Cardona et al., 2006, Cook et al., 2001, Fuhrmann et al., 2010). In addition to these regulatory molecules, healthy neurons have a sugar-coated exterior surface, designated as glycocalyx which is covered with sialic acids caps. Sialic acids can be recognized by microglial siglec receptors. This interaction signals the healthy state of neurons and suppresses microglial activation (Karlstetter and Langmann, 2014, Linnartz and Neumann, 2013). The retinal pigment epithelium (RPE) is also involved in modulation of microglial reactivity. The RPE is source of several cytokines in the eye including transforming growth factor-β (TGF-β) (Tanihara et al., 1993). Microarray analysis of murine primary microglia pre-stimulated with INF-γ and TNF-α and then with TGF-β revealed, that TGF-β can downregulate the expression of pro-inflammatory genes involved in chemotaxis, migration, apoptosis and host response to infection (Paglinawan et al., 2003). Thus, microglial reactivity is a complex process that is fine-tuned by the quality of the activating stimulus and the interaction with other retinal cells.

3.3.4 Microglia in the aging retina

In the entire CNS, including the retina, aging-related changes in microglial cells can be observed in healthy conditions and in responses to injury. Comparative studies between young and aged healthy mice revealed that microglia undergo phenotypic changes with increasing age. Resting microglia from aged mice compared to young ones appear smaller and stretched out fewer branched protrusions that were less motile (Damani et al., 2011). Furthermore the number and density of microglial cells increase with age. Of note is that the mosaic like arrangement of microglia in the retina became more irregular and the territory monitored by a single cells is smaller (Tremblay et al., 2012). Microglia cells which are in the young and healthy retina confied to the plexiform layers are also detected in the outer part in aged retinas (Wong, 2013, Ma et al., 2009).

The phenotypic changes occur along with altered microglial functions. Markers such as MHCII and pro-inflammatory cytokines like IL-6, TNFα- and IL-1β are upregulated with age, whereas cytokines associated with attenuation of microglial cells such as IL-4, IL-10 and TGF-β are generally downregulated. A further aging effect is that receptor interactions involved in suppression of microglial reactivity, such as CD200-CD200r and CX3CL1-CX3CR1 interactions, are significantly weaker with age (Matt and Johnson, 2016). These age-related changes promote inadequate microglial behavior also in response to injuries. Investigations in a laser -induced retinal injury model revealed that process motility as well as migration capacity was slowed down in aged microglia. Although the capability to respond to pathological stimuli was reduced, once activated the cells failed to transform back into a “resting” state (Damani et al., 2011). Since aging is a risk factor and microglia can contribute to degenerative diseases of the CNS, age-dependent microglial alterations like reduction of neuroprotective function, increase of neurotoxicity and inadequate responses to injury, are possible drivers for pathological processes (Flanary et al., 2007).

3.3.5 Microglia reactivity in retinal degenerative diseases

Several studies revealed an association between enhanced microglial reactivity and neurodegeneration. It is still discussed whether microglial reactivity is just the consequence of pathological alterations or if microglia cells are actively involved in the progression of degenerative diseases (Figure 4) (Karlstetter et al., 2015, Masuda and Prinz, 2016, Zhao et al., 2015, Giulian, 1999). An increasing number of studies indicate that microglial activation is an early event and precedes or accompanies degeneration of photoreceptors in various retinal degeneration models (Zhang et al., 2004, Zeiss and Johnson, 2004, Gehrig et al., 2007, Ebert et al., 2009, Zhao et al., 2015). For instance, an association between microglial proliferation and ongoing degenerative processes was detectable in the *Pde6b*^{rd1} mice, an inherited model of retinal degeneration (Zeiss and Johnson, 2004). Also in the RS1h knockout mouse that shows several features of X-linked juvenile retinoschisis (XLRS), microarray analysis revealed an upregulation of microglial-related genes starting at postnatal day p11, before any occurrence of photoreceptor apoptosis (Gehrig et al., 2007, Ebert et al., 2009).

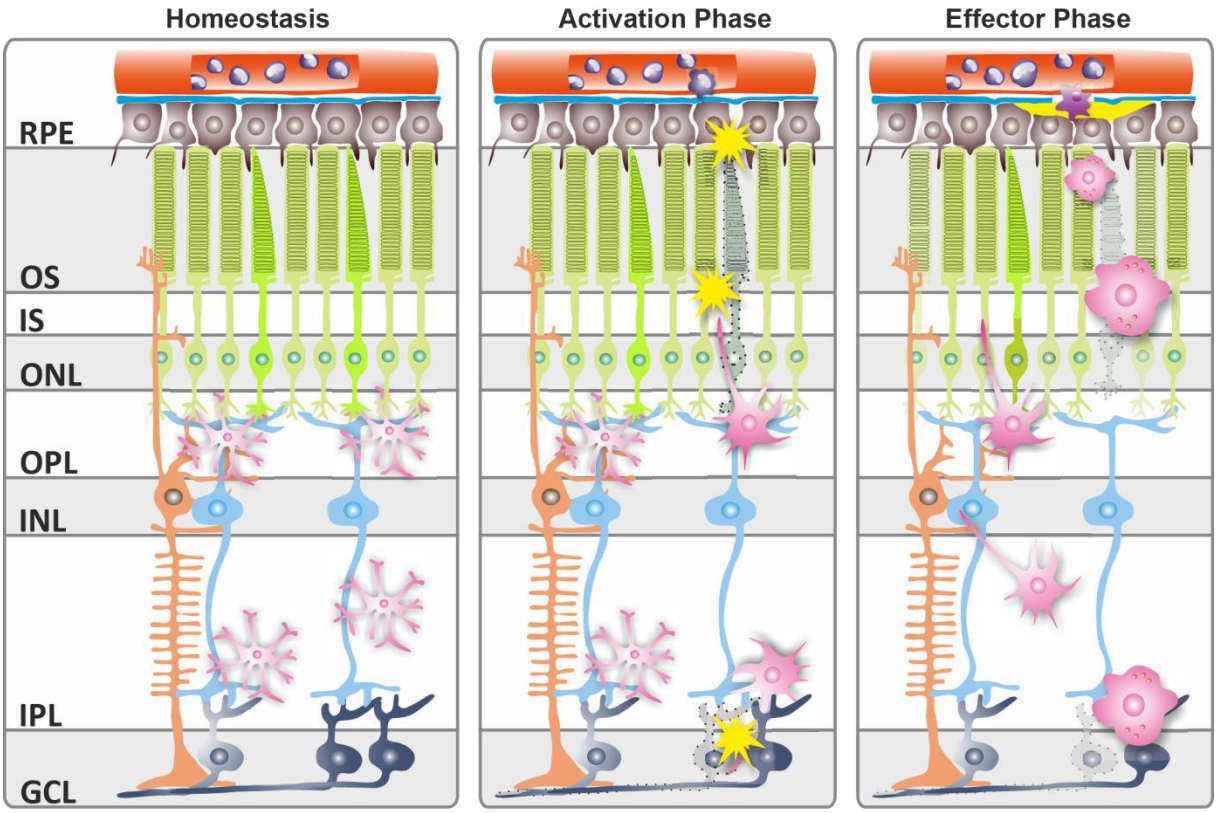

Figure 4: Schematic representation of microglial action during retinal degenerations. (A) Under homeostatic conditions ramified microglia mainly populate the plexiform layers and keep up tissue maintenance by phagocytoses of cell debris, secretion of neurotrophic factors and scan their environment in regard of pathological alterations. **(B)** Several factors signaling damage or abnormal function are sensed by microglia and lead to their activation. **(C)** Microglia and in case of breakdown of the blood-retina barrier, recruited blood-derived precursors migrate to the lesion sites, where they transform into amoeboid reactive phagocytes. These effector cells may be protective or detrimental depending on their immunological phenotype and the local cytokine milieu. RPE, retinal pigment epithelium; ONL, outer nuclear layer; OPL, outer plexiform layer; INL, inner nuclear layer; IPL, inner plexiform layer; GCL, ganglion cell layer (modified from (Karlstetter et al., 2010a)

Furthermore analysis of human retinal sections from patients with AMD, late-onset retinal degeneration (L-ORD) or retinitis pigmentosa (RP) revealed an accumulation of amoeboid shaped microglia in regions of ongoing photoreceptor death. Of note is that these microglia cells contained rhodopsin-positive cytoplasmatic inclusions, indicating that they phagocytosed photoreceptor cell debris and are possibly also involved in cell death of adjacent cells by production of neurotoxic factors (Gupta et al., 2003). Despite the fact that microglia cells basically exert several functions to keep-up tissue homeostasis and support neurons e.g. by production of different neurotrophic factors, many different studies revealed that microglia cells that lose their autoregulatory capacity can actively participate in the initiation and perturbation of retinal degenerative diseases. (Harada et al., 2002, Karlstetter et al., 2015). In line

with this, in vitro studies that compared the neurotoxic potential of activated versus non-activated supernatant of microglia and Müller cells, revealed that activated microglia cells induce much more photoreceptor cell death than conditioned medium from non-activated microglia or Müller cells. These findings suggest that soluble factors produced by reactive microglia such as NO, pro-inflammatory cytokines, complement factors or proteinases may contribute to induction of cell death during degenerative processes (Roque et al., 1999).

Which factors are involved in microglial activation is an open field of research. It was reported that stimulation with Toll-like receptor (TLR) ligands disturb the ability of microglial cells to distinguish between dead and alive, resulting in phagocytosis of viable neurons (Brown and Neher, 2014). The phagocytosis of stressed, but still viable neurons is designated as “phagoptosis” or primary phagocytosis. Phagoptosis generally mediates turnover of different cells like neutrophils or erythrocytes and is one form of cell death; however experiments in models of brain inflammation indicate that this process also contributes to neuron loss during degeneration. An important factor for phagoptosis induction seems to be the expression of ‘eat me’ signals, like the reversible expression of phosphatidylserine (PS) or the loss of ‘don’t eat me’ signals, as blocking of phagocytic signaling in microglia prevents neuron loss without inhibiting inflammation (Brown and Neher, 2012). In line with that, Zhao et al. showed that microglial phagocytosis of living photoreceptors is also involved in cell death in the CX3CR1 $^{GFP/+}$/rd10 retinal degeneration model that mimics features of retinitis pigmentosa. Depletion of microglial cells as well as blockage of microglial phagocytosis in the same model attenuated photoreceptor degeneration, suggesting reactive microglia as key players of cell death during degeneration (Zhao et al., 2015).

3.4 Modulation of microglial cells as a therapeutic strategy

The observation that microglia cells can be actively involved in retinal degeneration brings them into focus as a potential therapeutic target. Although causative genetic defects and contributing factors can vary tremendously, different pathologies share the common feature of innate immune activation. Microglial reactivity and inflammation is a general hallmark of neurodegenerative diseases. Therefore,

modulation of microglial cells could be a good therapeutic strategy to diminish degenerative processes in different diseases. Several compounds including natural occurring substances, synthetic pharmaceuticals as well as endogenous factors are investigated with regard to their immune modulatory competence.

3.4.1 Endogenous factors: AMWAP, micro RNAs and Interferon-β

After activation, microglia must be able to return back into a normal ramified scanning state. As loss of auto-regulatory function can have detrimental effects, microglia possess endogenous control mechanisms. Activated microglia/macrophe whey acidic protein (AMWAP) is produced by microglial cells and acts in a paracrine fashion. Overexpression of AMWAP as well as treatment of microglia cells with recombinant AMWAP reduced reactivity and limited their neurotoxic potential. Thus, AMWAP is an efficient endogenous counter-regulator of pro-inflammatory activity and a possibly therapeutic modulator of microglial reactivity (Karlstetter et al., 2010b, Aslanidis et al., 2015).

Further endogenous molecules that are able to modulate microglial cells are MicoRNAs (miRNAs). miRNAs are small non-coding RNA molecules that are involved in the regulation of diverse physiological processes including functions of the immune system. Different miRNAs were identified to control microglial reactivity, proposing epigenetic regulation by miRNAs as a potential therapeutic application (Cardoso et al., 2016). For example, overexpression of the microglial specific miR-124 in a model of experimental autoimmune encephalomyelitis (EAE) promoted the formation of a resting microglial phenotype, suppressed microglial activation and clearly ameliorated disease symptoms (Ponomarev et al., 2011).

Interferon-β (IFN-β) is a body own cytokine, but is also therapeutically used for the treatment of multiple sclerosis (MS) (Waubant et al., 2003, Kasper and Reder, 2014, Teige et al., 2003). Data from our research group recently revealed an important role for INF-β in a laser-induced mouse model of choroidal neovascularization (CNV), which mimics several features of age-related macular degeneration (AMD). Complete absence of IFNAR or specific deletion in microglia enhanced lesion size and microglial reactivity, whereas treatment with INF- β reduced CNV and microgliosis (Lückoff et al., 2016).

3.4.2 Natural compounds: Luteolin, Curcumin, Crocin and DHA

Different naturally occurring substances can modulate microglial reactivity and reduce their neurotoxic potential. Luteolin is a plant derived flavone that displays anti-oxidative and anti-inflammatory capacity in micromolar concentrations (Seelinger et al., 2008). In vitro studies with LPS-pre-activated BV-2 microglial cells revealed that Luteolin can reduce pro-inflammatory and pro-apoptotic gene expression as well as production of NO; whereas markers associated with enhanced phagocytosis, ramification, chemotaxis and anti-oxidative pathways were clearly upregulated, resulting in less neurotoxicity on photoreceptor cells (Dirscherl et al., 2010).

Similar findings were reported for Curcumin, a spice often found in curry powder (Oyagbemi et al., 2009). Transcriptome analysis of resting and activated microglia showed that treatment with curcumin potently downregulates transcripts that are associated with microglial activation. Furthermore, supernatant from curcumin challenged microglia were less toxic to photoreceptors cells compared to controls (Karlstetter et al., 2011).

A further plant-derived compound with microglial modulative capacity is crocin, a carotenoid that can be found in stigmas of safran or fruits of gardenia. Crocin was shown to reduce LPS, interferon-γ and amyloid-β induced microglial NO production and cell death *ex vivo* in hippocampal slice cultures as well as *in vivo* in light induced retinal degeneration and even improved retinal function measured by electroretinograms (ERG)(Nam et al., 2010, Yamauchi et al., 2011).

Another naturally occurring substance that also influences microglial reactivity is docosahexaenoic acid (DHA), which can be found in fish oil and some seeds. DHA is derived from an essential polyunsaturated fatty acid (PUFA) that must be obtained from dietary sources. DHA is an important structural fatty acid in brain and retina and is responsible for its integrity and functionality (Singh, 2005). Levels of DHA were shown to decrease during different forms of retinal degeneration, including retinoschisin deficient mice, a model of inherited retinal degeneration (Schaefer et al., 1995, Ebert et al., 2009). Dietary intervention with DHA alone or combined with curcumin reduced microgliosis and enhanced photoreceptor survival in retinoschisin deficient mice as well as in a model of neuronal lipofuscinosis (NCL) (Ebert et al., 2009, Mirza et al., 2013).

3.4.3 Minocycline

Minocycline is a semisynthetic tetracycline which is in use against a wide range of infectious diseases caused by gram-positive and gram-negative bacteria for at least 30 years. The ability to bind bacterial 30s ribosomal subunit results in blockage of protein synthesis and is mainly responsible for minocycline's anti-biotic effect. Beside the bacteriostatic action minocycline exerts several other biological activities, including anti-inflammatory and anti-apoptotic effects, neuroprotective capacity as well as inhibition of proteolysis, angiogenesis and tumor metastasis. In various disease models reaching from inflammatory diseases (dermatitis, atherosclerosis), autoimmune disorders (inflammatory bowel disease, rheumathoid arthritis) and neurodegenerative disorders (Parkinson's disease, Alzheimer's disease, Multiple sclerosis, amyotrophic lateral sclerosis, spinal cord injury, Huntington's disease and Ischemic injury) beneficial effects were observed. Accountable for the broad application possibilities is at least partially the rapid absorption, long half-life, good bioavailability and lipophilic properties that allow overcoming of the blood-brain barrier (Garrido-Mesa et al., 2013, Du et al., 2001, Wu et al., 2002b, Biscaro et al., 2012, Brundula et al., 2002, Nikodemova et al., 2010, Wang et al., 2003, Wu et al., 2002a).

In the eye several studies reported minocycline to act immune modulatory and neuroprotective. Glaucoma is a disease caused by degeneration of retinal ganglion cell axons. In DBA/2J mice, a chronic glaucoma model, microglial activation and migration into the optic nerve head are thought to be involved in disease progression. Treatment with minocycline was able to calm down microglial reactivity and to improve axonal integrity and transport. However, minocycline failed to reduce Müller cell and astrocyte gliosis as well as high intraocular pressure (IOP) (Bosco et al., 2008). Furthermore, administration of minocycline successfully preserved outer retinal structure and improved retinal function in a model of green light-induced degeneration that mimics features of dry AMD. Of note is that protection was accompanied by a reduced number of CD11b+ cells in the outer retina (Zhang et al., 2004). Additionally, different studies independently revealed that minocycline was able to reduce microgliosis and preserved retinal structure and function in different models for retinitis pigmentosa. For instance, Yang et al reported that minocycline treatment reduced iNOS expression in the retina and the authors suggested that

minocycline's neuroprotective effect could be at least partially mediated by blockage of microglial NO production (Yang et al., 2007a). Peng et al identified microglial activation to be an early event in the rd 10 model of RP and suggests minocycline to act neuroprotective through an anti-inflammatory and anti-apoptotic mechanism. Interestingly they also observed that microglia, dysregulated by Cx3cr1 deficiency, results in enhanced degeneration in rd 10 mice, suggesting microglial cells to be critically involved in disease progression (Peng et al., 2014). In contrast, others also proposed a microglia independent mechanism (Hughes et al., 2004). Of not is also minocycline's beneficial effect in the treatment of diabetic retinopathy. Diabetic retinopathy is characterized by intra-retinal vascular leakage and neuronal degeneration and there is increasing evidence that inflammatory processes including activation of microglial cells are involved. In a streptozotocin (STZ) induced model of diabetic retinopathy minocycline administration successfully suppressed the production of cytotoxins produced by reactive microglial cells and reduced neuronal apoptosis (Krady et al., 2005). In line with that, minocycline has already been tested in a phase I/II clinical trial for the treatment of diabetic macular edema (DME). In patients treatment with minocycline improved visual function and decreased vascular leakage, although retinal thickness was reported to decrease (Cukras et al., 2012)

It is still not fully clear which mechanisms are mainly responsible for the observed immune modulatory and neuroprotective capacity of minocycline. Proposed mechanisms include the modulation of microglial reactivity (Wang et al., 2005, Henry et al., 2008, Zhang et al., 2004), mitochondrial stabilization, interference with caspase dependent and independent cell death pathways (Chen et al., 2000, Wang et al., 2003, Wang et al., 2004), inhibition of p38 MAPKinase phosphorylation (Matsui et al., 2010, Hua et al., 2005), blockage of matrix metalloproteases (MMP) activity (Brundula et al., 2002, Park et al., 2011, Koistinaho et al., 2005, Xiao et al., 2012) and anti-oxidative as well as direct radical scavenging activity (Kraus et al., 2005) (Plane et al., 2010).

3.4.4 Translocator protein (18κDa) (TSPO) and its ligands

Translocator protein (18κDa) (TSPO) until 2006 also known as peripheral-type benzodiazepine receptor (PBR) is a transmembrane protein in the outer mitochondrial membrane (Papadopoulos et al., 2006, Anholt et al., 1986). TSPO is

an evolutionary well conserved gene and its expression is detectable in different organs like kidney, heart, testis, ovary and brain but highest expression levels were found in steroid-synthesizing tissue such as adrenal glands (Gavish et al., 1999). Within the brain TSPO is expressed in reactive astrocytes (Kuhlmann and Guilarte, 2000, Maeda et al., 2007) and in microglial cells (Casellas et al., 2002, Gavish et al., 1999, Park et al., 1996). In addition, detection has also been reported for some neuronal cell types for example in neurons of the olfactory bulb (Anholt et al., 1984), in neuro- and glioblastoma cell lines (Decaudin et al., 2002), rat dorsal root sensory neurons (Karchewski et al., 2004) and in cultures of rat cortical astrocytes (Jayakumar et al., 2002).

Both older hydropathy profile analysis (Joseph-Liauzun et al., 1998) as well as recently published nuclear-magnetic resonance (NMR) analysis (Jaremko et al., 2014) show that TSPO has a five transmembrane α-helix structure (Figure 5, A).

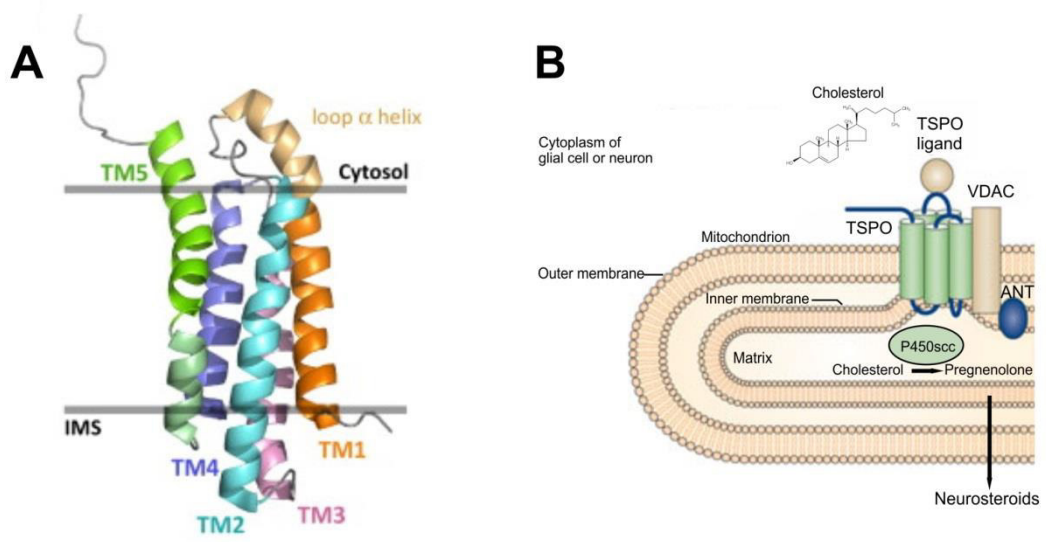

Figure 5: TSPO structure and mitochondrial localization. (A) Structure of TSPO in the outer mitochondrial membrane (side view) showing the five a-helix transmembrane structure (TM1–5). IMS, intermembrane space. **(B)** TSPO is localized in the outer mitochondrial membrane where it forms a complex with the voltage-dependent anion channel (VDAC) and the adenine nucleotide transporter (ANT). TSPO mediates the transition of cholesterol from the inner to the outer mitochondrial membrane. Cholesterin-monooxygenase P450 scc converts cholesterol into pregnenolone, a precursor for several neurosteroids. A is modified from (Selvaraj and Stocco, 2015), B is modified from (Rupprecht et al., 2010), Cholesterol structure modified from (Palmer, 2004)

Protein interaction studies proposed that TSPO forms a complex with other proteins of the inner and outer mitochondrial membrane such as the voltage-dependent anion channel (VDAC) and the adenine nucleotide transporter (ANT) (Garnier et al., 1994,

Veenman et al., 2008). TSPO, as part of this complex reaching from the inner to the outer mitochondrial membrane, is thought to mediate the transport of lipophilic substances such as cholesterol across the intermembrane space (McEnery et al., 1992, Papadopoulos et al., 2006). At the inner mitochondrial membrane the cholesterol side-chain cleaving enzyme cytochrome P450 (P450 scc) converts cholesterol to pregnenolone, a precursor for several neurosteroids (Figure 5, B) (Veenman et al., 2007, Papadopoulos et al., 2007). TSPO is thought to be involved in this crucial a rate-limiting step in steroidogenesis (Lacapere and Papadopoulos, 2003, Papadopoulos et al., 2006, Papadopoulos et al., 2007). In line with this role, TSPO ligands were reported to stimulate production of steroid hormones and neurosteroids in steroidogenic cells and isolated mitochondria (Mukhin et al., 1989, Papadopoulos et al., 1990). Additionally, knocking out TSPO or blocking TSPO with antisense oligodeoxynucleotides (ODNs) suppresses steroid production in Leydig tumor cells (Papadopoulos et al., 1997a, Hauet et al., 2005). Other described functions for TSPO include mitochondrial respiration (Hirsch et al., 1989, Gavish et al., 1999), formation of the mitochondrial permeability transition pore (MPTP) (Zamzami and Kroemer, 2001), cell proliferation (Corsi et al., 2008) and apoptosis (Veenman et al., 2008). Investigations with new established CRISPR/Cas9-mediated TSPO knock-out steroidogenic MA-10 Leydig cells, furthermore propose a role for TSPO in regulation of mitochondrial energy metabolism by modulation of fatty acid oxidation (FAO) (Tu et al., 2016). Of note is that many of the functions were detected in experiments using TSPO ligands.

Two separate studies have however shown that a global TSPO knockout is not lethal as was previosly thought, with the absence of TSPO having no impact on steroidogenesis. This raised a lot of doubt and controversy to the functions ascribed to TSPO (Papadopoulos et al., 1997b, Tu et al., 2014a, Banati et al., 2014). Stimulation of TSPO-knockout in MA-10 mouse Leydig tumor cells with TSPO ligand PK11195 also revealed that enhancement of steroid production is TSPO independent (Tu et al., 2014b). Leading to further speculation that some of the observed effects of TSPO ligands on steroidogenesis are just side effects and not TSPO specific (Selvaraj and Stocco, 2015). There is also conflicting evidence on the role of TSPO as regulator of the mitochondrial permeability transition pore (MPTP), a function associated with cell death induction. More recently published data propose that the

complex of TSPO, VDAC and ANT is not involved in this process (Baines et al., 2007, Kokoszka et al., 2004, Selvaraj and Stocco, 2015).

Independent of the discussion about TSPO function several studies show a strong upregulation of TSPO during different neuropathologies (Rupprecht et al., 2010). In humans, TSPO upregulation is observed in neurological disorders like Alzheimer's disease (Edison et al., 2008, Yasuno et al., 2008), Multiple sclerosis (Banati et al., 2000, Versijpt et al., 2005), Parkinson's disease (Gerhard et al., 2006) Amyotrophic lateral sclerosis (Turner et al., 2004), dementia (Cagnin et al., 2004), and stroke (Gerhard et al., 2005). This is why TSPO serves as a biomarker for brain damage and neurodegeneration. Radio labeled TSPO-ligands are used to detect TSPO expression by positon emission tomography (PET) or single photon emission computed tomography (SPECT), allowing to localize damaged areas or active disease processes (Vivash and O'Brien, 2016, Chauveau et al., 2008, Chen and Guilarte, 2008). However, human studies with healthy volunteers revealed variations in the binding affinity of TSPO ligands, so that results of TSPO density analysis have to be interpreted carefully (Owen et al., 2011b).

Besides their use as diagnostic tools to visualize TSPO expression, TSPO ligands have been shown to be potent in resolving neuroinflammation and neurodegeneration in various disease models (Rupprecht et al., 2010). Endogenous ligands for TSPO include cholesterol (Li et al., 2001), porphyrins (Verma et al., 1987), diazem-binding inhibitor (DBI) and its proteolytic products: octadecaneuropeptide (ODN) and triakontatetraneuropeptide (TTN) (Costa and Guidotti, 1991, Mocchetti and Santi, 1991). The production of DBI-derived ligands is upregulated in response to peripheral nerve injury, suggesting a role for TSPO and its endogenous ligands in nerve regeneration (Lacor et al., 1999). In the retina, DBI-derived ligands produced by astrocytes and Müller cells, were shown to negatively regulate microglial reactivity, by suppression of reactive-oxygen species (ROS) production, TNF-α expression and blockage of microglial proliferation. This suggests DBI-TSPO signaling in the retina to be important for macroglia-microglial interaction and essential for returning activated microglial into a quiescent state after an inflammatory response (Wang et al., 2014).

Synthetic TSPO ligands were primarily developed as neuroimaging agents. Nevertheless classical TSPO ligands such as PK11195 or Ro-5 4864 as well as more recently developed ligands have been reported to exert anti-inflammatory (Ryu et al.,

2005) , neuroprotective (Bordet et al., 2007, Veiga et al., 2005), immune suppressive (Daugherty et al., 2013), regenerative (Girard et al., 2012) and anti-anxiety activity (Rupprecht et al., 2009, Rupprecht et al., 2010). For example, treatment with PK 11195 reduced pro-inflammatory cytokine production, microglial reactivity and neuronal death in a model of quinolinic acid-induced brain lesion (Ryu et al., 2005). Similarly administration of Ro-5 4864 prevented neuron loss in two independent models of brain damage (Veiga et al., 2005, Soustiel et al., 2008). Another TSPO ligand, Etifoxine was shown to be protective in an experimental murine model for multiple sclerosis (MS). Etifoxine improved recovery from MS symptoms was accompanied by clearly reduced immune cell infiltration in the spinal cord and improved oligodendroglial regeneration (Daugherty et al., 2013). In an experimental model for amytrophic lateral sclerosis (ALS), characterized by death of cortical and spinal cord motor neurons, treatment with the TSPO ligand olesoxime (TRO 19622) reduced neuronal cell death and promoted regeneration (Bordet et al., 2007). Furthermore in psychiatric disorders, the TSPO ligand, XBD173 (AC-5216, Emapunil), diminished experimentally induced panic attacks in rodents and exerted antipanic capacity in human volunteers (Rupprecht et al., 2009).

However, how the different TSPO ligands exert neuroprotection and other beneficial effects remains largely unresolved. Possible mechanisms include the modulation of microglial cells, hence glial cells upregulate TSPO in response to pathological alterations and TSPO ligands were shown to reduce microgliosis (Rupprecht et al., 2010). In addition, beneficial effects of TSPO ligands have been associated with changes in neurosteroid production (Giatti et al., 2009, Barron et al., 2013, Selvaraj and Stocco, 2015). However, considering recent findings which challenge TSPO's role in steroidogenesis further approaches are needed to elucidate the exact function of TSPO and how TSPO ligands work to mediate therapeutic effects.

3.5 Aims of the thesis

There is increasing evidence that microglial reactivity actively contributes to the development and perturbation of retinal degenerations. Observations in different brain pathologies revealed furthermore an upregulation of TSPO in activated microglial cells. Moreover ligands for TSPO were effective in resolving degenerative CNS pathologies. Thus, attenuation of chronic microglial activation via TSPO ligands might represent a promising approach to diminish degenerative processes in the retina.

Therefore the study aimed to elucidate the role of TSPO as potential biomarker for retinal microgliosis and possible therapeutic target for the modulation of microglial cells. A comprehensive in vitro approach, testing key microglial functions, was performed to determine the capacity of TSPO ligand, XBD173 to interfere with microglial reactivity and resultant neurotoxicity *in vitro*. A further question addressed in this thesis was whether XBD173 might modulate microglial reactivity *in vivo* and thereby reduce light induced retinal degeneration.

A further goal of the thesis was to determine whether minocycline, an antibiotic with additional anti-inflammatory properties is able to reduce microglial neurotoxicity and to protect the retina from degeneration. Therefore a model of bright white light-induced retinal degeneration, mimicking features of inherited degenerations such as microgliosis and death of photoreceptors, was used to assess the immunomodulatory and neuroprotective effects of minocycline during retinal degeneration.

4 Results

4.1 Translocator protein (18 kDa) (TSPO) is expressed in reactive retinal microglia and modulates microglial inflammation and phagocytosis

Marcus Karlstetter, Caroline Nothdurfter, Alexander Aslanidis, Katharina Moeller, Felicitas Horn, **Rebecca Scholz**, Harald Neumann, Bernhard H F Weber, Rainer Rupprecht* and Thomas Langmann*

Background: The translocator protein (18 kDa) (TSPO) is a mitochondrial protein expressed on reactive glial cells and a biomarker for gliosis in the brain. TSPO ligands have been shown to reduce neuroinflammation in several mouse models of neurodegeneration. Here, we analyzed TSPO expression in mouse and human retinal microglia and studied the effects of the TSPO ligand XBD173 on microglial functions.

Methods: TSPO protein analyses were performed in retinoschisin-deficient mouse retinas and human retinas. Lipopolysaccharide (LPS)-challenged BV-2 microglial cells were treated with XBD173 and TSPO shRNAs in vitro and pro-inflammatory markers were determined by qRT-PCR. The migration potential of microglia was determined with wound healing assays and the proliferation was studied with Fluorescence Activated Cell Sorting (FACS) analysis. Microglial neurotoxicity was estimated by nitrite measurement and quantification of caspase 3/7 levels in 661 W photoreceptors cultured in the presence of microglia-conditioned medium. The effects of XBD173 on filopodia formation and phagocytosis were analyzed in BV-2 cells and human induced pluripotent stem (iPS) cell-derived microglia (iPSdM). The morphology of microglia was quantified in mouse retinal explants treated with XBD173.

Results: TSPO was strongly up-regulated in microglial cells of the dystrophic mouse retina and also co-localized with microglia in human retinas. Constitutive TSPO expression was high in the early postnatal Day 3 mouse retina and declined to low levels in the adult tissue. TSPO mRNA and protein were also strongly induced in LPS-challenged BV-2 microglia while the TSPO ligand XBD173 efficiently suppressed transcription of the pro-inflammatory marker genes chemokine (C-C motif) ligand 2 (CCL2), interleukin 6 (IL6) and inducible nitric oxide (NO)-synthase

(iNOS). Moreover, treatment with XBD173 significantly reduced the migratory capacity and proliferation of microglia, their level of NO secretion and their neurotoxic activity on 661 W photoreceptor cells. Furthermore, XBD173 treatment of murine and human microglial cells promoted the formation of filopodia and increased their phagocytic capacity to ingest latex beads or photoreceptor debris. Finally, treatment with XBD173 reversed the amoeboid alerted phenotype of microglial cells in explanted organotypic mouse retinal cultures after challenge with LPS.

Conclusions: These findings suggest that TSPO is highly expressed in reactive retinal microglia and a promising target to control microglial reactivity during retinal degeneration.

Own contribution to publication I:

To exclude that TSPO is significantly expressed in Müller cells or retinal neurons, I established, performed and analyzed glial fibrillary acid protein (GFAP)/TSPO and microtubule-associated protein 2 (MAP2)/TSPO co-stainings in wildtype as well as in Rs1h $^{-/y}$ mice (Fig.1. J-M). To determine the effect of XBD173 on microglial proliferation I established, performed and analyzed CFSE-based flow cytometry analysis (Fig. 4 C) and created the respective images

Contribution of co-authors to publication I:

Marcus Karlstetter conceptualized parts of the project, finalized images, managed collaborations and carried out qRT-PCR analysis and neurotoxicity assays (Fig. 3 A-H). Caroline Nothdurfter carried out pregnenolone ELISA (Fig. 7 A). Alexander Aslanidis carried out immunohistochemistry (Fig. 1 A-I), quantitative real-time PCR and Western blot (Fig. 2 A-E) analyses of TSPO expression in the retina and performed migration assays (Fig. 4 A, B). Alexander Aslanidis and Felicitas Horn performed morphological analyses and phagocytosis assays with BV-2 microglial cells and iPSdM cells (Fig. 5 A-H, Fig. 6 A-D). Katharina Moeller performed aminoglutethimide phagocytosis assays (Fig. 7 B) and optimized and carried out retinal explant experiments (Fig. 8 A-E). Prof. Harald Neumann provided iPSdM cells. Prof. Bernhard Weber provided valuable suggestions and critically read the manuscript. Prof. Rainer Rupprecht supplied the synthetic TSPO ligand XBD173 and provided valuable suggestions. Prof. Thomas Langmann, as principal investigator, coordinated the project and wrote the manuscript.

4.2 Targeting translocator protein (18 kDa) (TSPO) dampens pro-inflammatory microglia reactivity in the retina and protects from degeneration

Rebecca Scholz, Albert Caramoy, Mohajeet B. Bhuckory, Khalid Rashid, Mei Chen, Heping Xu, Christian Grimm and Thomas Langmann*

Background: Reactive microglia are commonly seen in retinal degenerative diseases, and neurotoxic microglia responses can contribute to photoreceptor cell death. We and others have previously shown that translocator protein (18 kDa) (TSPO) is highly induced in retinal degenerations and that the selective TSPO ligand XBD173 (AC-5216, emapunil) exerts strong anti-inflammatory effects on microglia in vitro and ex vivo. Here, we investigated whether targeting TSPO with XBD173 has immuno-modulatory and neuroprotective functions in two mouse models of acute retinal degeneration using bright white light exposure.

Methods: BALB/cJ and Cx3cr1GFP/+ mice received intraperitoneal injections of 10 mg/kg XBD173 or vehicle for five consecutive days, starting 1 day prior to exposure to either 15,000 lux white light for 1 h or 50,000 lux focal light for 10 min, respectively. The effects of XBD173 treatment on microglia and Müller cell reactivity were analyzed by immuno-stainings of retinal sections and flat mounts, fluorescence-activated cell sorting (FACS) analysis, and mRNA expression of microglia markers using quantitative real-time PCR (qRT-PCR). Optical coherence tomography (OCT), terminal deoxynucleotidyl transferase dUTP nick end labeling (TUNEL) stainings, and morphometric analyses were used to quantify the extent of retinal degeneration and photoreceptor apoptosis.

Results: Four days after the mice were challenged with bright white light, a large number of amoeboid-shaped alerted microglia appeared in the degenerating outer retina, which was nearly completely prevented by treatment with XBD173. This treatment also down-regulated the expression of TSPO protein in microglia but did not change the TSPO levels in the retinal pigment epithelium (RPE). RT-PCR analysis showed that the microglia/macrophage markers Cd68 and activated microglia/macrophage whey acidic protein (Amwap) as well as the pro-inflammatory genes Ccl2 and Il6 were reduced after XBD173 treatment. Light-induced degeneration of the outer retina was nearly fully blocked by XBD173 treatment. We further confirmed these findings in an independent mouse model of focal light

damage. Retinas of animals receiving XBD173 therapy displayed significantly more ramified non-reactive microglia and more viable arrestin-positive cone photoreceptors than vehicle controls.

Conclusions: Targeting TSPO with XBD173 effectively counter-regulates microgliosis and ameliorates light-induced retinal damage, highlighting a new pharmacological concept for the treatment of retinal degenerations.

Own contribution to publication II:

I designed, performed and analyzed all experiments, except of focal light damage analysis (Fig 6 A-J), created all images and helped to finalize the manuscript draft. I independently handled the revision phase of this project. I presented posters and oral presentations on several national and international meetings during my PhD.

Contribution of co-authors to publication II:

Albert Caramoy helped with OCT analyses. Mohajeet B. Bhuckory and Mei Chen carried out focal light exposure experiments coordinated by Prof. Heping Xu. Prof. Heping Xu and Prof. Christian Grimm provided valuable suggestions and critically read the manuscript. Khalid Rashid critically read the manuscript. Prof. Thomas Langmann, as principal investigator, coordinated the project and wrote the manuscript.

4.3 Minocycline counter-regulates pro-inflammatory microglia responses in the retina and protects from degeneration

Rebecca Scholz, Markus Sobotka, Albert Caramoy, Thomas Stempfl, Christoph Moehle and Thomas Langmann*

Background: Microglia reactivity is a hallmark of retinal degenerations and overwhelming microglial responses contribute to photoreceptor death. Minocycline, a semi-synthetic tetracycline analog, has potent anti-inflammatory and neuroprotective effects. Here, we investigated how minocycline affects microglia in vitro and studied its immuno-modulatory properties in a mouse model of acute retinal degeneration using bright white light exposure.

Methods: LPS-treated BV-2 microglia were stimulated with 50 µg/ml minocycline for 6 or 24 h, respectively. Pro-inflammatory gene transcription was determined by real-time RT-PCR and nitric oxide (NO) secretion was assessed using the Griess reagent. Caspase 3/7 levels were determined in 661W photoreceptors cultured with microglia-conditioned medium in the absence or presence of minocycline supplementation. BALB/cJ mice received daily intraperitoneal injections of 45 mg/kg minocycline, starting 1 day before exposure to 15.000 lux white light for 1 hour. The effect of minocycline treatment on microglial reactivity was analyzed by immunohistochemical stainings of retinal sections and flat-mounts, and messenger RNA (mRNA) expression of microglia markers was determined using real-time RT-PCR and RNA-sequencing. Optical coherence tomography (OCT) and terminal deoxynucleotidyl transferase dUTP nick end labeling (TUNEL) stainings were used to measure the extent of retinal degeneration and photoreceptor apoptosis.

Results: Stimulation of LPS-activated BV-2 microglia with minocycline significantly diminished the transcription of the pro-inflammatory markers CCL2, IL6, and inducible nitric oxide synthase (iNOS). Minocycline also reduced the production of NO and dampened microglial neurotoxicity on 661W photoreceptors. Furthermore, minocycline had direct protective effects on 661W photoreceptors by decreasing caspase 3/7 activity. In mice challenged with white light, injections of minocycline strongly decreased the number of amoeboid alerted microglia in the outer retina and

down-regulated the expression of the microglial activation marker translocator protein (18 kDa) (TSPO), CD68, and activated microglia/macrophage whey acidic protein (AMWAP) already 1 day after light exposure. Furthermore, RNA-seq analyses revealed the potential of minocycline to globally counter-regulate pro-inflammatory gene transcription in the light-damaged retina. The severe thinning of the outer retina and the strong induction of photoreceptor apoptosis induced by light challenge were nearly completely prevented by minocycline treatment as indicated by a preserved retinal structure and a low number of apoptotic cells.

Conclusions: Minocycline potently counter-regulates microgliosis and light-induced retinal damage, indicating a promising concept for the treatment of retinal pathologies.

Own contribution to publication III:

To determine the neurotoxic potential of differentially stimulated microglia and on 661W photoreceptors I designed, performed and analyzed caspase 3/7 activity measurements (Fig 2 B). I performed immunohistochemical stainings (microglial markers: iba1, tspo) in retinal sections and flat-mounts to analyze the effect of minocycline treatment on microglial reactivity four days after light exposure. Furthermore I specified activation of Müller cells by staining of glial fibrillary protein (GFAP) (Fig. 3 A-L). To determine whether microglial activation is an early event after light exposure and precedes photoreceptor apoptosis, microglial morphology and location were analyzed by immunostainings of retinal sections (Fig 5 A-C) as early as one day after light exposure. I additionally carried out time kinetic experiments to analyze mRNA expression levels of microglia associated markers (Fig 5 D-I). To analyze structural changes of the retina, I immunostained retinal sections with DAPI (Fig 7 H-J). I analyzed the amount of apoptotic cells by TUNEL-labeling (Fig 7 K-M) and performed RNA analyses to determine the level of caspase 8 mRNA which is involved in programmed cell death (Fig. 7 N). To analyze how fast microglia cells react to light stimuli, I performed immunostainings and mRNA analysis four hours after light exposure (Fig S1 A-F). I created all images and wrote the manuscript draft. I independently handled the revision phase of this project

Contribution of co-authors to publication III:

Under my supervision, Markus Sobotka carried out qRT-PCR analysis in BV-2 microglial cells (Fig. 1A-F) and retinas (Fig 4 A-F) and performed nitric oxide (NO)

measurements (Fig. 2A). Supported by Albert Caramoy and me, Markus Sobotka carried out and analyzed OCT analyses (Fig. 7 A-G). Thomas Stempfl and Christoph Moehle performed RNA sequencing and wrote the respecting part of the manuscript (Fig. 6 A-C). Prof. Thomas Langmann, as principal investigator, obtained funding, supervised the project, created the RNA sequencing image and tables (Fig 6 A-C, S2, S3) and corrected the manuscript.

5 Discussion

5.1 TSPO-reactivity marker and target for therapy

Microglial activation is a general hallmark of neurodegenerative diseases. There is increasing evidence that loss of auto-regulatory capacity of microglia cells, resulting in chronic activation, contributes to neuronal cell death in the CNS including the retina (Karlstetter et al., 2015). From brain pathologies it is known that activated microglia express enhanced levels of TSPO (Rupprecht et al., 2010). However, knowledge about TSPO expression in retinal microglia was missing. Therefore, in the current study, we aimed at elucidating the role of TSPO as a possible reactivity marker for microglia in the retina and hypothesized that TSPO could be a target for neuroprotective therapy in this tissue.

5.1.1 TSPO as a microglial reactivity marker in retinal degeneration

From different neuropathies affecting the brain or the peripheral nervous system (PNS), it is well known that TSPO is upregulated in reactive microglial cells and sometimes in astrocytes and that this mitochondrial protein is a suitable biomarker to detect and localize neuro-inflammatory events using radio-labeled TSPO ligands (Vowinckel et al., 1997, Cagnin et al., 2004, Turner et al., 2004, Gerhard et al., 2005, Gerhard et al., 2006, Maeda et al., 2007, Miyoshi et al., 2009). Here, we showed for the first time that human and mouse retinal microglia cells express TSPO. Microglial TSPO was upregulated in the degenerating retinoschisin-deficient as well light-damaged retina. TSPO expression in both models overlapped with the peak of microglial reactivity. This implicates that TSPO could also be a suitable biomarker for detecting gliosis in retinal diseases. Our work was subsequently confirmed by Wang et al. investigating the expression of TSPO in different models of retinal inflammation and injury (LPS- induced inflammation/ NMDA-induced excitotoxicity, subretinal hemorrhage and optic nerve crush) (Wang et al., 2014). Microglial TSPO expression was also observed in myosin VI deficient mice with a phenotype reflecting some similarities of age-related macular degeneration, further highlighting TSPO as a biomarker of retinal degeneration (Schubert et al., 2015). Studies from other groups as well as our own data therefore raise hope for using TSPO ligands in the future as

in vivo imaging tools to monitor microgliosis during retinal degenerations. However there are several limitations. For instance, one widely used TSPO ligand ^{11}C-PK11195 has been reported to possess relatively low brain permeability and to bind unspecifically to plasma proteins. This results in low specificity of PET images, making the detection of minor alterations during neuroinflammation difficult (Vivash and O'Brien, 2016, Owen and Matthews, 2011). Moreover, it was noticed that there exists genetic variation in the binding affinity of TSPO ligands and some patients even completely lack tracer binding. Responsible for this is a single nucleotide polymorphism (rs6971) in exon 4 of the TSPO gene causing an alanine147-to-threonine substitution (Owen et al., 2011a, Owen et al., 2012, Fujita et al., 2008). It is therefore necessary to test whether this polymorphism is present in patients to correctly interpret TSPO-binding studies.

Considering a different role of TSPO expressing cells like microglia or astrocytes during degeneration, difficulties in data interpretation of TSPO ligand binding studies may occur (Vivash and O'Brien, 2016, Lavisse et al., 2012). In the eye we and others detected TSPO expression in different cell types such as microglia cells, astrocytes and cells of the retinal pigment epithelium (RPE) (Scholz et al., 2015a, Wang et al., 2014). We have shown that TSPO is constitutively expressed in the RPE whereas microglia show a low basal expression but strong upregulation during degenerative changes. Hence, due to the unspecific nature of TSPO ligands used for *in vivo* imaging and low resolution of PET images, subtle changes in the relatively low number of retinal microglial cells might be hard to distinguish from the high background signal resulting from strongly expressing TSPO cells such as the RPE. Therefore to circumvent this problem and construe in vivo imaging pictures more accurately, the development of cell type specific radio-ligands would be very helpful.

5.1.2 Understanding TSPO induction in microglial cells

TSPO is upregulated in response to highly diverse stimuli such as neuronal degeneration (Edison et al., 2008), mechanic induced injury (Karchewski et al., 2004) , recovery responses from injury (Lacor et al., 1999), autoimmune processes (Daugherty et al., 2013, Vowinckel et al., 1997), challenge to external stressors like light (Scholz et al., 2015a, Scholz et al., 2015b), hereditary alterations or bacterial

compounds (Karlstetter et al., 2014). Due to the complexity of diseases and models reflecting microglial TSPO upregulation, it is hard to decipher the factors and pathways involved in microglial TSPO regulation. We and others found TSPO upregulation in microglial cells after stimulation with TLR4 ligand LPS (Karlstetter et al., 2014, Wang et al., 2014). Therefore damage-associated molecular patterns recognized by TLR4 and subsequent downstream signaling are good candidates for microglial TSPO induction. Indeed, pharmacological blockage of TLR 4 by LPS-RS in a rat model of neuropathic pain prevented TSPO upregulation and neuropathic pain (Wei et al., 2013). Since microglial cells express several immuno-regulatory surface receptors in addition to TLRs, it seems unlikely that TSPO regulation solely depends on TLR signaling.

5.1.3 Transcriptional regulation of TSPO

TSPO protein expression was investigated in different cells under both homeostatic and disease conditions, highest TSPO expression levels were detectable in steroid synthesizing tissue (Gavish et al., 1999). But there is only scarce information about the transcriptional regulation of TSPO in different cell types. Studies using cells with high (MA-10 mouse tumor Leydig cells) and low (NIH-3T3 mouse fibroblasts) basal TSPO expression level revealed that protein kinase c epsilon (PKC ε) is crucially involved in the control of TSPO on transcriptional level. PKC ε was proposed to regulate TSPO expression via a mitogen-activated protein kinase (MAPK) (Raf-1-/MEK1/2-ERK1/2) signal transduction pathway, acting at least partially through Stat3 and c-Jun transcription factors (Batarseh et al., 2010, Batarseh and Papadopoulos, 2010). But it was shown that PKC ε is not expressed in microglia cells (Slepko et al., 1999). Further investigations will be needed to elucidate microglia-specific regulation of TSPO transcription in health and disease.

5.1.4 Immune modulation and neuroprotection by TSPO ligand XBD173

We initially showed that XBD173 could reverse LPS induced microglial reactivity and dampen its neurotoxic potential on photoreceptors *in vitro*. Based on these findings

we tested XBD173 in two independent murine models of light-induced retinal degeneration. This TSPO directed therapy revealed reduced numbers and less amoeboid shaped, reactive microglial cells in the outer retina and preserved the retinal structure (Scholz et al., 2015a).

Our findings are in agreement with studies using other TSPO ligands in pathologies of the brain or the peripheral nervous system that revealed neuroprotective effects accompanied by a reduction of immune cell reactivity (Daugherty et al., 2013, Barron et al., 2013, Girard et al., 2008, Ryu et al., 2005). For instance, treatment of experimental autoimmune encephalomyelitis (EAE) with Etifoxine attenuated disease severity, improved symptomatic recovery and reduced immune cell infiltration (Daugherty et al., 2013). The same ligand also promoted axonal regeneration in a model of traumatic nerve injury (Girard et al., 2012). Comparable to our findings that showed less GFAP expression in Müller cells and less microglial reactivity in mice treated with XBD173, administration of TSPO ligand, Ro5-4864 in Alzheimer's disease reduced both GFAP and Iba1 immunoreactivity and attenuated neuropathological alterations as well as behavioral deficits (Barron et al., 2013).

Although modulation of microglia is very likely involved in XBD173's neuroprotective effect, TSPO function and the exact mechanism of action are still uncertain. In our *in vitro* study, treatment of LPS-activated BV-2 microglia with XBD173 dampened pro-inflammatory marker gene expression of CCL2, IL6 and iNOS, whereas TSPO knockdown with two different shRNAs abrogated the suppressing effects. Transcripts of the same markers were also reduced in retinas of XBD173- treated mice four days after light challenge. In line with suppressed iNOS transcripts, XBD173 also suppressed microglial toxic NO production. Moreover microglial conditioned medium from XBD173 stimulated cells was less neurotoxic on 661W photoreceptors compared to controls. Indeed, elevated levels of NO are detectable in retinal degeneration and depending on the amount and duration, supposed to contribute to the disease process (Hoey et al., 1997, Yang et al., 2007a). Therefore suppression of pro-inflammatory signaling is very likely involved in this TSPO-directed therapy approach. Supporting this hypothesis, studies using the TSPO agonist PK11195 also revealed suppression of pro-inflammatory gene transcription. For instance, stimulation of human LPS-activated microglial cells with PK11195 reduced gene expression of cyclooxygenase-2 (COX-2) and tumor necrosis factor-a (TNF-a) (Choi

et al., 2002). In line with that, administration of the same compound also decreased mRNA levels of the pro-inflammatory cytokines IL1β, IL6, TNFα and iNOS as well as microglial reactivity in quinolinic acid induced brain degeneration (Ryu et al., 2005).

As mentioned previously, XBD173 dampened CCL2 gene expression *in vitro* and *in vivo*, which could be important for the observed neuroprotective effect. Studies investigating the role of CCL2/CCR2 signaling in models of AMD suggest an important role of this cytokine in degenerative processes, as knockout of these factor or pharmacological blockage prevents inflammatory microglia and monocyte recruitment and photoreceptor degeneration (Sennlaub et al., 2013, Raoul et al., 2010).

Our *in vitro* studies further showed XBD173's capacity to suppress microglial migration and proliferation, suggesting TSPO to be involved in the control of these functions. In line with this, TTN, a DBI-derived endogenous TSPO ligand, produced by Müller cells and astrocytes, significantly reduced microglial proliferation in the retina (Wang et al., 2014). Indeed high TSPO expression is positively correlated to enhanced proliferative capacity in human breast cancer cell lines (Hardwick et al., 1999). The same is also true for TSPO overexpressing glioma cells, which show enhanced proliferation, transmigration and motility (Rechichi et al., 2008). As enhanced proliferation is a sign of microglial reactivity, the ability of the synthetic ligand XBD173 as well as the endogenous ligand TTN to ameliorate these responses further proves their potency in limiting pro-inflammatory responses in microglia (Wang et al., 2014).

Phagocytosis is generally enhanced during pathological conditions, however, phagocytosis itself is not a sign of pro-inflammatory activation, as high phagocytic capacity is also important to maintain physiological conditions (Sierra et al., 2013). In the current study, XBD173 stimulation of human iPSdM and murine BV2 microglial cells resulted in increased phagocytosis of both latex beads and apoptotic photoreceptor debris. XBD173 administration furthermore promoted the formation of filopodia in the human and the murine cell culture system as well as in retinal explants. It is not yet clear how XBD173 mediates these effects. However, since pro-inflammatory substances such as LPS induce an increase in Ca^{2+} ions in microglia cells leading to concomitant actin organization, it is plausible that XBD173 could influence filopodia formation and the ramified morphology by changing Ca^{2+} levels

(Bader et al., 1994). Indeed, the TSPO ligand PK11195 reduced LPS-induced increase of intracellular Ca^{2+} in human microglial cells (Choi et al., 2002).

TSPO is supposed to control a rate limiting step in steroidogenesis (Papadopoulos et al., 2006, Papadopoulos et al., 2007, Rupprecht et al., 2010) and we detected elevated levels of the neurosteroid precursor pregnenolon after XBD173 stimulation in microglial supernatant. Furthermore, blocking the rate limiting enzymatic conversion of cholesterol to pregnenolone by aminoglutethimide (AMG) reduced the phagocytic capacity of microglial cells suggesting a role for pregnenolone derived steroids in control of microglial functions. Interestingly, Giatti et al. observed that TSPO ligand, Ro5 4864 effectively reduced the severity of diabetic neuropathy through a local increase of neurosteroids (Giatti et al., 2009). Furthermore, progesterone and its metabolite allopregnanolone, both derived from pregnenolone, downregulated pro-apoptotic genes (caspase 3, bax, bad) and enhanced expression of anti-apoptotic bcl-2 in a model of traumatic brain injury, ultimately resulting in neuroprotection (Djebaili et al., 2005, Djebaili et al., 2004, Yao et al., 2005). Moreover, progesterone was recently tested in the rd1 mouse model of retinitis pigmentosa. Progesterone was able to decrease gliosis, the amount of cell death, increased ONL thickness and also improved retinal function detectable by an improved ERG b wave amplitude (Sanchez-Vallejo et al., 2015). These data allow speculations that neuroprotection by intervention with TSPO ligands to be possibly mediated by influencing neurosteroid production.

Retinal TSPO expression was not limited to microglial cells and TSPO was also detectable in astrocytes and the RPE. Furthermore, XBD173 treatment did not change TSPO expression in these cells as it was seen in microglia. This indicates potential different functions for TSPO in astrocytes and RPE than microglia. Moreover, it raises the question whether the protective effect of XBD173 is exclusively mediated by modulation of microglial cells. Analyses of human RPE cells revealed a correlation between aging and mitochondrial dysfunction, resulting in increased susceptibility of RPE cells to oxidative stress (He et al., 2010). Interestingly, mitochondrial damage in RPE cells, possibly resulting in dysfunction, was recently associated with the development of AMD (Terluk et al., 2015). Therefore it has to be examined whether XBD173's neuroprotection could also be mediated by influencing mitochondrial function in RPE cells.

5.1.5 TSPO - future challenges and perspectives

As light damage is an inducible, fast progressive model and caused by one specific trigger, it would be interesting to test XBD173's efficiency to suppress neurodegeneration also in a slow degeneration model of inherited retinal dystrophy. Since some retinopathies like AMD also comprise an uncontrolled growth of blood vessels, it would be interesting to test combinatorial therapeutic strategies targeting both microglial cells and newly formed blood vessels.

Creation of cell type specific TSPO knock out mice, lacking TSPO in microglial or RPE cells would allow studying the cell type specific role of TSPO. Furthermore these conditional knockout mice would enable to investigate which cell type is essentially responsible for the before described neuroprotective effect in light induced degeneration. Considering high constitutive expression of TSPO in RPE, it would moreover be very interesting to study if and how XBD173 stimulation affects RPE cells.

Insights from new established complete TSPO knockout mice, that were against expectations viable, bring old understanding of TSPO as a cholesterol transporter and theories of mechanism of action of different TSPO ligands to stagger. Future efforts should aim at elucidating the exact role of TSPO under physiological and pathological conditions and in different cell types (Tu et al., 2014a, Banati et al., 2014). More recently published literature proposes a role for TSPO in oxidative stress response and fatty acid oxidation (Tu et al., 2016, Batoko et al., 2015b, Batoko et al., 2015a). How these functions are influenced by TSPO ligands and contribute to the detected immunomodulatory and neuroprotective effects has to be figured out.

5.2 Minocycline in retinal degeneration

Minocycline is an approved antibiotic for the use against gram positive and negative bacteria. Several studies revealed further properties including anti-inflammatory and anti-apoptotic activities and inhibited proteolysis, angiogenesis and tumor metastasis (Garrido-Mesa et al., 2013, Domercq and Matute, 2004). Our investigations aimed at

elucidating how minocycline modulates microglia cells and if minocycline can protect from white light-induced degeneration. Of note is that light is also a promoting factor in human retinal degenerations and is therefore more than an artificial stimulus (Cruickshanks et al., 1993, Swaroop et al., 2009, Wenzel et al., 2005).

5.2.1 Immune modulation and retinal degeneration rescue by Minocycline

Our minocycline intervention study revealed that minocycline counter-regulated the early pro-inflammatory microglial response and protected the retina from light induced photoreceptor death. This neuroprotective effect was in good agreement with other models of retinal degeneration such as glaucoma, retinitis pigmentosa or diabetic retinopathy (Bosco et al., 2008, Yang et al., 2007a, Krady et al., 2005). We have analyzed microglia and noticed less amoeboid cells in the outer retina and lower expression of TSPO, AMWAP and CD68 in the Minocycline treatment group. This indicates that Minocycline counter-regulates retinal microglial reactivity. In agreement, minocycline treatment in a model of diabetic retinopathy also repressed pro-inflammatory mediators and cytotoxins, which are known to be released from reactive microglia (Krady et al., 2005). Similarly, Minocycline specifically increased the number of ramified microglia in a DBA/2J mouse glaucoma model. The reduction of microglia activation was coupled to improved retinal ganglion cell (RGC) function (Bosco et al., 2008). Peng and colleagues also showed that inhibition of microglial activation with Minocycline reduced photoreceptor apoptosis in the murine rd 10 model of retinitis pigmentosa (Peng et al., 2014).

We also analyzed potential mechanisms how minocycline could mediate immune modulation and neuroprotection. The analyses with BV-2 microglia and the light damage model revealed efficient suppression of key microglial activation pathways (CCL2, IL6, iNOS) by minocycline. Similar to our findings, pro-inflammatory molecules like IL6, IL1β and TNF-α, TLR 2, Cox1, Cox 2 and iNOS were suppressed by minocycline stimulation of BV-2 microglia (Henry et al., 2008, Wang et al., 2005, Peng et al., 2014). Reduced transcripts of pro-inflammatory markers (IL-1β, TNF-α) were furthermore detected in minocycline treated mice that mimic diabetic retinopathy and retinitis pigmentosa (Krady et al., 2005, Peng et al., 2014). Thus

minocycline seem to be very effective in diminishing pro-inflammatory gene expression.

Nitric oxide (NO) is a toxic molecule that is capable of damaging photoreceptors and other retinal cells when secreted from microglia. We showed that minocycline reduced microglial NO production after LPS challenge and reduced neurotoxicity of microglial conditioned medium on photoreceptor cells. Interestingly, adding minocycline directly to photoreceptors also reduced microglial mediated cell death. Several studies revealed an association between NO production and degenerative processes and substances blocking NO production were reported to reduce degeneration (Yang et al., 2007a, Hoey et al., 1997, Nagayama et al., 1998, Yang et al., 2007b).

Minocycline could also act directly on photoreceptors to inhibit apoptosis. A protein, involved in apoptosis induction, is B-cell lymphoma 2 (Bcl-2) that can interfere with pro-apoptotic proteins such as Bax, Bak and Bid and thereby block mitochondrial cytochrome-c release and caspase dependent induction of cell death. Likewise, minocycline treatment of rd 10 retinitis pigmentosa mice and animals with retinal vein occlusion enhanced anti-apoptotic Bcl-2 expression, suppressed pro-apoptotic Bax levels and caspase 3/7 activity and thereby exerted neuroprotection (Wang et al., 2004, Peng et al., 2014, Sun et al., 2013). Additionally, Minocycline reduced apoptosis-inducing factor (AIF) mediated cell death in a model of Huntington's disease (Wang et al., 2003, Chen et al., 2000).

Minocycline could also directly act neuroprotective via its free radical scavenging properties. Rat brain homogenate lipid peroxidation 2,2-diphenyl-1-picrylhydrazyl (DPPH) radical scavenging assays revealed that minocycline exerts anti-oxidative capacity comparable to Vitamin E (Kraus et al., 2005). Other studies report that treatment with minocycline enhanced transcription of anti-oxidative nuclear respiratory factor 2 (Nrf 2) regulated genes like NAD(P)H dehydrogenase (quinone) 1 (NQO1) and heme oxygenase 1 (HO-1) (Sakata et al., 2012). It was proposed that minocycline's anti-oxidative action relies on the one hand on its chemical structure and on the other hand on its modulatory capacity of certain enzymes, like nitric oxide synthase or lipoxygenase (Plane et al., 2010).

Beside the so far elucidated options, how minocycline mediates neuroprotection, further mechanisms were proposed. It was reported that minocycline has the ability to attenuate p38 mitogen-activated protein kinase (p38 MAPK) phosphorylation in spinal cord microglia and neurons and thereby act anti-nociceptive in models of tissue injury and inflammation-evoked pain (Hua et al., 2005). Similarly, Matsui and colleagues reported that both Minocycline and an inhibitor of p38 repress release of pro-inflammatory substances like nitric oxide (NO) and prostaglandine E2 (PGE2) in spinal cord microglia, which are thought to be implicated in nociceptive signaling (Matsui et al., 2010).

Minocycline could also mediate neuroprotection by blocking Matrix metalloproteinases (MMPs). MMPs are involved in the transition of leukocytes across barriers, a critical aspect in CNS pathologies with enhanced immune cell infiltration such as multiple sclerosis. It was shown that minocycline can block MMP activity, resulting in less severe disease outcome in experimental autoimmune encephalomyelitis (Brundula et al., 2002). In line with these findings, interfering with MMPS by Minocycline was also able to decrease infarct size in models of cerebral ischemia (Park et al., 2011, Koistinaho et al., 2005). In the eye, minocycline administration reduced neovascularization in a model of alkali burn-induced corneal neovascularization, possibly by diminishing MMPs (MMP2/9/13), proinflammatory cytokine (IL-1 β, IL-6) production as well as angiogenic factors (VEGF, bFGF) (Xiao et al., 2012).

Taken together, different mechanisms are discussed how minocycline can exert neuroprotection but most studies revealed that reduction of microglial reactivity is a key event.

5.2.2 Minocycline – future challenges and perspectives

Minocycline was able to reduce microglial reactivity and prevented light induced retinal degeneration, reflected in a preserved outer nuclear layer (Scholz et al., 2015b). This is in agreement with other studies showing neuroprotection in degenerative diseases of the CNS (Garrido-Mesa et al., 2013). The good CNS permeability and bioavailability and the fact that minocycline is already in use in patients as an antibiotic makes the transfer from bench to bedside way easier. For

the usage of minocycline in retinopathies, data from a first clinical trial, testing minocycline as medication for diabetic macular edema, are available. Minocycline improved visual function, central macular edema and vascular leakage compared to historical controls (Cukras et al., 2012). Because of the promising findings from preclinical and clinical trials extension of minocycline application to further retinal degenerative pathologies with microglial contribution is conceivable. Since some retinopathies like AMD also comprise a detrimental growth of blood vessels, it would be interesting to test combinatorial therapeutic strategies targeting both microglial cells and angiogenesis.

Possible challenges to transfer minocycline to the clinic include the occurrence of side effects such as tissue hyperpigmentation, serious hypersensitivity reactions and autoimmune disorders (Kim and Suh, 2009). Hence the application regimen of minocycline in pre-clinical studies varies there might also be difficulties to find an effective dosage to treat retinopathies in patients. Differences between laboratory animals and patients such as variations in the half-life of minocycline need to be considered (Noble et al., 2009).

5.3 Conclusion

There are only limited strategies for treating inherited and complex retinal degenerations and to detect microgliosis in the eye.

This thesis suggests that the brain degeneration biomarker TSPO may also be used to detect gliosis in the eye. Treatment with TSPO-ligand, XBD173 reduced the neurotoxic potential of microglial cells and prevented light-induced retinal degeneration. Therefore TSPO is a promising target to control microglial reactivity and to treat retinal degeneration.

In addition findings revealed that minocycline ameliorates light-induced retinal damage by counter-regulation of microglial reactivity and direct effects on photoreceptors. Taken together the data highlight microglia-directed treatment strategies, as a promising therapeutic option for retinal degenerative diseases.

References

AJAMI, B., BENNETT, J. L., KRIEGER, C., TETZLAFF, W. & ROSSI, F. M. 2007. Local self-renewal can sustain CNS microglia maintenance and function throughout adult life. *Nat Neurosci,* 10**,** 1538-43.

ALLIOT, F., GODIN, I. & PESSAC, B. 1999. Microglia derive from progenitors, originating from the yolk sac, and which proliferate in the brain. *Brain Res Dev Brain Res,* 117**,** 145-52.

ANHOLT, R. R., MURPHY, K. M., MACK, G. E. & SNYDER, S. H. 1984. Peripheral-type benzodiazepine receptors in the central nervous system: localization to olfactory nerves. *J Neurosci,* 4**,** 593-603.

ANHOLT, R. R., PEDERSEN, P. L., DE SOUZA, E. B. & SNYDER, S. H. 1986. The peripheral-type benzodiazepine receptor. Localization to the mitochondrial outer membrane. *J Biol Chem,* 261**,** 576-83.

ASLANIDIS, A., KARLSTETTER, M., SCHOLZ, R., FAUSER, S., NEUMANN, H., FRIED, C., PIETSCH, M. & LANGMANN, T. 2015. Activated microglia/macrophage whey acidic protein (AMWAP) inhibits NFkappaB signaling and induces a neuroprotective phenotype in microglia. *J Neuroinflammation,* 12**,** 77.

BADER, M. F., TAUPENOT, L., ULRICH, G., AUNIS, D. & CIESIELSKI-TRESKA, J. 1994. Bacterial endotoxin induces [Ca2+]i transients and changes the organization of actin in microglia. *Glia,* 11**,** 336-44.

BAINES, C. P., KAISER, R. A., SHEIKO, T., CRAIGEN, W. J. & MOLKENTIN, J. D. 2007. Voltage-dependent anion channels are dispensable for mitochondrial-dependent cell death. *Nat Cell Biol,* 9**,** 550-5.

BALASHOV, N. A. & BERNSTEIN, P. S. 1998. Purification and identification of the components of the human macular carotenoid metabolism pathways. . *Invest Ophthal Vis Sci.,* 39**,** 38.

BANATI, R. B., MIDDLETON, R. J., CHAN, R., HATTY, C. R., KAM, W. W., QUIN, C., GRAEBER, M. B., PARMAR, A., ZAHRA, D., CALLAGHAN, P., FOK, S., HOWELL, N. R., GREGOIRE, M., SZABO, A., PHAM, T., DAVIS, E. & LIU, G. J. 2014. Positron emission tomography and functional characterization of a complete PBR/TSPO knockout. *Nat Commun,* 5**,** 5452.

BANATI, R. B., NEWCOMBE, J., GUNN, R. N., CAGNIN, A., TURKHEIMER, F., HEPPNER, F., PRICE, G., WEGNER, F., GIOVANNONI, G., MILLER, D. H., PERKIN, G. D., SMITH, T., HEWSON, A. K., BYDDER, G., KREUTZBERG, G. W., JONES, T., CUZNER, M. L. & MYERS, R. 2000. The peripheral benzodiazepine binding site in the brain in multiple sclerosis: quantitative in vivo imaging of microglia as a measure of disease activity. *Brain,* 123 (Pt 11)**,** 2321-37.

BARRON, A. M., GARCIA-SEGURA, L. M., CARUSO, D., JAYARAMAN, A., LEE, J. W., MELCANGI, R. C. & PIKE, C. J. 2013. Ligand for translocator protein reverses pathology in a mouse model of Alzheimer's disease. *J Neurosci,* 33**,** 8891-7.

BATARSEH, A., LI, J. & PAPADOPOULOS, V. 2010. Protein kinase C epsilon regulation of translocator protein (18 kDa) Tspo gene expression is mediated through a MAPK pathway targeting STAT3 and c-Jun transcription factors. *Biochemistry,* 49**,** 4766-78.

BATARSEH, A. & PAPADOPOULOS, V. 2010. Regulation of translocator protein 18 kDa (TSPO) expression in health and disease states. *Mol Cell Endocrinol,* 327**,** 1-12.

BATOKO, H., JURKIEWICZ, P. & VELJANOVSKI, V. 2015a. Translocator proteins, porphyrins and abiotic stress: new light? *Trends Plant Sci,* 20**,** 261-3.

BATOKO, H., VELJANOVSKI, V. & JURKIEWICZ, P. 2015b. Enigmatic Translocator protein (TSPO) and cellular stress regulation. *Trends Biochem Sci,* 40**,** 497-503.

BERGER, W., KLOECKENER-GRUISSEM, B. & NEIDHARDT, J. 2010. The molecular basis of human retinal and vitreoretinal diseases. *Prog Retin Eye Res,* 29**,** 335-75.

BESSIS, A., BECHADE, C., BERNARD, D. & ROUMIER, A. 2007. Microglial control of neuronal death and synaptic properties. *Glia,* 55**,** 233-8.

BISCARO, B., LINDVALL, O., TESCO, G., EKDAHL, C. T. & NITSCH, R. M. 2012. Inhibition of microglial activation protects hippocampal neurogenesis and improves cognitive deficits in a transgenic mouse model for Alzheimer's disease. *Neurodegener Dis,* 9**,** 187-98.

BOMMAS-EBERT, U., TEUBNER, P. & VOß, R. 2006. *Kurzlehrbuch Anatomie und Embryologie*, Thieme.
BORDET, T., BUISSON, B., MICHAUD, M., DROUOT, C., GALEA, P., DELAAGE, P., AKENTIEVA, N. P., EVERS, A. S., COVEY, D. F., OSTUNI, M. A., LACAPERE, J. J., MASSAAD, C., SCHUMACHER, M., STEIDL, E. M., MAUX, D., DELAAGE, M., HENDERSON, C. E. & PRUSS, R. M. 2007. Identification and characterization of cholest-4-en-3-one, oxime (TRO19622), a novel drug candidate for amyotrophic lateral sclerosis. *J Pharmacol Exp Ther,* 322**,** 709-20.
BOSCO, A., INMAN, D. M., STEELE, M. R., WU, G., SOTO, I., MARSH-ARMSTRONG, N., HUBBARD, W. C., CALKINS, D. J., HORNER, P. J. & VETTER, M. L. 2008. Reduced retina microglial activation and improved optic nerve integrity with minocycline treatment in the DBA/2J mouse model of glaucoma. *Invest Ophthalmol Vis Sci,* 49**,** 1437-46.
BOWMAKER, J. K. & DARTNALL, H. J. 1980. Visual pigments of rods and cones in a human retina. *J Physiol,* 298**,** 501-11.
BRINGMANN, A., PANNICKE, T., GROSCHE, J., FRANCKE, M., WIEDEMANN, P., SKATCHKOV, S. N., OSBORNE, N. N. & REICHENBACH, A. 2006. Muller cells in the healthy and diseased retina. *Prog Retin Eye Res,* 25**,** 397-424.
BROWN, G. C. & NEHER, J. J. 2012. Eaten alive! Cell death by primary phagocytosis: 'phagoptosis'. *Trends Biochem Sci,* 37**,** 325-32.
BROWN, G. C. & NEHER, J. J. 2014. Microglial phagocytosis of live neurons. *Nat Rev Neurosci,* 15**,** 209-16.
BRUNDULA, V., REWCASTLE, N. B., METZ, L. M., BERNARD, C. C. & YONG, V. W. 2002. Targeting leukocyte MMPs and transmigration: minocycline as a potential therapy for multiple sclerosis. *Brain,* 125**,** 1297-308.
CAGNIN, A., ROSSOR, M., SAMPSON, E. L., MACKINNON, T. & BANATI, R. B. 2004. In vivo detection of microglial activation in frontotemporal dementia. *Ann Neurol,* 56**,** 894-7.
CAMPBELL, M. & HUMPHRIES, P. 2012. The blood-retina barrier: tight junctions and barrier modulation. *Adv Exp Med Biol,* 763**,** 70-84.
CARDONA, A. E., PIORO, E. P., SASSE, M. E., KOSTENKO, V., CARDONA, S. M., DIJKSTRA, I. M., HUANG, D., KIDD, G., DOMBROWSKI, S., DUTTA, R., LEE, J. C., COOK, D. N., JUNG, S., LIRA, S. A., LITTMAN, D. R. & RANSOHOFF, R. M. 2006. Control of microglial neurotoxicity by the fractalkine receptor. *Nat Neurosci,* 9**,** 917-24.
CARDOSO, A. L., GUEDES, J. R. & DE LIMA, M. C. 2016. Role of microRNAs in the regulation of innate immune cells under neuroinflammatory conditions. *Curr Opin Pharmacol,* 26**,** 1-9.
CARSON, M. J., DOOSE, J. M., MELCHIOR, B., SCHMID, C. D. & PLOIX, C. C. 2006. CNS immune privilege: hiding in plain sight. *Immunol Rev,* 213**,** 48-65.
CASELLAS, P., GALIEGUE, S. & BASILE, A. S. 2002. Peripheral benzodiazepine receptors and mitochondrial function. *Neurochem Int,* 40**,** 475-86.
CHAO, C. C., HU, S., MOLITOR, T. W., SHASKAN, E. G. & PETERSON, P. K. 1992. Activated microglia mediate neuronal cell injury via a nitric oxide mechanism. *J Immunol,* 149**,** 2736-41.
CHAUVEAU, F., BOUTIN, H., VAN CAMP, N., DOLLE, F. & TAVITIAN, B. 2008. Nuclear imaging of neuroinflammation: a comprehensive review of [11C]PK11195 challengers. *Eur J Nucl Med Mol Imaging,* 35**,** 2304-19.
CHEN, M., ONA, V. O., LI, M., FERRANTE, R. J., FINK, K. B., ZHU, S., BIAN, J., GUO, L., FARRELL, L. A., HERSCH, S. M., HOBBS, W., VONSATTEL, J. P., CHA, J. H. & FRIEDLANDER, R. M. 2000. Minocycline inhibits caspase-1 and caspase-3 expression and delays mortality in a transgenic mouse model of Huntington disease. *Nat Med,* 6**,** 797-801.
CHEN, M. & XU, H. 2015. Parainflammation, chronic inflammation, and age-related macular degeneration. *J Leukoc Biol*.
CHEN, M. K. & GUILARTE, T. R. 2008. Translocator protein 18 kDa (TSPO): molecular sensor of brain injury and repair. *Pharmacol Ther,* 118**,** 1-17.

CHITNIS, T., IMITOLA, J., WANG, Y., ELYAMAN, W., CHAWLA, P., SHARUK, M., RADDASSI, K., BRONSON, R. T. & KHOURY, S. J. 2007. Elevated neuronal expression of CD200 protects Wlds mice from inflammation-mediated neurodegeneration. *Am J Pathol,* 170**,** 1695-712.

CHOI, H. B., KHOO, C., RYU, J. K., VAN BREEMEN, E., KIM, S. U. & MCLARNON, J. G. 2002. Inhibition of lipopolysaccharide-induced cyclooxygenase-2, tumor necrosis factor-alpha and [Ca2+]i responses in human microglia by the peripheral benzodiazepine receptor ligand PK11195. *J Neurochem,* 83**,** 546-55.

COLEMAN, H. R., CHAN, C.-C., FERRIS, F. L. & CHEW, E. Y. 2008. Age-related macular degeneration. *The Lancet,* 372**,** 1835-1845.

COOK, D. N., CHEN, S. C., SULLIVAN, L. M., MANFRA, D. J., WIEKOWSKI, M. T., PROSSER, D. M., VASSILEVA, G. & LIRA, S. A. 2001. Generation and analysis of mice lacking the chemokine fractalkine. *Mol Cell Biol,* 21**,** 3159-65.

COOKE BAILEY, J. N., SOBRIN, L., PERICAK-VANCE, M. A., HAINES, J. L., HAMMOND, C. J. & WIGGS, J. L. 2013. Advances in the genomics of common eye diseases. *Hum Mol Genet,* 22**,** R59-65.

CORSI, L., GEMINIANI, E. & BARALDI, M. 2008. Peripheral benzodiazepine receptor (PBR) new insight in cell proliferation and cell differentiation review. *Curr Clin Pharmacol,* 3**,** 38-45.

COSTA, E. & GUIDOTTI, A. 1991. Diazepam binding inhibitor (DBI): a peptide with multiple biological actions. *Life Sci,* 49**,** 325-44.

CRUICKSHANKS, K. J., KLEIN, R. & KLEIN, B. E. 1993. Sunlight and age-related macular degeneration. The Beaver Dam Eye Study. *Arch Ophthalmol,* 111**,** 514-8.

CUKRAS, C. A., PETROU, P., CHEW, E. Y., MEYERLE, C. B. & WONG, W. T. 2012. Oral minocycline for the treatment of diabetic macular edema (DME): results of a phase I/II clinical study. *Invest Ophthalmol Vis Sci,* 53**,** 3865-74.

DAMANI, M. R., ZHAO, L., FONTAINHAS, A. M., AMARAL, J., FARISS, R. N. & WONG, W. T. 2011. Age-related alterations in the dynamic behavior of microglia. *Aging Cell,* 10**,** 263-76.

DAUGHERTY, D. J., SELVARAJ, V., CHECHNEVA, O. V., LIU, X. B., PLEASURE, D. E. & DENG, W. 2013. A TSPO ligand is protective in a mouse model of multiple sclerosis. *EMBO Mol Med,* 5**,** 891-903.

DECAUDIN, D., CASTEDO, M., NEMATI, F., BEURDELEY-THOMAS, A., DE PINIEUX, G., CARON, A., POUILLART, P., WIJDENES, J., ROUILLARD, D., KROEMER, G. & POUPON, M. F. 2002. Peripheral benzodiazepine receptor ligands reverse apoptosis resistance of cancer cells in vitro and in vivo. *Cancer Res,* 62**,** 1388-93.

DICK, A. D. 2003. Control of myeloid activity during retinal inflammation. *Journal of Leukocyte Biology,* 74**,** 161-166.

DIRSCHERL, K., KARLSTETTER, M., EBERT, S., KRAUS, D., HLAWATSCH, J., WALCZAK, Y., MOEHLE, C., FUCHSHOFER, R. & LANGMANN, T. 2010. Luteolin triggers global changes in the microglial transcriptome leading to a unique anti-inflammatory and neuroprotective phenotype. *J Neuroinflammation,* 7**,** 3.

DJEBAILI, M., GUO, Q., PETTUS, E. H., HOFFMAN, S. W. & STEIN, D. G. 2005. The neurosteroids progesterone and allopregnanolone reduce cell death, gliosis, and functional deficits after traumatic brain injury in rats. *J Neurotrauma,* 22**,** 106-18.

DJEBAILI, M., HOFFMAN, S. W. & STEIN, D. G. 2004. Allopregnanolone and progesterone decrease cell death and cognitive deficits after a contusion of the rat pre-frontal cortex. *Neuroscience,* 123**,** 349-59.

DOMERCQ, M. & MATUTE, C. 2004. Neuroprotection by tetracyclines. *Trends Pharmacol Sci,* 25**,** 609-12.

DU, Y., MA, Z., LIN, S., DODEL, R. C., GAO, F., BALES, K. R., TRIARHOU, L. C., CHERNET, E., PERRY, K. W., NELSON, D. L., LUECKE, S., PHEBUS, L. A., BYMASTER, F. P. & PAUL, S. M. 2001. Minocycline prevents nigrostriatal dopaminergic neurodegeneration in the MPTP model of Parkinson's disease. *Proc Natl Acad Sci U S A,* 98**,** 14669-74.

EBERT, S., WEIGELT, K., WALCZAK, Y., DROBNIK, W., MAUERER, R., HUME, D. A., WEBER, B. H. & LANGMANN, T. 2009. Docosahexaenoic acid attenuates microglial activation and delays early retinal degeneration. *J Neurochem,* 110**,** 1863-75.

EDISON, P., ARCHER, H. A., GERHARD, A., HINZ, R., PAVESE, N., TURKHEIMER, F. E., HAMMERS, A., TAI, Y. F., FOX, N., KENNEDY, A., ROSSOR, M. & BROOKS, D. J. 2008. Microglia, amyloid, and cognition in Alzheimer's disease: An [11C](R)PK11195-PET and [11C]PIB-PET study. *Neurobiol Dis,* 32**,** 412-9.

FERRARI, S., DI IORIO, E., BARBARO, V., PONZIN, D., SORRENTINO, F. S. & PARMEGGIANI, F. 2011. Retinitis pigmentosa: genes and disease mechanisms. *Curr Genomics,* 12**,** 238-49.

FLANARY, B. E., SAMMONS, N. W., NGUYEN, C., WALKER, D. & STREIT, W. J. 2007. Evidence that aging and amyloid promote microglial cell senescence. *Rejuvenation Res,* 10**,** 61-74.

FRADE, J. M. & BARDE, Y. A. 1998. Nerve growth factor: two receptors, multiple functions. *Bioessays,* 20**,** 137-45.

FUHRMANN, M., BITTNER, T., JUNG, C. K., BURGOLD, S., PAGE, R. M., MITTEREGGER, G., HAASS, C., LAFERLA, F. M., KRETZSCHMAR, H. & HERMS, J. 2010. Microglial Cx3cr1 knockout prevents neuron loss in a mouse model of Alzheimer's disease. *Nat Neurosci,* 13**,** 411-3.

FUJITA, M., IMAIZUMI, M., ZOGHBI, S. S., FUJIMURA, Y., FARRIS, A. G., SUHARA, T., HONG, J., PIKE, V. W. & INNIS, R. B. 2008. Kinetic analysis in healthy humans of a novel positron emission tomography radioligand to image the peripheral benzodiazepine receptor, a potential biomarker for inflammation. *Neuroimage,* 40**,** 43-52.

GARNIER, M., DIMCHEV, A. B., BOUJRAD, N., PRICE, J. M., MUSTO, N. A. & PAPADOPOULOS, V. 1994. In vitro reconstitution of a functional peripheral-type benzodiazepine receptor from mouse Leydig tumor cells. *Mol Pharmacol,* 45**,** 201-11.

GARRIDO-MESA, N., ZARZUELO, A. & GALVEZ, J. 2013. Minocycline: far beyond an antibiotic. *Br J Pharmacol,* 169**,** 337-52.

GAVISH, M., BACHMAN, I., SHOUKRUN, R., KATZ, Y., VEENMAN, L., WEISINGER, G. & WEIZMAN, A. 1999. Enigma of the Peripheral Benzodiazepine Receptor. *PHARMACOLOGICAL REVIEWS,* 51**,** 630-646.

GEHRIG, A., LANGMANN, T., HORLING, F., JANSSEN, A., BONIN, M., WALTER, M., POTHS, S. & WEBER, B. H. 2007. Genome-wide expression profiling of the retinoschisin-deficient retina in early postnatal mouse development. *Invest Ophthalmol Vis Sci,* 48**,** 891-900.

GERHARD, A., PAVESE, N., HOTTON, G., TURKHEIMER, F., ES, M., HAMMERS, A., EGGERT, K., OERTEL, W., BANATI, R. B. & BROOKS, D. J. 2006. In vivo imaging of microglial activation with [11C](R)-PK11195 PET in idiopathic Parkinson's disease. *Neurobiol Dis,* 21**,** 404-12.

GERHARD, A., SCHWARZ, J., MYERS, R., WISE, R. & BANATI, R. B. 2005. Evolution of microglial activation in patients after ischemic stroke: a [11C](R)-PK11195 PET study. *Neuroimage,* 24**,** 591-5.

GIATTI, S., PESARESI, M., CAVALETTI, G., BIANCHI, R., CAROZZI, V., LOMBARDI, R., MASCHI, O., LAURIA, G., GARCIA-SEGURA, L. M., CARUSO, D. & MELCANGI, R. C. 2009. Neuroprotective effects of a ligand of translocator protein-18 kDa (Ro5-4864) in experimental diabetic neuropathy. *Neuroscience,* 164**,** 520-9.

GINHOUX, F., GRETER, M., LEBOEUF, M., NANDI, S., SEE, P., GOKHAN, S., MEHLER, M. F., CONWAY, S. J., NG, L. G., STANLEY, E. R., SAMOKHVALOV, I. M. & MERAD, M. 2010. Fate mapping analysis reveals that adult microglia derive from primitive macrophages. *Science,* 330**,** 841-5.

GIRARD, C., LIU, S., ADAMS, D., LACROIX, C., SINEUS, M., BOUCHER, C., PAPADOPOULOS, V., RUPPRECHT, R., SCHUMACHER, M. & GROYER, G. 2012. Axonal regeneration and neuroinflammation: roles for the translocator protein 18 kDa. *J Neuroendocrinol,* 24**,** 71-81.

GIRARD, C., LIU, S., CADEPOND, F., ADAMS, D., LACROIX, C., VERLEYE, M., GILLARDIN, J. M., BAULIEU, E. E., SCHUMACHER, M. & SCHWEIZER-GROYER, G. 2008. Etifoxine improves peripheral nerve regeneration and functional recovery. *Proc Natl Acad Sci U S A,* 105**,** 20505-10.

GIULIAN, D. 1999. Microglia and the immune pathology of Alzheimer disease. *Am J Hum Genet,* 65**,** 13-8.

GRIMM, C. & REME, C. E. 2013. Light damage as a model of retinal degeneration. *Methods Mol Biol,* 935**,** 87-97.

GRIMM, C., WENZEL, A., HAFEZI, F., YU, S., REDMOND, T. M. & REME, C. E. 2000. Protection of Rpe65-deficient mice identifies rhodopsin as a mediator of light-induced retinal degeneration. *Nat Genet,* 25**,** 63-6.

GRIMM, C., WENZEL, A., WILLIAMS, T., ROL, P., HAFEZI, F. & REME, C. 2001. Rhodopsin-mediated blue-light damage to the rat retina: effect of photoreversal of bleaching. *Invest Ophthalmol Vis Sci,* 42**,** 497-505.

GUPTA, N., BROWN, K. E. & MILAM, A. H. 2003. Activated microglia in human retinitis pigmentosa, late-onset retinal degeneration, and age-related macular degeneration. *Experimental Eye Research,* 76**,** 463-471.

HANISCH, U. K. & KETTENMANN, H. 2007. Microglia: active sensor and versatile effector cells in the normal and pathologic brain. *Nat Neurosci,* 10**,** 1387-94.

HARADA, T., HARADA, C., KOHSAKA, S., WADA, E., YOSHIDA, K., OHNO, S., MAMADA, H., TANAKA, K., PARADA, L. F. & WADA, K. 2002. Microglia-Muller glia cell interactions control neurotrophic factor production during light-induced retinal degeneration. *J Neurosci,* 22**,** 9228-36.

HARDWICK, M., FERTIKH, D., CULTY, M., LI, H., VIDIC, B. & PAPADOPOULOS, V. 1999. Peripheral-type benzodiazepine receptor (PBR) in human breast cancer: correlation of breast cancer cell aggressive phenotype with PBR expression, nuclear localization, and PBR-mediated cell proliferation and nuclear transport of cholesterol. *Cancer Res,* 59**,** 831-42.

HAUET, T., YAO, Z. X., BOSE, H. S., WALL, C. T., HAN, Z., LI, W., HALES, D. B., MILLER, W. L., CULTY, M. & PAPADOPOULOS, V. 2005. Peripheral-type benzodiazepine receptor-mediated action of steroidogenic acute regulatory protein on cholesterol entry into leydig cell mitochondria. *Mol Endocrinol,* 19**,** 540-54.

HE, Y., GE, J., BURKE, J. M., MYERS, R. L., DONG, Z. Z. & TOMBRAN-TINK, J. 2010. Mitochondria impairment correlates with increased sensitivity of aging RPE cells to oxidative stress. *J Ocul Biol Dis Infor,* 3**,** 92-108.

HENRY, C. J., HUANG, Y., WYNNE, A., HANKE, M., HIMLER, J., BAILEY, M. T., SHERIDAN, J. F. & GODBOUT, J. P. 2008. Minocycline attenuates lipopolysaccharide (LPS)-induced neuroinflammation, sickness behavior, and anhedonia. *J Neuroinflammation,* 5**,** 15.

HIRSCH, J. D., BEYER, C. F., MALKOWITZ, L., BEER, B. & BLUME, A. J. 1989. Mitochondrial benzodiazepine receptors mediate inhibition of mitochondrial respiratory control. *Mol Pharmacol,* 35**,** 157-63.

HOEK, R. M., RUULS, S. R., MURPHY, C. A., WRIGHT, G. J., GODDARD, R., ZURAWSKI, S. M., BLOM, B., HOMOLA, M. E., STREIT, W. J., BROWN, M. H., BARCLAY, A. N. & SEDGWICK, J. D. 2000. Down-regulation of the macrophage lineage through interaction with OX2 (CD200). *Science,* 290**,** 1768-71.

HOEY, S., GRABOWSKI, P. S., RALSTON, S. H., FORRESTER, J. V. & LIVERSIDGE, J. 1997. Nitric oxide accelerates the onset and increases the severity of experimental autoimmune uveoretinitis through an IFN-gamma-dependent mechanism. *J Immunol,* 159**,** 5132-42.

HUA, X. Y., SVENSSON, C. I., MATSUI, T., FITZSIMMONS, B., YAKSH, T. L. & WEBB, M. 2005. Intrathecal minocycline attenuates peripheral inflammation-induced hyperalgesia by inhibiting p38 MAPK in spinal microglia. *Eur J Neurosci,* 22**,** 2431-40.

HUGHES, E. H., SCHLICHTENBREDE, F. C., MURPHY, C. C., BRODERICK, C., VAN ROOIJEN, N., ALI, R. R. & DICK, A. D. 2004. Minocycline delays photoreceptor death

in the rds mouse through a microglia-independent mechanism. *Exp Eye Res,* 78**,** 1077-84.
HUME, D. A., PERRY, V. H. & GORDON, S. 1983. Immunohistochemical localization of a macrophage-specific antigen in developing mouse retina: phagocytosis of dying neurons and differentiation of microglial cells to form a regular array in the plexiform layers. *J Cell Biol,* 97**,** 253-7.
ITO, D., IMAI, Y., OHSAWA, K., NAKAJIMA, K., FUKUUCHI, Y. & KOHSAKA, S. 1998. Microglia-specific localisation of a novel calcium binding protein, Iba1. *Brain Res Mol Brain Res,* 57**,** 1-9.
JAGER, R. D., MIELER, W. F. & MILLER, J. W. 2008. Age-related macular degeneration. *N Engl J Med,* 358**,** 2606-17.
JAREMKO, L., JAREMKO, M., GILLER, K., BECKER, S. & ZWECKSTETTER, M. 2014. Structure of the mitochondrial translocator protein in complex with a diagnostic ligand. *Science,* 343**,** 1363-6.
JAYAKUMAR, A. R., PANICKAR, K. S. & NORENBERG, M. D. 2002. Effects on free radical generation by ligands of the peripheral benzodiazepine receptor in cultured neural cells. *J Neurochem,* 83**,** 1226-34.
JOLY, S., FRANCKE, M., ULBRICHT, E., BECK, S., SEELIGER, M., HIRRLINGER, P., HIRRLINGER, J., LANG, K. S., ZINKERNAGEL, M., ODERMATT, B., SAMARDZIJA, M., REICHENBACH, A., GRIMM, C. & REME, C. E. 2009. Cooperative phagocytes: resident microglia and bone marrow immigrants remove dead photoreceptors in retinal lesions. *Am J Pathol,* 174**,** 2310-23.
JOSEPH-LIAUZUN, E., DELMAS, P., SHIRE, D. & FERRARA, P. 1998. Topological analysis of the peripheral benzodiazepine receptor in yeast mitochondrial membranes supports a five-transmembrane structure. *J Biol Chem,* 273**,** 2146-52.
KARCHEWSKI, L. A., BLOECHLINGER, S. & WOOLF, C. J. 2004. Axonal injury-dependent induction of the peripheral benzodiazepine receptor in small-diameter adult rat primary sensory neurons. *Eur J Neurosci,* 20**,** 671-83.
KARLSTETTER, M., EBERT, S. & LANGMANN, T. 2010a. Microglia in the healthy and degenerating retina: insights from novel mouse models. *Immunobiology,* 215**,** 685-91.
KARLSTETTER, M. & LANGMANN, T. 2014. Microglia in the aging retina. *Adv Exp Med Biol,* 801**,** 207-12.
KARLSTETTER, M., LIPPE, E., WALCZAK, Y., MOEHLE, C., ASLANIDIS, A., MIRZA, M. & LANGMANN, T. 2011. Curcumin is a potent modulator of microglial gene expression and migration. *J Neuroinflammation,* 8**,** 125.
KARLSTETTER, M., NOTHDURFTER, C., ASLANIDIS, A., MOELLER, K., HORN, F., SCHOLZ, R., NEUMANN, H., RUPPRECHT, R. & LANGMANN, T. 2014. Translocator protein (18 kDa) (TSPO) is expressed in reactive retinal microglia and modulates microglial inflammation and phagocytosis. *The Journal of Neuroinflammation,* 11.
KARLSTETTER, M., SCHOLZ, R., RUTAR, M., WONG, W. T., PROVIS, J. M. & LANGMANN, T. 2015. Retinal microglia: just bystander or target for therapy? *Prog Retin Eye Res,* 45**,** 30-57.
KARLSTETTER, M., WALCZAK, Y., WEIGELT, K., EBERT, S., VAN DEN BRULLE, J., SCHWER, H., FUCHSHOFER, R. & LANGMANN, T. 2010b. The novel activated microglia/macrophage WAP domain protein, AMWAP, acts as a counter-regulator of proinflammatory response. *J Immunol,* 185**,** 3379-90.
KARPERIEN, A., AHAMMER, H. & JELINEK, H. F. 2013. Quantitating the subtleties of microglial morphology with fractal analysis. *Front Cell Neurosci,* 7**,** 3.
KASPER, L. H. & REDER, A. T. 2014. Immunomodulatory activity of interferon-beta. *Ann Clin Transl Neurol,* 1**,** 622-31.
KETTENMANN, H., HANISCH, U. K., NODA, M. & VERKHRATSKY, A. 2011. Physiology of microglia. *Physiol Rev,* 91**,** 461-553.
KEZIC, J. & MCMENAMIN, P. G. 2008. Differential turnover rates of monocyte-derived cells in varied ocular tissue microenvironments. *J Leukoc Biol,* 84**,** 721-9.

KIERDORF, K., ERNY, D., GOLDMANN, T., SANDER, V., SCHULZ, C., PERDIGUERO, E. G., WIEGHOFER, P., HEINRICH, A., RIEMKE, P., HOLSCHER, C., MULLER, D. N., LUCKOW, B., BROCKER, T., DEBOWSKI, K., FRITZ, G., OPDENAKKER, G., DIEFENBACH, A., BIBER, K., HEIKENWALDER, M., GEISSMANN, F., ROSENBAUER, F. & PRINZ, M. 2013a. Microglia emerge from erythromyeloid precursors via Pu.1- and Irf8-dependent pathways. *Nat Neurosci,* 16**,** 273-80.

KIERDORF, K., KATZMARSKI, N., HAAS, C. A. & PRINZ, M. 2013b. Bone marrow cell recruitment to the brain in the absence of irradiation or parabiosis bias. *PLoS One,* 8**,** e58544.

KIM, H. S. & SUH, Y. H. 2009. Minocycline and neurodegenerative diseases. *Behav Brain Res,* 196**,** 168-79.

KIMBREL, E. A. & LANZA, R. 2015. Current status of pluripotent stem cells: moving the first therapies to the clinic. *Nat Rev Drug Discov,* 14**,** 681-92.

KOISTINAHO, M., MALM, T. M., KETTUNEN, M. I., GOLDSTEINS, G., STARCKX, S., KAUPPINEN, R. A., OPDENAKKER, G. & KOISTINAHO, J. 2005. Minocycline protects against permanent cerebral ischemia in wild type but not in matrix metalloprotease-9-deficient mice. *J Cereb Blood Flow Metab,* 25**,** 460-7.

KOKOSZKA, J. E., WAYMIRE, K. G., LEVY, S. E., SLIGH, J. E., CAI, J., JONES, D. P., MACGREGOR, G. R. & WALLACE, D. C. 2004. The ADP/ATP translocator is not essential for the mitochondrial permeability transition pore. *Nature,* 427**,** 461-5.

KOLB, H. 2005. Gross Anatomy of the Eye.

KRADY, J. K., BASU, A., ALLEN, C. M., XU, Y., LANOUE, K. F., GARDNER, T. W. & LEVISON, S. W. 2005. Minocycline reduces proinflammatory cytokine expression, microglial activation, and caspase-3 activation in a rodent model of diabetic retinopathy. *Diabetes,* 54**,** 1559-65.

KRAUS, R. L., PASIECZNY, R., LARIOSA-WILLINGHAM, K., TURNER, M. S., JIANG, A. & TRAUGER, J. W. 2005. Antioxidant properties of minocycline: neuroprotection in an oxidative stress assay and direct radical-scavenging activity. *J Neurochem,* 94**,** 819-27.

KUHLMANN, A. C. & GUILARTE, T. R. 2000. Cellular and subcellular localization of peripheral benzodiazepine receptors after trimethyltin neurotoxicity. *J Neurochem,* 74**,** 1694-704.

LACAPERE, J. J. & PAPADOPOULOS, V. 2003. Peripheral-type benzodiazepine receptor: structure and function of a cholesterol-binding protein in steroid and bile acid biosynthesis. *Steroids,* 68**,** 569-85.

LACOR, P., GANDOLFO, P., TONON, M. C., BRAULT, E., DALIBERT, I., SCHUMACHER, M., BENAVIDES, J. & FERZAZ, B. 1999. Regulation of the expression of peripheral benzodiazepine receptors and their endogenous ligands during rat sciatic nerve degeneration and regeneration: a role for PBR in neurosteroidogenesis. *Brain Res,* 815**,** 70-80.

LAMB, T. D., COLLIN, S. P. & PUGH, E. N., JR. 2007. Evolution of the vertebrate eye: opsins, photoreceptors, retina and eye cup. *Nat Rev Neurosci,* 8**,** 960-76.

LANGMANN, T. 2007. Microglia activation in retinal degeneration. *J Leukoc Biol,* 81**,** 1345-51.

LAVISSE, S., GUILLERMIER, M., HERARD, A. S., PETIT, F., DELAHAYE, M., VAN CAMP, N., BEN HAIM, L., LEBON, V., REMY, P., DOLLE, F., DELZESCAUX, T., BONVENTO, G., HANTRAYE, P. & ESCARTIN, C. 2012. Reactive astrocytes overexpress TSPO and are detected by TSPO positron emission tomography imaging. *J Neurosci,* 32**,** 10809-18.

LEE, J. E., LIANG, K. J., FARISS, R. N. & WONG, W. T. 2008. Ex vivo dynamic imaging of retinal microglia using time-lapse confocal microscopy. *Invest Ophthalmol Vis Sci,* 49**,** 4169-76.

LI, H., YAO, Z., DEGENHARDT, B., TEPER, G. & PAPADOPOULOS, V. 2001. Cholesterol binding at the cholesterol recognition/ interaction amino acid consensus (CRAC) of the peripheral-type benzodiazepine receptor and inhibition of steroidogenesis by an HIV TAT-CRAC peptide. *Proc Natl Acad Sci U S A,* 98**,** 1267-72.

LI, Y. Q., CHEN, P., JAIN, V., REILLY, R. M. & WONG, C. S. 2004. Early radiation-induced endothelial cell loss and blood-spinal cord barrier breakdown in the rat spinal cord. *Radiat Res,* 161**,** 143-52.

LINNARTZ, B. & NEUMANN, H. 2013. Microglial activatory (immunoreceptor tyrosine-based activation motif)- and inhibitory (immunoreceptor tyrosine-based inhibition motif)-signaling receptors for recognition of the neuronal glycocalyx. *Glia,* 61**,** 37-46.

LÜCKOFF, A., CARAMOY, A., SCHOLZ, R., PRINZ, M., KALINKE, U. & LANGMANN, T. 2016. Interferon-beta signaling in retinal mononuclear phagocytes attenuates pathological neovascularization. *EMBO Mol Med*.

MA, W., ZHAO, L., FONTAINHAS, A. M., FARISS, R. N. & WONG, W. T. 2009. Microglia in the mouse retina alter the structure and function of retinal pigmented epithelial cells: a potential cellular interaction relevant to AMD. *PLoS One,* 4**,** e7945.

MAEDA, J., HIGUCHI, M., INAJI, M., JI, B., HANEDA, E., OKAUCHI, T., ZHANG, M. R., SUZUKI, K. & SUHARA, T. 2007. Phase-dependent roles of reactive microglia and astrocytes in nervous system injury as delineated by imaging of peripheral benzodiazepine receptor. *Brain Res,* 1157**,** 100-11.

MASUDA, T. & PRINZ, M. 2016. Microglia: A Unique Versatile Cell in the Central Nervous System. *ACS Chem Neurosci*.

MATSUI, T., SVENSSON, C. I., HIRATA, Y., MIZOBATA, K., HUA, X. Y. & YAKSH, T. L. 2010. Release of prostaglandin E(2) and nitric oxide from spinal microglia is dependent on activation of p38 mitogen-activated protein kinase. *Anesth Analg,* 111**,** 554-60.

MATT, S. M. & JOHNSON, R. W. 2016. Neuro-immune dysfunction during brain aging: new insights in microglial cell regulation. *Curr Opin Pharmacol,* 26**,** 96-101.

MCENERY, M. W., SNOWMAN, A. M., TRIFILETTI, R. R. & SNYDER, S. H. 1992. Isolation of the mitochondrial benzodiazepine receptor: association with the voltage-dependent anion channel and the adenine nucleotide carrier. *Proc Natl Acad Sci U S A,* 89**,** 3170-4.

MILDNER, A., SCHMIDT, H., NITSCHE, M., MERKLER, D., HANISCH, U. K., MACK, M., HEIKENWALDER, M., BRUCK, W., PRILLER, J. & PRINZ, M. 2007. Microglia in the adult brain arise from Ly-6ChiCCR2+ monocytes only under defined host conditions. *Nat Neurosci,* 10**,** 1544-53.

MIRZA, M., VOLZ, C., KARLSTETTER, M., LANGIU, M., SOMOGYI, A., RUONALA, M. O., TAMM, E. R., JAGLE, H. & LANGMANN, T. 2013. Progressive retinal degeneration and glial activation in the CLN6 (nclf) mouse model of neuronal ceroid lipofuscinosis: a beneficial effect of DHA and curcumin supplementation. *PLoS One,* 8**,** e75963.

MIYOSHI, M., ITO, H., ARAKAWA, R., TAKAHASHI, H., TAKANO, H., HIGUCHI, M., OKUMURA, M., OTSUKA, T., KODAKA, F., SEKINE, M., SASAKI, T., FUJIE, S., SEKI, C., MAEDA, J., NAKAO, R., ZHANG, M. R., FUKUMURA, T., MATSUMOTO, M. & SUHARA, T. 2009. Quantitative analysis of peripheral benzodiazepine receptor in the human brain using PET with (11)C-AC-5216. *J Nucl Med,* 50**,** 1095-101.

MOCCHETTI, I. & SANTI, M. R. 1991. Diazepam binding inhibitor peptide: cloning and gene expression. *Neuropharmacology,* 30**,** 1365-71.

MORROW, E. M., FURUKAWA, T. & CEPKO, C. L. 1998. Vertebrate photoreceptor cell development and disease. *Trends Cell Biol,* 8**,** 353-8.

MUKHIN, A. G., PAPADOPOULOS, V., COSTA, E. & KRUEGER, K. E. 1989. Mitochondrial benzodiazepine receptors regulate steroid biosynthesis. *Proc Natl Acad Sci U S A,* 86**,** 9813-6.

NAGAYAMA, M., ZHANG, F. & IADECOLA, C. 1998. Delayed treatment with aminoguanidine decreases focal cerebral ischemic damage and enhances neurologic recovery in rats. *J Cereb Blood Flow Metab,* 18**,** 1107-13.

NAM, K. N., PARK, Y. M., JUNG, H. J., LEE, J. Y., MIN, B. D., PARK, S. U., JUNG, W. S., CHO, K. H., PARK, J. H., KANG, I., HONG, J. W. & LEE, E. H. 2010. Anti-inflammatory effects of crocin and crocetin in rat brain microglial cells. *Eur J Pharmacol,* 648**,** 110-6.

NG, T. F. & STREILEIN, J. W. 2001. Light-induced migration of retinal microglia into the subretinal space. *Invest Ophthalmol Vis Sci,* 42**,** 3301-10.
NIKODEMOVA, M., LEE, J., FABRY, Z. & DUNCAN, I. D. 2010. Minocycline attenuates experimental autoimmune encephalomyelitis in rats by reducing T cell infiltration into the spinal cord. *J Neuroimmunol,* 219**,** 33-7.
NIMMERJAHN, A., KIRCHHOFF, F. & HELMCHEN, F. 2005. Resting microglial cells are highly dynamic surveillants of brain parenchyma in vivo. *Science,* 308**,** 1314-8.
NOBLE, W., GARWOOD, C. J. & HANGER, D. P. 2009. Minocycline as a potential therapeutic agent in neurodegenerative disorders characterised by protein misfolding. *Prion* 3**,** 78-83.
ORGANISCIAK, D. T., DARROW, R. M., BARSALOU, L., KUTTY, R. K. & WIGGERT, B. 2000. Circadian-dependent retinal light damage in rats. *Invest Ophthalmol Vis Sci,* 41**,** 3694-701.
OWEN, D. R., GUNN, R. N., RABINER, E. A., BENNACEF, I., FUJITA, M., KREISL, W. C., INNIS, R. B., PIKE, V. W., REYNOLDS, R., MATTHEWS, P. M. & PARKER, C. A. 2011a. Mixed-affinity binding in humans with 18-kDa translocator protein ligands. *J Nucl Med,* 52**,** 24-32.
OWEN, D. R., LEWIS, A. J., REYNOLDS, R., RUPPRECHT, R., ESER, D., WILKINS, M. R., BENNACEF, I., NUTT, D. J. & PARKER, C. A. 2011b. Variation in binding affinity of the novel anxiolytic XBD173 for the 18 kDa translocator protein in human brain. *Synapse,* 65**,** 257-9.
OWEN, D. R. & MATTHEWS, P. M. 2011. Imaging brain microglial activation using positron emission tomography and translocator protein-specific radioligands. *Int Rev Neurobiol,* 101**,** 19-39.
OWEN, D. R., YEO, A. J., GUNN, R. N., SONG, K., WADSWORTH, G., LEWIS, A., RHODES, C., PULFORD, D. J., BENNACEF, I., PARKER, C. A., STJEAN, P. L., CARDON, L. R., MOOSER, V. E., MATTHEWS, P. M., RABINER, E. A. & RUBIO, J. P. 2012. An 18-kDa translocator protein (TSPO) polymorphism explains differences in binding affinity of the PET radioligand PBR28. *J Cereb Blood Flow Metab,* 32**,** 1-5.
OYAGBEMI, A. A., SABA, A. B. & IBRAHEEM, A. O. 2009. Curcumin: from food spice to cancer prevention. *Asian Pac J Cancer Prev,* 10**,** 963-7.
PAGLINAWAN, R., MALIPIERO, U., SCHLAPBACH, R., FREI, K., REITH, W. & FONTANA, A. 2003. TGFbeta directs gene expression of activated microglia to an anti-inflammatory phenotype strongly focusing on chemokine genes and cell migratory genes. *Glia,* 44**,** 219-31.
PALMER, M. 2004. Cholesterol and the activity of bacterial toxins. *FEMS Microbiol Lett,* 238**,** 281-9.
PAPADOPOULOS, V., AMRI, H., LI, H., BOUJRAD, N., VIDIC, B. & GARNIER, M. 1997a. Targeted disruption of the peripheral-type benzodiazepine receptor gene inhibits steroidogenesis in the R2C Leydig tumor cell line. *J Biol Chem,* 272**,** 32129-35.
PAPADOPOULOS, V., AMRI, H., BOUJRAD, N., CASCIO, C., CULTY, M., GARNIER,, M., H., M., LI, H., VIDIC, B., BROWN, A. S., REVERSA, J. L., BERNASSAU, & J. M., D., K. 1997b. Peripheral benzodiazepine receptor in cholesterol transport and steroidogenesis. . *Steroids,* 62**,** 21-28.
PAPADOPOULOS, V., BARALDI, M., GUILARTE, T. R., KNUDSEN, T. B., LACAPERE, J. J., LINDEMANN, P., NORENBERG, M. D., NUTT, D., WEIZMAN, A., ZHANG, M. R. & GAVISH, M. 2006. Translocator protein (18kDa): new nomenclature for the peripheral-type benzodiazepine receptor based on its structure and molecular function. *Trends Pharmacol Sci,* 27**,** 402-9.
PAPADOPOULOS, V., LIU, J. & CULTY, M. 2007. Is there a mitochondrial signaling complex facilitating cholesterol import? *Mol Cell Endocrinol,* 265-266**,** 59-64.
PAPADOPOULOS, V., MUKHIN, A. G., COSTA, E. & KRUEGER, K. E. 1990. The peripheral-type benzodiazepine receptor is functionally linked to Leydig cell steroidogenesis. *J Biol Chem,* 265**,** 3772-9.

PARK, C. H., CARBONI, E., WOOD, P. L. & GEE, K. W. 1996. Characterization of peripheral benzodiazepine type sites in a cultured murine BV-2 microglial cell line. *Glia,* 16**,** 65-70.
PARK, C. H., SHIN, T. K., LEE, H. Y., KIM, S. J. & LEE, W. S. 2011. Matrix metalloproteinase inhibitors attenuate neuroinflammation following focal cerebral ischemia in mice. *Korean J Physiol Pharmacol,* 15**,** 115-22.
PENG, B., XIAO, J., WANG, K., SO, K. F., TIPOE, G. L. & LIN, B. 2014. Suppression of microglial activation is neuroprotective in a mouse model of human retinitis pigmentosa. *J Neurosci,* 34**,** 8139-50.
PEREZ-CERDA, F., SANCHEZ-GOMEZ, M. V. & MATUTE, C. 2015. Pio del Rio Hortega and the discovery of the oligodendrocytes. *Front Neuroanat,* 9**,** 92.
PLANE, J. M., SHEN, Y., PLEASURE, D. E. & DENG, W. 2010. Prospects for minocycline neuroprotection. *Arch Neurol,* 67**,** 1442-8.
PONOMAREV, E. D., VEREMEYKO, T., BARTENEVA, N., KRICHEVSKY, A. M. & WEINER, H. L. 2011. MicroRNA-124 promotes microglia quiescence and suppresses EAE by deactivating macrophages via the C/EBP-alpha-PU.1 pathway. *Nat Med,* 17**,** 64-70.
RANSOHOFF, R. M. 2007. Microgliosis: the questions shape the answers. *Nat Neurosci,* 10**,** 1507-9.
RAOUL, W., AUVYNET, C., CAMELO, S., GUILLONNEAU, X., FEUMI, C., COMBADIERE, C. & SENNLAUB, F. 2010. CCL2/CCR2 and CX3CL1/CX3CR1 chemokine axes and their possible involvement in age-related macular degeneration. *J Neuroinflammation,* 7**,** 87.
RECHICHI, M., SALVETTI, A., CHELLI, B., COSTA, B., DA POZZO, E., SPINETTI, F., LENA, A., EVANGELISTA, M., RAINALDI, G., MARTINI, C., GREMIGNI, V. & ROSSI, L. 2008. TSPO over-expression increases motility, transmigration and proliferation properties of C6 rat glioma cells. *Biochim Biophys Acta,* 1782**,** 118-25.
RIO-HORTEGA, P. D. 1939. The Microglia. *The Lancet,* 233 (6036)**,** 1023-1026.
ROQUE, R. S., ROSALES, A. A., JINGJING, L., AGARWAL, N. & AL-UBAIDI, M. R. 1999. Retina-derived microglial cells induce photoreceptor cell death in vitro. *Brain Res,* 836**,** 110-9.
ROUMIER, A., BECHADE, C., PONCER, J. C., SMALLA, K. H., TOMASELLO, E., VIVIER, E., GUNDELFINGER, E. D., TRILLER, A. & BESSIS, A. 2004. Impaired synaptic function in the microglial KARAP/DAP12-deficient mouse. *J Neurosci,* 24**,** 11421-8.
RUPPRECHT, R., PAPADOPOULOS, V., RAMMES, G., BAGHAI, T. C., FAN, J., AKULA, N., GROYER, G., ADAMS, D. & SCHUMACHER, M. 2010. Translocator protein (18 kDa) (TSPO) as a therapeutic target for neurological and psychiatric disorders. *Nat Rev Drug Discov,* 9**,** 971-88.
RUPPRECHT, R., RAMMES, G., ESER, D., BAGHAI, T. C., SCHÜLE, C., NOTHDURFTER, C., TROXLER, T., GENTSCH, C., KALKMAN, H. O., CHAPERON, F., UZUNOV, V., H. MCALLISTER, K. H., BERTAINA-ANGLADE, V., DRIEU LA ROCHELLE, C., TUERCK, D., FLOESSER, A., KIESE, B., SCHUMACHER, M., LANDGRAF, R., HOLSBOER, F. & KUCHER, K. 2009. Translocator Protein (18 kD) as Target for Anxiolytics Without Benzodiazepine-Like Side Effects. *sciencexpress***,** 2.
RYU, J. K., CHOI, H. B. & MCLARNON, J. G. 2005. Peripheral benzodiazepine receptor ligand PK11195 reduces microglial activation and neuronal death in quinolinic acid-injected rat striatum. *Neurobiol Dis,* 20**,** 550-61.
SAKATA, H., NIIZUMA, K., YOSHIOKA, H., KIM, G. S., JUNG, J. E., KATSU, M., NARASIMHAN, P., MAIER, C. M., NISHIYAMA, Y. & CHAN, P. H. 2012. Minocycline-preconditioned neural stem cells enhance neuroprotection after ischemic stroke in rats. *J Neurosci,* 32**,** 3462-73.
SANCHEZ-VALLEJO, V., BENLLOCH-NAVARRO, S., LOPEZ-PEDRAJAS, R., ROMERO, F. J. & MIRANDA, M. 2015. Neuroprotective actions of progesterone in an in vivo model of retinitis pigmentosa. *Pharmacol Res,* 99**,** 276-88.
SCHAEFER, E. J., ROBINS, S. J., PATTON, G. M., SANDBERG, M. A., WEIGEL-DIFRANCO, C. A., ROSNER, B. & BERSON, E. L. 1995. Red blood cell membrane

phosphatidylethanolamine fatty acid content in various forms of retinitis pigmentosa. *J Lipid Res,* 36**,** 1427-33.
SCHAFER, D. P., LEHRMAN, E. K., KAUTZMAN, A. G., KOYAMA, R., MARDINLY, A. R., YAMASAKI, R., RANSOHOFF, R. M., GREENBERG, M. E., BARRES, B. A. & STEVENS, B. 2012. Microglia sculpt postnatal neural circuits in an activity and complement-dependent manner. *Neuron,* 74**,** 691-705.
SCHOLZ, R., CARAMOY, A., BHUCKORY, M. B., RASHID, K., CHEN, M., XU, H., GRIMM, C. & LANGMANN, T. 2015a. Targeting translocator protein (18 kDa) (TSPO) dampens pro-inflammatory microglia reactivity in the retina and protects from degeneration. *J Neuroinflammation,* 12**,** 201.
SCHOLZ, R., SOBOTKA, M., CARAMOY, A., STEMPFL, T., MOEHLE, C. & LANGMANN, T. 2015b. Minocycline counter-regulates pro-inflammatory microglia responses in the retina and protects from degeneration. *Journal of Neuroinflammation,* 12.
SCHUBERT, T., GLEISER, C., HEIDUSCHKA, P., FRANZ, C., NAGEL-WOLFRUM, K., SAHABOGLU, A., WEISSCHUH, N., ESKE, G., ROHBOCK, K., RIEGER, N., PAQUET-DURAND, F., WISSINGER, B., WOLFRUM, U., HIRT, B., SINGER, W., RUTTIGER, L., ZIMMERMANN, U. & KNIPPER, M. 2015. Deletion of myosin VI causes slow retinal optic neuropathy and age-related macular degeneration (AMD)-relevant retinal phenotype. *Cell Mol Life Sci,* 72**,** 3953-69.
SCHULZ, C., GOMEZ PERDIGUERO, E., CHORRO, L., SZABO-ROGERS, H., CAGNARD, N., KIERDORF, K., PRINZ, M., WU, B., JACOBSEN, S. E., POLLARD, J. W., FRAMPTON, J., LIU, K. J. & GEISSMANN, F. 2012. A lineage of myeloid cells independent of Myb and hematopoietic stem cells. *Science,* 336**,** 86-90.
SEDEL, F., BECHADE, C., VYAS, S. & TRILLER, A. 2004. Macrophage-derived tumor necrosis factor alpha, an early developmental signal for motoneuron death. *J Neurosci,* 24**,** 2236-46.
SEELINGER, G., MERFORT, I. & SCHEMPP, C. M. 2008. Anti-oxidant, anti-inflammatory and anti-allergic activities of luteolin. *Planta Med,* 74**,** 1667-77.
SELVARAJ, V. & STOCCO, D. M. 2015. The changing landscape in translocator protein (TSPO) function. *Trends Endocrinol Metab,* 26**,** 341-8.
SENNLAUB, F., AUVYNET, C., CALIPPE, B., LAVALETTE, S., POUPEL, L., HU, S. J., DOMINGUEZ, E., CAMELO, S., LEVY, O., GUYON, E., SAEDERUP, N., CHARO, I. F., ROOIJEN, N. V., NANDROT, E., BOURGES, J. L., BEHAR-COHEN, F., SAHEL, J. A., GUILLONNEAU, X., RAOUL, W. & COMBADIERE, C. 2013. CCR2(+) monocytes infiltrate atrophic lesions in age-related macular disease and mediate photoreceptor degeneration in experimental subretinal inflammation in Cx3cr1 deficient mice. *EMBO Mol Med,* 5**,** 1775-93.
SIERRA, A., ABIEGA, O., SHAHRAZ, A. & NEUMANN, H. 2013. Janus-faced microglia: beneficial and detrimental consequences of microglial phagocytosis. *Front Cell Neurosci,* 7**,** 6.
SINGH, M. 2005. Essential Fatty Acids, DHA and Human Brain. *Indian J Pediatr* 72**,** 239-242.
SLEPKO, N., PATRIZIO, M. & LEVI, G. 1999. Expression and translocation of protein kinase C isoforms in rat microglial and astroglial cultures. *J Neurosci Res,* 57**,** 33-8.
SOUSTIEL, J. F., ZAAROOR, M., VLODAVSKY, E., VEENMAN, L., WEIZMAN, A. & GAVISH, M. 2008. Neuroprotective effect of Ro5-4864 following brain injury. *Exp Neurol,* 214**,** 201-8.
STRAUSS, O. 2005. The retinal pigment epithelium in visual function. *Physiol Rev,* 85**,** 845-81.
SUN, C., LI, X. X., HE, X. J., ZHANG, Q. & TAO, Y. 2013. Neuroprotective effect of minocycline in a rat model of branch retinal vein occlusion. *Exp Eye Res,* 113**,** 105-16.
SUNG, C. H. & CHUANG, J. Z. 2010. The cell biology of vision. *J Cell Biol,* 190**,** 953-63.
SWAROOP, A., CHEW, E. Y., RICKMAN, C. B. & ABECASIS, G. R. 2009. Unraveling a multifactorial late-onset disease: from genetic susceptibility to disease mechanisms for age-related macular degeneration. *Annu Rev Genomics Hum Genet,* 10**,** 19-43.

TANIHARA, H., YOSHIDA, M., MATSUMOTO, M. & YOSHIMURA, N. 1993. Identification of transforming growth factor-beta expressed in cultured human retinal pigment epithelial cells. *Invest Ophthalmol Vis Sci,* 34**,** 413-9.

TEIGE, I., TRESCHOW, A., TEIGE, A., MATTSSON, R., NAVIKAS, V., LEANDERSON, T., HOLMDAHL, R. & ISSAZADEH-NAVIKAS, S. 2003. IFN-beta gene deletion leads to augmented and chronic demyelinating experimental autoimmune encephalomyelitis. *J Immunol,* 170**,** 4776-84.

TERLUK, M. R., KAPPHAHN, R. J., SOUKUP, L. M., GONG, H., GALLARDO, C., MONTEZUMA, S. R. & FERRINGTON, D. A. 2015. Investigating mitochondria as a target for treating age-related macular degeneration. *J Neurosci,* 35**,** 7304-11.

TRAVIS, G. H., GOLCZAK, M., MOISE, A. R. & PALCZEWSKI, K. 2007. Diseases caused by defects in the visual cycle: retinoids as potential therapeutic agents. *Annu Rev Pharmacol Toxicol,* 47**,** 469-512.

THE EYE DISEASES PREVALANCE RESEARCH GROUP 2004 Causes and Prevalence of Visual Impairment Among Adults in the United States. *Arch Ophthalmol. ,* 122**,** 477-485.

TREMBLAY, M. E., ZETTEL, M. L., ISON, J. R., ALLEN, P. D. & MAJEWSKA, A. K. 2012. Effects of aging and sensory loss on glial cells in mouse visual and auditory cortices. *Glia,* 60**,** 541-58.

TU, L. N., MOROHAKU, K., MANNA, P. R., PELTON, S. H., BUTLER, W. R., STOCCO, D. M. & SELVARAJ, V. 2014a. Peripheral benzodiazepine receptor/translocator protein global knock-out mice are viable with no effects on steroid hormone biosynthesis. *J Biol Chem,* 289**,** 27444-54.

TU, L. N., ZHAO, A. H., HUSSEIN, M., STOCCO, D. M. & SELVARAJ, V. 2016. Translocator protein (TSPO) affects mitochondrial fatty acid oxidation in steroidogenic cells. *Endocrinology***,** en20151795.

TU, L. N., ZHAO, A. H., STOCCO, D. M. & SELVARAJ, V. 2014b. PK11195 effect on steroidogenesis is not mediated through the translocator protein (TSPO). *Endocrinology***,** en20141707.

TURNER, M. R., CAGNIN, A., TURKHEIMER, F. E., MILLER, C. C., SHAW, C. E., BROOKS, D. J., LEIGH, P. N. & BANATI, R. B. 2004. Evidence of widespread cerebral microglial activation in amyotrophic lateral sclerosis: an [11C](R)-PK11195 positron emission tomography study. *Neurobiol Dis,* 15**,** 601-9.

VEENMAN, L., PAPADOPOULOS, V. & GAVISH, M. 2007. Channel-like functions of the 18-kDa translocator protein (TSPO): regulation of apoptosis and steroidogenesis as part of the host-defense response. *Curr Pharm Des,* 13**,** 2385-405.

VEENMAN, L., SHANDALOV, Y. & GAVISH, M. 2008. VDAC activation by the 18 kDa translocator protein (TSPO), implications for apoptosis. *J Bioenerg Biomembr,* 40**,** 199-205.

VEIGA, S., AZCOITIA, I. & GARCIA-SEGURA, L. M. 2005. Ro5-4864, a peripheral benzodiazepine receptor ligand, reduces reactive gliosis and protects hippocampal hilar neurons from kainic acid excitotoxicity. *J Neurosci Res,* 80**,** 129-37.

VELERI, S., LAZAR, C. H., CHANG, B., SIEVING, P. A., BANIN, E. & SWAROOP, A. 2015. Biology and therapy of inherited retinal degenerative disease: insights from mouse models. *Dis Model Mech,* 8**,** 109-29.

VERMA, A., NYE, J. S. & SNYDER, S. H. 1987. Porphyrins are endogenous ligands for the mitochondrial (peripheral-type) benzodiazepine receptor. *Proc Natl Acad Sci U S A,* 84**,** 2256-60.

VERSIJPT, J., DEBRUYNE, J. C., VAN LAERE, K. J., DE VOS, F., KEPPENS, J., STRIJCKMANS, K., ACHTEN, E., SLEGERS, G., DIERCKX, R. A., KORF, J. & DE REUCK, J. L. 2005. Microglial imaging with positron emission tomography and atrophy measurements with magnetic resonance imaging in multiple sclerosis: a correlative study. *Mult Scler,* 11**,** 127-34.

VIVASH, L. & O'BRIEN, T. J. 2016. Imaging Microglial Activation with TSPO PET: Lighting Up Neurologic Diseases? *J Nucl Med,* 57**,** 165-8.

VOWINCKEL, E., REUTENS, D., BECHER, B., VERGE, G., EVANS, A., OWENS, T. & ANTEL, J. P. 1997. PK11195 binding to the peripheral benzodiazepine receptor as a marker of microglia activation in multiple sclerosis and experimental autoimmune encephalomyelitis. *J Neurosci Res,* 50**,** 345-53.

WANG, A. L., YU, A. C., LAU, L. T., LEE, C., WU LE, M., ZHU, X. & TSO, M. O. 2005. Minocycline inhibits LPS-induced retinal microglia activation. *Neurochem Int,* 47**,** 152-8.

WANG, J., WEI, Q., WANG, C. Y., HILL, W. D., HESS, D. C. & DONG, Z. 2004. Minocycline up-regulates Bcl-2 and protects against cell death in mitochondria. *J Biol Chem,* 279**,** 19948-54.

WANG, M., WANG, X., ZHAO, L., MA, W., RODRIGUEZ, I. R., FARISS, R. N. & WONG, W. T. 2014. Macroglia-microglia interactions via TSPO signaling regulates microglial activation in the mouse retina. *J Neurosci,* 34**,** 3793-806.

WANG, X., ZHU, S., DROZDA, M., ZHANG, W., STAVROVSKAYA, I. G., CATTANEO, E., FERRANTE, R. J., KRISTAL, B. S. & FRIEDLANDER, R. M. 2003. Minocycline inhibits caspase-independent and -dependent mitochondrial cell death pathways in models of Huntington's disease. *Proc Natl Acad Sci U S A,* 100**,** 10483-7.

WANG, X. J., YE, M., ZHANG, Y. H. & CHEN, S. D. 2007. CD200-CD200R regulation of microglia activation in the pathogenesis of Parkinson's disease. *J Neuroimmune Pharmacol,* 2**,** 259-64.

WAUBANT, E., GOODKIN, D., BOSTROM, A., BACCHETTI, P., HIETPAS, J., LINDBERG, R. & LEPPERT, D. 2003. IFNbeta lowers MMP-9/TIMP-1 ratio, which predicts new enhancing lesions in patients with SPMS. *Neurology,* 60**,** 52-7.

WEI, X. H., WEI, X., CHEN, F. Y., ZANG, Y., XIN, W. J., PANG, R. P., CHEN, Y., WANG, J., LI, Y. Y., SHEN, K. F., ZHOU, L. J. & LIU, X. G. 2013. The upregulation of translocator protein (18 kDa) promotes recovery from neuropathic pain in rats. *J Neurosci,* 33**,** 1540-51.

WENZEL, A., GRIMM, C., SAMARDZIJA, M. & REME, C. E. 2005. Molecular mechanisms of light-induced photoreceptor apoptosis and neuroprotection for retinal degeneration. *Prog Retin Eye Res,* 24**,** 275-306.

WENZEL, A., GRIMM, C., SEELIGER, M. W., JAISSLE, G., HAFEZI, F., KRETSCHMER, R., ZRENNER, E. & REME, C. E. 2001a. Prevention of photoreceptor apoptosis by activation of the glucocorticoid receptor. *Invest Ophthalmol Vis Sci,* 42**,** 1653-9.

WENZEL, A., REME, C. E., WILLIAMS, T. P., HAFEZI, F. & GRIMM, C. 2001b. The Rpe65 Leu450Met variation increases retinal resistance against light-induced degeneration by slowing rhodopsin regeneration. *J Neurosci,* 21**,** 53-8.

WONG, W. T. 2013. Microglial aging in the healthy CNS: phenotypes, drivers, and rejuvenation. *Front Cell Neurosci,* 7**,** 22.

WU, D., CHOI, D., JACKSON-LEWIS, V., ISCHIROPOULOS, VILA, M., TIEU, K., TEISMANN, P. & SERGE PRZEDBORSKI, S. 2002a. Blockade of Microglial Activation Is Neuroprotective in the 1-Methyl-4-Phenyl-1,2,3,6-Tetrahydropyridine Mouse Model of Parkinson Disease. *The Journal of Neuroscience,* 22**,** 1763–1771.

WU, D. C., JACKSON-LEWIS, V., VILA, M., TIEU, K., TEISMANN, P., VADSETH, C., CHOI, D. K., ISCHIROPOULOS, H. & PRZEDBORSKI, S. 2002b. Blockade of microglial activation is neuroprotective in the 1-methyl-4-phenyl-1,2,3,6-tetrahydropyridine mouse model of Parkinson disease. *J Neurosci,* 22**,** 1763-71.

XIAO, O., XIE, Z. L., LIN, B. W., YIN, X. F., PI, R. B. & ZHOU, S. Y. 2012. Minocycline inhibits alkali burn-induced corneal neovascularization in mice. *PLoS One,* 7**,** e41858.

XU, H., CHEN, M., MAYER, E. J., FORRESTER, J. V. & DICK, A. D. 2007. Turnover of resident retinal microglia in the normal adult mouse. *Glia,* 55**,** 1189-98.

YAMAUCHI, M., TSURUMA, K., IMAI, S., NAKANISHI, T., UMIGAI, N., SHIMAZAWA, M. & HARA, H. 2011. Crocetin prevents retinal degeneration induced by oxidative and endoplasmic reticulum stresses via inhibition of caspase activity. *Eur J Pharmacol,* 650**,** 110-9.

YANG, L.-P., LI, Y., ZHU, X.-A. & TSO, M. O. M. 2007a. Minocycline delayed photoreceptor death in the rds mice through iNOS-dependent mechanism. *Molecular Vision,* 13**,** 1073-82.
YANG, L. P., ZHU, X. A. & TSO, M. O. 2007b. Minocycline and sulforaphane inhibited lipopolysaccharide-mediated retinal microglial activation. *Mol Vis,* 13**,** 1083-93.
YAO, X. L., LIU, J., LEE, E., LING, G. S. & MCCABE, J. T. 2005. Progesterone differentially regulates pro- and anti-apoptotic gene expression in cerebral cortex following traumatic brain injury in rats. *J Neurotrauma,* 22**,** 656-68.
YASUNO, F., OTA, M., KOSAKA, J., ITO, H., HIGUCHI, M., DORONBEKOV, T. K., NOZAKI, S., FUJIMURA, Y., KOEDA, M., ASADA, T. & SUHARA, T. 2008. Increased binding of peripheral benzodiazepine receptor in Alzheimer's disease measured by positron emission tomography with [11C]DAA1106. *Biol Psychiatry,* 64**,** 835-41.
YAU, K. W. & HARDIE, R. C. 2009. Phototransduction motifs and variations. *Cell,* 139**,** 246-64.
YOUNG, R. W. 1967. The renewal of photoreceptor cell outer segments. *J Cell Biol,* 33**,** 61-72.
ZAMZAMI, N. & KROEMER, G. 2001. The mitochondrion in apoptosis: how Pandora's box opens. *Nat Rev Mol Cell Biol, 2***,** 67-71.
ZEISS, C. J. & JOHNSON, E. A. 2004. Proliferation of microglia, but not photoreceptors, in the outer nuclear layer of the rd-1 mouse. *Invest Ophthalmol Vis Sci,* 45**,** 971-6.
ZHANG, C., LEI, B., LAM, T. T., YANG, F., SINHA, D. & TSO, M. O. 2004. Neuroprotection of photoreceptors by minocycline in light-induced retinal degeneration. *Invest Ophthalmol Vis Sci,* 45**,** 2753-9.
ZHAO, L., ZABEL, M. K., WANG, X., MA, W., SHAH, P., FARISS, R. N., QIAN, H., PARKHURST, C. N., GAN, W. B. & WONG, W. T. 2015. Microglial phagocytosis of living photoreceptors contributes to inherited retinal degeneration. *EMBO Mol Med*.
ZHOU, R. & CASPI, R. R. 2010. Ocular immune privilege. *F1000 Biol Rep,* 2.

Publications

JOURNAL OF NEUROINFLAMMATION

RESEARCH Open Access

Translocator protein (18 kDa) (TSPO) is expressed in reactive retinal microglia and modulates microglial inflammation and phagocytosis

Marcus Karlstetter[1†], Caroline Nothdurfter[2†], Alexander Aslanidis[1], Katharina Moeller[1], Felicitas Horn[1], Rebecca Scholz[1], Harald Neumann[3], Bernhard H F Weber[4], Rainer Rupprecht[2*†] and Thomas Langmann[1*†]

Abstract

Background: The translocator protein (18 kDa) (TSPO) is a mitochondrial protein expressed on reactive glial cells and a biomarker for gliosis in the brain. TSPO ligands have been shown to reduce neuroinflammation in several mouse models of neurodegeneration. Here, we analyzed TSPO expression in mouse and human retinal microglia and studied the effects of the TSPO ligand XBD173 on microglial functions.

Methods: TSPO protein analyses were performed in retinoschisin-deficient mouse retinas and human retinas. Lipopolysaccharide (LPS)-challenged BV-2 microglial cells were treated with XBD173 and TSPO shRNAs *in vitro* and pro-inflammatory markers were determined by qRT-PCR. The migration potential of microglia was determined with wound healing assays and the proliferation was studied with Fluorescence Activated Cell Sorting (FACS) analysis. Microglial neurotoxicity was estimated by nitrite measurement and quantification of caspase 3/7 levels in 661 W photoreceptors cultured in the presence of microglia-conditioned medium. The effects of XBD173 on filopodia formation and phagocytosis were analyzed in BV-2 cells and human induced pluripotent stem (iPS) cell-derived microglia (iPSdM). The morphology of microglia was quantified in mouse retinal explants treated with XBD173.

Results: TSPO was strongly up-regulated in microglial cells of the dystrophic mouse retina and also co-localized with microglia in human retinas. Constitutive TSPO expression was high in the early postnatal Day 3 mouse retina and declined to low levels in the adult tissue. TSPO mRNA and protein were also strongly induced in LPS-challenged BV-2 microglia while the TSPO ligand XBD173 efficiently suppressed transcription of the pro-inflammatory marker genes chemokine (C-C motif) ligand 2 (CCL2), interleukin 6 (IL6) and inducible nitric oxide (NO)-synthase (iNOS). Moreover, treatment with XBD173 significantly reduced the migratory capacity and proliferation of microglia, their level of NO secretion and their neurotoxic activity on 661 W photoreceptor cells. Furthermore, XBD173 treatment of murine and human microglial cells promoted the formation of filopodia and increased their phagocytic capacity to ingest latex beads or photoreceptor debris. Finally, treatment with XBD173 reversed the amoeboid alerted phenotype of microglial cells in explanted organotypic mouse retinal cultures after challenge with LPS.

Conclusions: These findings suggest that TSPO is highly expressed in reactive retinal microglia and a promising target to control microglial reactivity during retinal degeneration.

Keywords: Translocator protein (18 kDa), Microglia, Retinal degeneration, Phagocytosis

* Correspondence:rainer.rupprecht@medbo.de; thomas.langmann@uk-koeln.de
†Equal contributors
[2]Department of Psychiatry and Psychotherapy, University of Regensburg, D-93053 Regensburg, Germany
[1]Department of Ophthalmology, University of Cologne, D-50931 Cologne, Germany
Full list of author information is available at the end of the article

Background

The translocator protein (18 kDa) (TSPO), previously known as the peripheral benzodiazepine receptor, is an integral part of the outer mitochondrial membrane [1] where it forms a complex with other mitochondrial proteins, such as the voltage-dependent anion channel (VDAC) and the adenine nucleotide transporter (ANT) [2]. TSPO mediates the transport of cholesterol into the inner mitochondrial membrane, where it serves as a precursor for steroids and neurosteroids [3]. Hence, the protein is constitutively expressed in steroidogenic tissues such as the adrenal gland, the gonads and the brain [4]. In the central nervous system TSPO is present both in neurons and activated glial cells [5-7]. Endogenous ligands of TSPO are cholesterol, porphyrins and active peptide fragments cleaved off from the diazepam binding inhibitor [8]. Glial up-regulation of TSPO is a major hallmark of neurodegenerative diseases [9] and various TSPO ligands have been developed as molecular markers to detect gliosis by means of Positron Emission Tomography (PET) imaging [10].

TSPO ligands are also under investigation as treatment options for a variety of neurological disorders, including Alzheimer's disease [11], multiple sclerosis [12], neuropathic pain [13], peripheral nerve injury [9] and anxiety disorders [14]. Classical synthetic TSPO ligands, such as the benzodiazepine derivative 4′-chlorodiazepam (Ro5-4864) and the isoquinoline carboxamide PK11195, directly enhance GABAergic neurotransmission [15]. TSPO ligands such as etifoxine and XBD173 (emapunil) stimulate the synthesis of neurosteroids and may exert anti-inflammatory and neuroprotective effects [16].

Inherited retinal degenerations are clinically and genetically heterogeneous diseases characterized by progressive vision loss [17]. Although the individual mechanisms of pathogenesis remain to be resolved, microglial activation is a common hallmark of retinal degeneration [18]. The retinoschisin-deficient ($Rs1h^{-/Y}$) mouse is a prototypic model for inherited retinal dystrophies with strong microglial reactivity [19,20]. Modulation of retinal microglia with docosahexaenoic acid could dampen microglial reactivity in $Rs1h^{-/Y}$ mice and thereby reduced retinal degeneration [21]. TSPO ligands could potentially have a similar effect and may target the neurodegenerative cascade via their anti-inflammatory and microglia modulating effects.

In this study, we showed that TSPO expression is directly connected to retinal microgliosis in a mouse model of retinal degeneration and in human retinal sections. Moreover, we demonstrated that the TSPO ligand XBD173 induces an anti-inflammatory, neuroprotective and pro-phagocytic phenotype in microglia using cultures of murine and human microglial cell lines as well as mouse retinal explants.

Methods

Animals

MacGreen [22], $Rs1h^{-/Y}$ [19] and wild-type mice were all on a pure C57BL/ 6 J background. Animals were maintained in an air-conditioned environment on a 12-hour light–dark schedule at 22°C, and had free access to food and water. The health of the animals was regularly monitored, and all procedures complied with the German Law on Animal Protection and the Institute for Laboratory Animal Research Guide for the Care and Use of Laboratory Animals, 2011.

Human tissue

Retinal samples of donors were obtained from the Eye Bank of the Center of Ophthalmology, University of Cologne, Germany. The donor age ranged between 54 and 72 years. Postmortem time ranged between 5 and 36 h. After dissection of the anterior segment, the remaining tissue included the posterior pole. The research followed the tenets of the Declaration of Helsinki.

Reagents

E. coli 0111:B4 lipopolysaccharide and aminoglutethimide were purchased from Sigma Aldrich (St. Louis, MO, USA). XBD173 (emapunil) was obtained by custom synthesis from APAC Pharmaceuticals (Ellicott City, MD, USA). XBD173 was dissolved in ethanol.

Cell culture and retinal explants

BV-2 microglia-like cells were cultured in RPMI/5% fetal calf serum (FCS) supplemented with 2 mM L-Glutamine and 195 nM β-mercaptoethanol. Isolation and culture of primary retinal microglia has been described previously [21]. BV-2 cells were stimulated with 50 ng/ml lipopolysaccharide (LPS) and various concentrations of XBD173 or ethanol as vehicle control. 661 W photoreceptor-like cells were a gift from Prof. Muayyad Al-Ubaidi (Department of Cell Biology, University of Oklahoma Health Sciences Center, Oklahoma City, OK, USA) and the culture conditions have been described elsewhere [23]. Human microglial cell lines (iPSdM) were generated from induced pluripotent stem (iPS) cell lines obtained by reprogramming from skin fibroblasts as previously described [24,25]. These cells proliferate without addition of growth factors and they were passaged 1:3 twice a week. The microglial phenotype was confirmed by flow cytometry (CD11b, CD16/32, CD36, CD45, CX3CR1). Retinas from MacGreen mice were rinsed in DMEM/Ham's F12 medium supplemented with 1% FCS and placed on 25 mm circular Nucleopore filters (VWR, Darmstadt, Germany) with the photoreceptor side facing the membrane. After 24 h of *in vitro* culture with vehicle, 1 μg/ml LPS, 20 μM XBD173 or 1 μg/ml LPS + 20 μM XBD173, retinas were fixed and imaged in flat-mounts. Ramified and

amoeboid microglial cells were directly imaged by green fluorescent protein (GFP) fluorescence using the Axioskop2 MOT Plus Apotome microscope (Carl Zeiss, Jena, Germany) and counted.

Scratch wound-healing assay

A total of 400,000 BV-2 microglial cells were grown in six-well plates as 80% confluent monolayers and were wounded with a sterile 100 μl pipette tip. Thereafter, the cells were stimulated with 50 ng/ml LPS, 50 μM XBD173, 50 ng/ml LPS + 50 μM XBD173, or ethanol as solvent control. Migration into the open scar was documented with microphotographs taken at different time points after wounding using a Nikon ECLIPSE TE2000 inverted microscope (Nikon, Tokyo, Japan). The number of migrating cells was quantified by counting all cells within a 0.4 mm^2 region in the center of each scratch. The number of migrated cells was then normalized to the average cell density to account for changes in proliferation. A minimum of five individual cultures was used to calculate the mean migratory capacity of each cell culture condition.

Proliferation assay

For carboxyfluorescein diacetate succinimidyl ester (CFSE) proliferation assays, BV-2 microglial cells were labeled with 1 μM CFSE (e-Bioscience, San Diego, CA, USA) and cultured (1.5×10^5 per well) in a six-well plate. After 24 h of culture with vehicle, 100 ng/ml LPS, 50 μM XBD173 or 100 ng/ml LPS + 50 μM XBD173, cells were stained with a fixable viability dye (e-Bioscience), to exclude dead cells from the analysis. The fluorescence intensity of CFSE-labeled BV-2 cells was analyzed by flow cytometry (FACS Canto II). Analysis of cell division was performed using FlowJo software (Treestar Inc., Ashland, OR, USA).

shRNA knock-down of TSPO in BV-2 cells

For knockdown of endogenous TSPO in BV-2 cells, shRNA vectors were obtained from the RNAi consortium (TRC). Briefly, BV-2 cells were transfected with 2.5 μg vector DNA using TransIT®-LT1 transfection reagent (Mirus Bio LLC, Madison, WI, USA) to express TSPO-specific or scrambled shRNAs. Twenty-four hours after transfection cells were stimulated with vehicle, 50 ng/ml LPS, 20 μM XBD173 or 50 ng/ml LPS + 20 μM XBD173 for 12 hours before cells were harvested for RNA isolation and mRNA expression analysis.

661 W photoreceptor apoptosis assay

To test microglial neurotoxicity, a culture system of 661 W photoreceptors with microglia-conditioned medium was established. 661 W photoreceptor cells were incubated for 48 h either in their own medium or with culture supernatants from unstimulated, 50 ng/ml LPS, 50 μM XBD173 or 50 ng/ml LPS + 50 μM XBD173 treated microglial cells. The 661 W cell morphology was assessed by phase contrast microscopy and apoptotic cell death was determined with the Caspase-Glo® 3/7 Assay (Promega GmbH, Mannheim, Germany). Cells were lysed and incubated with a luminogenic caspase-3/7 substrate, which contains the tetrapeptide sequence DEVD. Luminescence was then generated by addition of recombinant luciferase and was proportional to the amount of caspase activity present. The luminescent signal was read on an Infinite F200 pro plate reader (Tecan, Crailsheim, Germany). A blank reaction was used to measure background luminescence associated with the cell culture system and Caspase-Glo® 3/7 Reagent (Promega). The value for the blank reaction was subtracted from all experimental values. Negative control reactions were performed to determine the basal caspase activity of 661 W cells. Relative luciferase units (RLU) reflect the level of apoptotic cell death in the different 661 W cell cultures.

Nitrite measurement

Nitric oxide concentrations were determined by measuring the amount of nitrite produced by BV-2 microglial cells into the culture medium using the Griess reagent system (Promega). A 50 μl cell culture supernatant was collected and an equal volume of Griess reagent was added to each well. After incubation for 15 minutes at room temperature, the absorbance was read at 540 nm on an Infinite F200 pro plate reader (Tecan). The concentration of nitrite for each sample was calculated from a sodium nitrite standard curve.

Phagocytosis assays

BV-2 microglial cells were pre-treated for 2 h with compounds before 4 μl latex bead solution (Polystyrene microparticles, Sigma Aldrich, St. Louis, MO, USA) was added to the wells. Cells were incubated for 6 h and five micrographs per well were taken using an AxioVert.A1 inverted microscope (Carl Zeiss). The phagocytic activity was determined by calculating the number of cells which phagocytosed 10 or more latex beads compared to all cells per field. The conditions for human microglial cells (iPSdM) were the same with the modification that cells were pre-treated for 24 h, the incubation time with beads was 24 h and only fully saturated cells were counted as positive. To study the microglial uptake of apoptotic photoreceptor cell material, 661 W photoreceptor cells were starved with serum deprivation, harvested and fluorescently labeled using CellTracker CM-DiI (Invitrogen, Carlsbad, CA, USA). For phagocytosis, BV-2 microglial cells were pre-treated for 2 h with compounds before 400 μl stained apoptotic 661 W solution was added for further 6 h. iPSdM cells were pre-treated for 24 h before 400 μl stained apoptotic 661 W solution was added for further 24 h. Cells were then

fixed and nuclei were stained with 4′,6-diamidino-2-phenylindole. Fluorescence micrographs were taken and ImageJ software (National Institutes of Health, Bethesda, MD, USA) was used to determine the ratio of phagocytosed apoptotic photoreceptor fragments (red signal) relative to the total microglia cell number (DAPI signal).

Phalloidin staining

BV-2 microglial cells or human microglial cells (iPSdM) were grown on cover slips in six-well plates and the indicated compounds were added for 24 h. Thereafter, the cells were fixed, permeabilized with 0.1% Triton X-100 and f-actin was fluorescently labeled using 0.1 μg/ml Phalloidin-TRITC (Sigma). The nuclei were stained using 4′,6-diamidino-2-phenylindole and photomicrographs were taken with an Axioskop2 MOT Plus Apotome microscope (Carl Zeiss).

Immunohistochemistry

Immunohistochemical analyses were performed on 10 μm retinal sections embedded in optimal cutting temperature (OCT) compound (Hartenstein, Würzburg, Germany) or on retinal flat mounts. Samples were fixed in 4% paraformaldehyde, rinsed and rehydrated with PBS. Sections were blocked with a dried milk solution followed by an overnight incubation with primary antibodies at 4°C. Antibodies included rabbit anti-Iba1 antibody (Wako Chemicals, Neuss, Germany), rabbit anti-TSPO antibody (Abcam, Cambridge, UK), goat anti-MAP2 antibody (Santa Cruz Biotechnology, Santa Cruz, CA, USA), and goat anti-GFAP antibody (Santa Cruz Biotechnology). After washing, samples were labeled with a secondary antibody conjugated to Alexa488 (green) or Alexa594 (red) (Jackson Immuno-Research, West Grove, PA, USA) and counter-stained with DAPI. Sections and flat-mounts were mounted in DAKO fluorescent mounting medium (Dako Deutschland GmbH, Hamburg, Germany) and viewed with an Axioskop2 MOT Plus Apotome microscope (Carl Zeiss).

Western blot analysis

Mouse retinal tissue was homogenized in cold RIPA buffer (20 mM Na-phosphate buffer, 150 mM NaCl, 5 mM EDTA, 1% Triton X-100 and protease inhibitors) using a TissueLyser LT (Qiagen, Hilden, Germany). Insoluble debris was removed by centrifugation for 15 minutes at 16,000 g. LPS-treated and control BV-2 microglia were directly lysed in RIPA buffer. Protein concentrations were determined by Bradford assay (Roti-quant, Roth, Karlsruhe, Germany). A total of 10 μg of microglial or 30 μg of total-retina proteins were separated by SDS-PAGE on 15% gels with PageRuler pre-stained protein ladder (Thermo Scientific, Waltham, MA, USA). Proteins were then transferred to 0.45 μm nitrocellulose membranes (Biorad, Munich, Germany). After blocking in TBS-T containing 5% nonfat dry milk, membranes were incubated with primary antibodies against TSPO (ab109497, Abcam,) or Actin (sc-1616, Santa Cruz Biotechnology). Blots were then incubated with secondary goat anti-rabbit IgG-HRP or rabbit anti-goat IgG-HRP antibodies (sc-2004, sc-2768, Santa Cruz Biotechnology). Enhanced chemiluminescence signals were then visualized and imaged with the MultiImage II system (Alpha Innotech, Santa Clara, CA, USA).

RNA isolation and reverse transcription

Total RNA was extracted from total retina, BV-2 microglial cells or isolated retinal microglia according to the manufacturer's instructions using the RNeasy Mini Kit (Qiagen). Purity and integrity of the RNA was assessed on the Agilent 2100 Bioanalyzer with the RNA 6000 Nano LabChip® reagent set (Agilent Technologies, Santa Clara, CA, USA). The RNA was quantified spectrophotometrically and then stored at −80°C. First-strand cDNA synthesis was performed with the RevertAid™ H Minus First Strand cDNA Synthesis Kit (Fermentas, Schwerte, Germany).

Quantitative real-time RT-PCR

Amplifications of 50 ng cDNA were performed with an ABI7900HT machine (Applied Biosystems, Carlsbad, CA, USA) in 10 μl reaction mixtures containing 1 × TaqMan Universal PCR Master Mix (Applied Biosystems), 200 nM of primers and 0.25 μl of dual-labeled probe (Roche ProbeLibrary, Roche Applied Science, Basel, Switzerland). The reaction parameters were as follows: 2 minutes 50°C hold, 30 minutes 60°C hold and 5 minutes 95°C hold, followed by 45 cycles of 20 s 94°C melt and 1 minute 60°C anneal/extension. Primer sequences and Roche Library Probe numbers were as follows: CCL2, forward primer 5′-catccacgtgttggctca-3′, reverse primer 5′-gatcatcttgctggtgaatgagt-3′, probe #62; IL6, forward primer 5′-gatggatgctaccaaactggat-3′, reverse primer 5′-ccaggtagctatggtactccaga-3′, probe #6; iNOS, forward primer 5′-ctttgccacggacgagac-3′, reverse primer 5′- tcattgtactctgagggctga-3′, probe #13. Measurements were performed in triplicates and results were analyzed with an ABI sequence detector software version 2.3 using the ΔΔCt method for relative quantification.

Pregnenolone ELISA

BV-2 cells were seeded on 24-well plates in 1 ml/well of RPMI/5% FCS supplemented with 2 mM L-Glutamine and 195 nM β-mercaptoethanol. After cells had attached after 6 h, 50 ng/ml LPS and/or 20 μM XBD173 were added to each well. After 21 h, cells were washed twice with HEPES assay buffer (140 mM NaCl, 5 mM KCl, 1.8 mM $CaCl_2$, 1 mM $MgSO_4$, 10 mM glucose, 10 mM

HEPES/NaOH, pH 7.4) as described previously [26]. Then 1 ml of HEPES assay buffer supplemented with BSA (0.1%) and Trilostane (25 μM) (Sigma-Aldrich) was added to each well. Again 50 ng/ml LPS and/or 20 μM XBD173 were added. After 3 h the supernatants were removed to perform pregnenolone ELISA according to the manufacturer's recommendations (IBL International, Hamburg, Germany). In brief, 50 μl of each sample were pipetted into a rabbit anti-pregnenolone antibody coated 96-microwell Plate. A total of 100 μl of pregnenolone-HRP conjugate was then added. Ready-to-use-calibrators were provided by IBL international. After 1 h of incubation and washing 150 μl of tetramethylbenzidine/hydrogen peroxide (TMB) substrate was added. Assays were read with a Tecan Spectra at 450 nm. Data were analyzed by Magellan Data Analysis Software (Tecan).

Statistical analyses

Real-time quantitative RT-PCR data were analyzed with the ΔΔCt method using an unpaired Student's *t*-test. Assays for nitrite secretion, microglial migration and pregnenolone ELISAs were analyzed with an unpaired Student's *t* test. Caspase 3/7 assays and phagocytosis assays were analyzed with a Mann–Whitney *U*-test. $P < 0.05$ was considered as statistically significant.

Results

Induction of TSPO expression in activated microglia of the retina

To identify genes regulated during activation of microglia, we have previously performed DNA microarray analysis of isolated retinal microglial cells from degenerating retinoschisin-deficient ($Rs1h^{-/Y}$) and control macrophage/microglia MacGreen reporter mice [21]. Among the differently expressed transcripts, a significantly increased mRNA expression of TSPO was detected in activated retinal microglia (data not shown). Therefore, we determined the protein expression of TSPO in the retina and found a weak expression in the MacGreen reporter mouse, which was present in ramified microglia of the plexiform layers and astrocytes of the ganglion cell layer (Figure 1A-C). However, there was a remarkable increase of TSPO expression specifically in microglia of MacGreen/$Rs1h^{-/Y}$ retinas (Figure 1D-F). Notably, there was nearly a full overlap of TSPO signals with amoeboid microglial cells which migrated to the degenerating inner nuclear layer (Figure 1F). In the human retina, TSPO expression was also evident in inner plexiform layer microglial cells as demonstrated by Iba1 co-immunostaining as well as in astrocytes (Figure 1G-I). To exclude that TSPO is significantly expressed in Müller cells or retinal neurons, immunostainings for glial fibrillary acid protein (GFAP) and microtubule-associated protein 2 (MAP2) were performed. Neither wild-type retinas nor $Rs1h^{-/Y}$ retinas

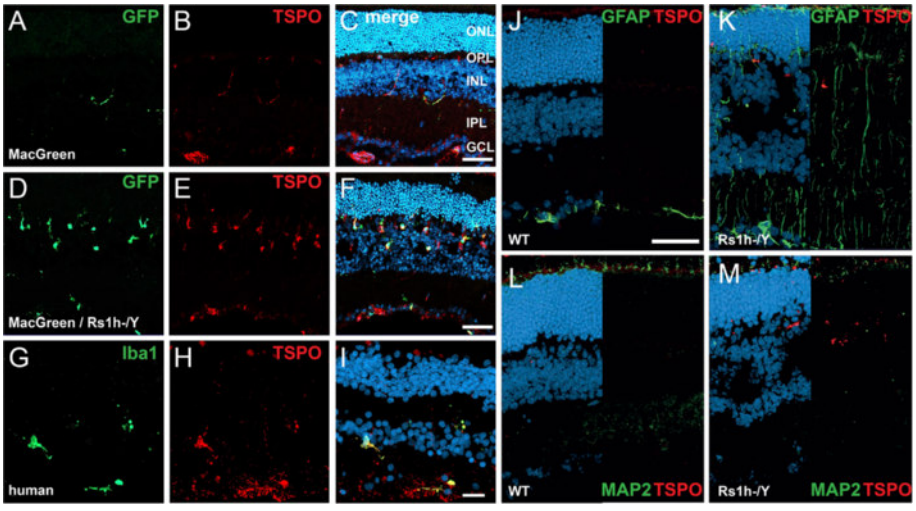

Figure 1 TSPO expression as a marker for microgliosis in degenerating and aging retinas. In MacGreen mice, representative photomicrographs show low TSPO expression in retinal microglia (green GFP signal and red TSPO immunofluorescence) and constitutive expression in astrocytes (red TSPO immunofluorescence) **(A-C)** but strong up-regulation in retinal microglia from MacGreen/$Rs1h^{-/Y}$ mice **(D-F)**. The overlap of TSPO and Iba1 immunostaining also indicates co-expression in human retinal microglia **(G-I)**. TSPO immunostaining staining does not co-localize with the Müller cell marker GFAP **(J, K)** or the neuronal microtubule marker MAP2 **(L, M)**. ONL, outer nuclear layer; OPL, outer plexiform layer; INL, inner nuclear layer; IPL, inner plexiform layer; GCL, ganglion cell layer, GFP, green fluorescent protein; TSPO, translocator protein (18 kDa); GFAP, glial fibrillary acid protein; MAP2, microtubule-associated protein 2. Scale bar, 50 μm.

displayed an overlap of TSPO signals with GFAP (Figure 1J, K) or MAP2 (Figure 1L, M), respectively.

To further verify the steep TSPO expression in reactive microglia, mRNA analysis of isolated retinal microglia from MacGreen and MacGreen/Rs1h$^{-/Y}$ retinas was performed. There was a strong and significant increase of TSPO mRNA in MacGreen/Rs1h$^{-/Y}$ microglia (12.01 ± 0.82, P <0.01) compared to MacGreen microglia (1.0 ± 1.07) (Figure 2A). TSPO induction was also confirmed on the protein level when total retinas of MacGreen/Rs1h$^{-/Y}$ mice compared to MacGreen mice were analyzed (Figure 2B). We next performed TSPO transcript analysis in early postnatal development of the mouse retina. TSPO was present at higher levels in early retinal development and turned to lower levels in the adult retina (Figure 2C). We then analyzed whether the induction of TSPO expression is also present in cultured BV-2 microglia, which were activated by LPS. Treatment of BV-2 cells with 50 ng/ml LPS elicited a highly significant increase in TSPO levels (4.11 ± 0.31, P <0.001) compared to vehicle-treated BV-2 cells (1.0 ± 0.80) (Figure 2D). The increase of TSPO in LPS-activated BV-2 microglia was also confirmed on the protein level using Western blot analysis (Figure 2E).

The selective TSPO ligand XBD173 dampens pro-inflammatory and neurotoxic microglial activation

We investigated whether stimulation of TSPO with the selective ligand XBD173 influences microglial reactivity. We first tested the mRNA expression of the chemo-attractant protein CCL2, the pro-inflammatory cytokine IL6 and iNOS in LPS-activated microglia upon treatment with three different doses of XBD173. The TSPO ligand significantly and dose-dependently suppressed mRNA levels of CCL2 (Figure 3A, P = 0.0014 for 20 μM XBD173 and P = 0.0003 for 50 μM XBD173 versus vehicle control), IL6 (Figure 3B, P = 0.0004 for 20 μM XBD173 and P = 0.0001 for 50 μM XBD173 versus vehicle control), and iNOS (Figure 3C, P = 0.0104 for 20 μM XBD173 and P = 0.0004 for 50 μM XBD173 versus vehicle control).

To test whether the anti-inflammatory effect of XBD173 depends on TSPO expression, shRNA mediated knock-down of TSPO was performed. Transfection of BV-2 cells with two different TSPO-specific shRNAs showed a 50 to 60% knock-down of TSPO mRNA levels compared to a scramble control (data not shown). The mRNA expression levels of CCL2 (Figure 3D), IL6 (Figure 3E) and iNOS (Figure 3F) were no longer suppressed by XBD173 treatment when either shRNA1 or shRNA2 that specifically target TSPO were present. This clearly implicates that the suppressing effect of XBD173 acts via TSPO in BV-2 cells.

When co-administered together with 50 ng/ml LPS, 50 μM XBD173 also strongly diminished NO-production from BV-2 microglial cells compared to vehicle-treated cells (Figure 3G, P <0.0001). We then performed an apoptosis assay of 661 W photoreceptor cells incubated in the presence of microglia-conditioned medium. LPS-activated microglial cells incubated in the presence of 50 μM XBD173 had a significantly lower pro-apoptotic effect on photoreceptor cells than microglia cultured with vehicle (Figure 3H, P <0.0022).

We then analyzed the effect of the TSPO ligand on microglial migration. Stimulation of BV-2 microglial cells

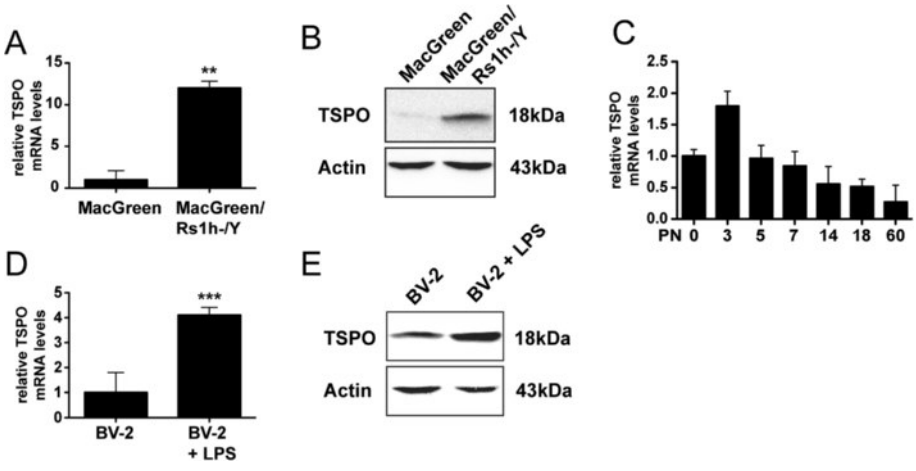

Figure 2 TSPO mRNA and protein expression in reactive microglia. (A) Strong induction of TSPO mRNA levels in isolated microglial cells from MacGreen/Rs1h$^{-/Y}$ mice compared to MacGreen mice. **(B)** TSPO protein induction in total retinas from MacGreen/Rs1h$^{-/Y}$ mice compared to MacGreen mice. **(C)** Temporal TSPO mRNA expression profiling shows a high early postnatal expression level and continuous decline to low levels in adult mouse retinas. **(D, E)** LPS activation of BV-2 microglial cells leads to the induction of TSPO transcripts **(D)** and protein **(E)**. Data show mean ± SD (n = 3/group, measured in triplicates) **P <0.01 MacGreen/Rs1h$^{-/Y}$ versus MacGreen; ***P <0.001 BV-2 + 50 ng/ml LPS versus BV-2. LPS, lipopolysaccharide; TSPO, translocator protein (18 kDa).

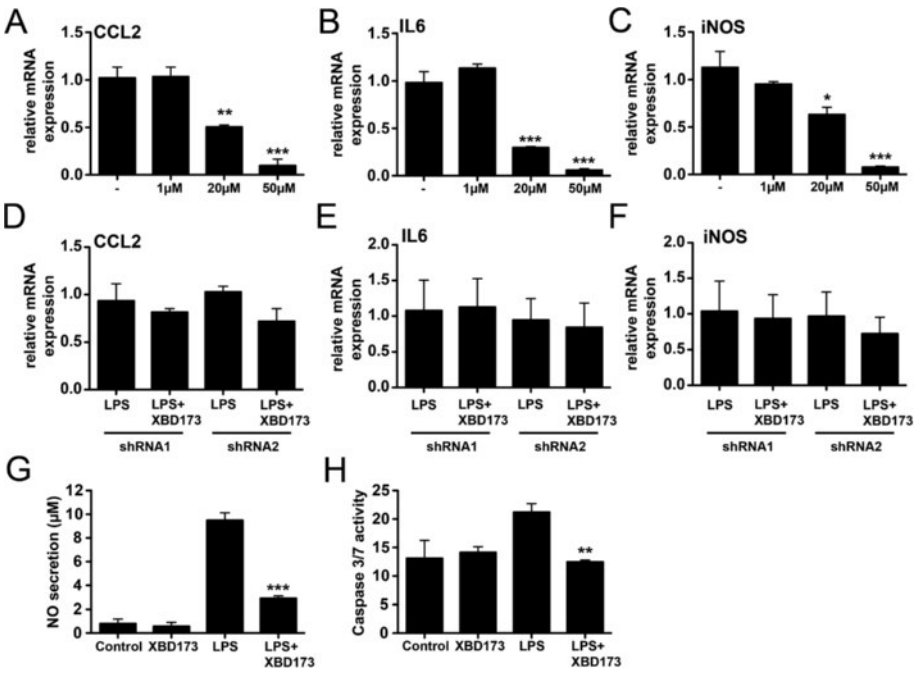

Figure 3 The TSPO agonist XBD173 dampens gene transcription of pro-inflammatory markers and reduces microglial neurotoxicity. LPS-activated BV-2 microglial cells were cultured in the presence of various concentrations of XBD173 for 24 h and the pro-inflammatory transcript markers CCL2 **(A)**, IL6 **(B)**, iNOS **(C)** were determined by *real time* qRT-PCR. Data show mean ± SD (n = 3/group, measured in triplicates) **P* <0.05, ***P* <0.01, ****P* <0.001 XBD173 + LPS versus LPS-treated cells. **(D-F)**, Knock-down of TSPO with two independent shRNAs abrogates the suppressing effects of XBD173 on CCL2 **(D)**, IL6 **(E)** and iNOS **(F)** gene expression in BV-2 cells. **(G)**, Production of NO as determined by detection of nitrite from BV-2 microglial cells treated with 50 μM XBD173 in the absence or presence of 50 ng/ml LPS. Data show mean ± SD (n = 9/group) ****P* <0.001 XBD173 + LPS versus LPS-treated cells. **(H)**, 661 W photoreceptor cell cultures were treated with conditioned media from BV-2 microglial cells for 48 hours. The supernatant from control-stimulated, 20 μM XBD173-treated, 50 ng/ml LPS-treated, or 20 μM XBD173 + 50 ng/ml LPS-treated cells was added to 661 W photoreceptor cells and apoptosis-related caspase 3/7 activation was determined. Data show mean ± SD (n = 6/group) ***P* <0.01 XBD173 + LPS versus LPS-treated cells. CCL2, (C-C motif) ligand 2; IL6, interleukin-6; iNOS, inducible nitric oxide synthase; LPS, lipopolysaccharide; NO, nitric oxide.

with 50 μM XBD173 strongly reduced the migration of BV-2 cells in a wound-healing scratch assay (Figure 4A). This effect was quantified and significant in non-activated microglia (Figure 4B, P <0.0008) as well as LPS-preactivated BV-2 cells (Figure 4B, P <0.0406). We constantly noticed a reduced cell number in our culture assays and, therefore, tested a potential anti-mitotic effect of XBD173. CFSE labeling and FACS analyses clearly demonstrated that XBD173 reduced the proliferation rate of both unstimulated and LPS-treated BV-2 cells (Figure 4C).

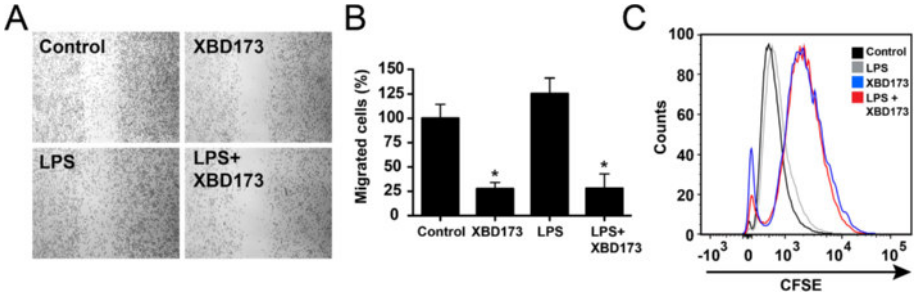

Figure 4 The TSPO agonist XBD173 reduces microglial migration and proliferation. (A) Scratch assay to mimic wound-healing in cultured BV-2 microglia treated with vehicle, 50 ng/ml LPS, 50 μM XBD173 or both. Microphotographs from scratched areas were quantified 8 h after treatment **(B)**. Data show mean ± SEM (n = 5/group) **P* <0.05 XBD173 versus control, **P* <0.001 XBD173 + LPS versus LPS-treated cells. **(C)**, CFSE-based proliferation assay of BV-2 microglial cells treated with vehicle, 100 ng/ml LPS, 50 μM XBD173 or 100 ng/ml LPS + 50 μM XBD173. The proliferation rate of BV-2 microglia was analyzed 24 hours after treatment using flow cytometry and a representative graph out of four repetitions is shown. CFSE, carboxyfluorescein diacetate succinimidyl ester; LPS, lipopolysaccharide; TSPO, translocator protein (18 kDa).

XBD173 increases filopodia formation and phagocytosis in murine and human microglia

To investigate further functional consequences of treatment with the TSPO ligand, we tested the effects of TSPO activation on the morphology and phagocytosis of murine BV-2 microglia and human microglial cells (iPSdM) derived from human induced pluripotent stem cells. Staining of the f-actin cytoskeleton with phalloidin indicated that XBD173 caused a prominent formation of filopodia in murine BV-2 cells either in the absence or presence of LPS (Figure 5A-D). This effect was even more pronounced in human iPSdM, which showed a large rim of flattened filopodia (Figure 5E-H).

This striking phenomenon of XBD173-induced filopodia formation prompted us to analyze the phagocytic capacity in detail using latex beads and CM-DiI-stained apoptotic 661 W photoreceptor material as a more physiological trigger. BV-2 microglial cells stimulated with XBD173 showed a significantly higher phagocytosis rate of latex beads in non-activated cells (Figure 6A, B, $P = 0.0013$) as well as LPS-preactivated cells (Figure 6A, B, $P = 0.0029$). A similar effect of XBD173 was noticed with fluorescent apoptotic 661 W photoreceptors in non-activated (Figure 6C, D, $P = 0.0192$) and LPS-incubated BV-2 cells (Figure 6C, D, $P = 0.0013$). XBD173 had a similar stimulating effect on the phagocytic potential of human microglial cells with strongly increased uptake of latex beads (Figure 6E, F, $P < 0.0001$) and CM-DiI-stained apoptotic 661 W membranes (Figure 6G, H, $P < 0.0001$).

To test whether the phenomenon of XBD173-induced phagocytosis is dependent on neurosteroid synthesis, we first quantified pregnenolone levels in BV-2 cells. Stimulation of BV-2 microglia with either 20 μM XBD173 alone (Figure 7A, $P < 0.0005$) or together with 50 ng/ml LPS (Figure 7A, $P < 0.0074$) strongly increased pregnenolone levels measured in the cell culture supernatant. We next performed bead phagocytosis assays with BV-2 cells stimulated with 20 μM XBD173 in the presence or absence of the CYP11A1 inhibitor aminoglutethimide. As previously shown in Figure 6, BV-2 cells stimulated with XBD173 showed a higher phagocytosis potential than control cells (Figure 7B, $P < 0.0001$). Interestingly, this effect was completely prevented when the cells were co-incubated with 20 μM XBD173 and 100 μM aminoglutethimide (Figure 7B). These data suggest that the phagocytosis promoting effect of XBD173 requires pregnenolone synthesis.

XBD173 reduces the number of LPS-alerted amoeboid microglia in living retinal explants

Finally, we analyzed whether the XBD173-dependent morphological transformation of microglial cells can also be observed in the *ex vivo* retina. Retinas from MacGreen reporter mice were used to enable easy GFP-based analysis of microglial ramification. Retinal explants cultured for 24 h *in vitro* retained their ramified morphology (Figure 8A) and the microglial network was not significantly affected by XBD173 alone (Figure 8B). In contrast, retinal microglia dramatically changed their morphology in the presence of LPS with a large fraction of bloated amoeboid cells (Figure 8C). This LPS-induced morphological transition of microglia was effectively suppressed by XBD173 (Figure 8D). We then performed a quantitative analysis of ramified and amoeboid microglial cells in all retinal explants. As already indicated in Figure 7A-D, the number of amoeboid cells was significantly increased in LPS-treated cultures compared to vehicle-treated explants (Figure 8E, $P = 0.0012$). Interestingly, co-incubation of explants with LPS and XBD173 resulted in a strongly reduced number of alerted amoeboid microglia cells (Figure 8E, $P < 0.0001$). Thus, XBD173 was not only able to influence microglial reactivity *in vitro* but also significantly affected microglia in living mouse retinas.

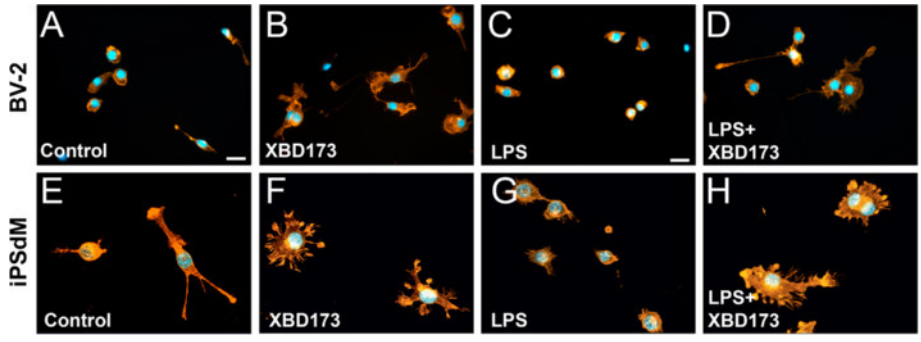

Figure 5 The TSPO ligand XBD173 promotes microglial filopodia formation. (A-D) Representative images of phalloidin-stained murine BV-2 microglial cells treated with 50 μM XBD173 in the absence or presence of 50 ng/ml LPS. **(E-H)** Representative images of phalloidin-stained human iPS-derived microglia (iPSdM) treated with 30 μM XBD173 in the absence or presence of 250 ng/ml LPS. LPS, lipopolysaccharide; TSPO, translocator protein (18 kDa).

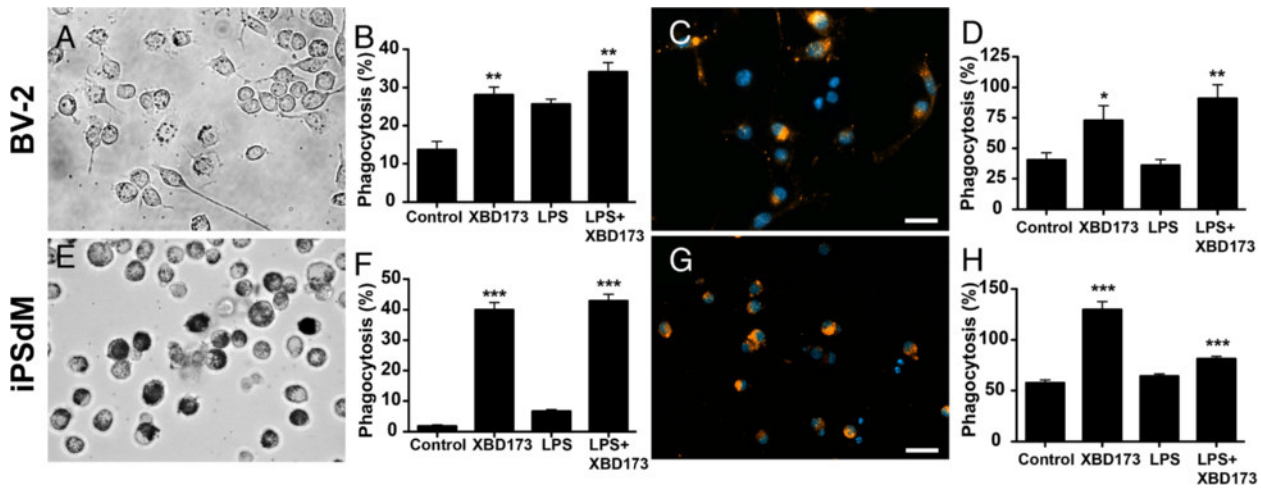

Figure 6 The TSPO ligand XBD173 increases microglial phagocytosis. Phagocytosis was monitored in BV-2 cells incubated with latex beads **(A, B)** or CM-DiI-stained apoptotic 661 W photoreceptor material **(C, D)**. Data show mean ± SEM (n = 9/group) ***P* <0.01 XBD173 + LPS versus LPS-treated cells, **P* <0.05 XBD173 versus vehicle-treated cells. Phagocytosis was monitored in human iPSdM cells incubated with latex beads **(E, F)** or CM-DiI-stained apoptotic 661 W photoreceptor material **(G, H)**. Data show mean ± SEM (n = 9/group) ****P* <0.01 XBD173 + LPS versus LPS-treated cell and XBD173 versus vehicle-treated cells. LPS, lipopolysaccharide; TSPO, translocator protein (18 kDa).

Discussion

Based on its selective expression in activated glial cells of the brain, TSPO is a marker for brain gliosis and TSPO ligands have been developed for *in vivo* imaging in human and mouse [27,28]. In the present study, we now show that selective up-regulation of TSPO is closely associated with the reactivity of microglia during retinal degeneration. To our knowledge, this is the first report to identify TSPO as a biomarker of activated microglia both in mouse and human retinal tissue. Major questions are why and how TSPO is up-regulated in reactive retinal microglia. Microgliosis in the retina of a mouse model of retinoschisin-deficiency starts at postnatal Day 14, peaks at P21 and then declines to lower levels [29]. The peak of microglial reactivity perfectly overlaps with high induction of TSPO expression levels. In the brain, TSPO detects activation of both microglia and astrocytes as a result of injury but also during recovery from injury [30,31], indicating that the presence of TSPO on activated glia may be a self-limiting mechanism of activation and proliferation. Our data of up-regulated TSPO expression in LPS-stimulated BV-2 microglia revealed that TLR4 signaling may play a crucial role in TSPO induction. In line with our experiments, up-regulation of TSPO in the recovery phase from neuropathic pain was prevented by pharmacological blockade of TLR4 [13]. We, therefore, hypothesize that retinal damage and the presence of damage-associated molecular patterns may trigger TLR4 signaling on microglia and thereby influence TSPO expression.

Our experiments demonstrate that the selective TSPO ligand XBD173 efficiently reversed the LPS-triggered

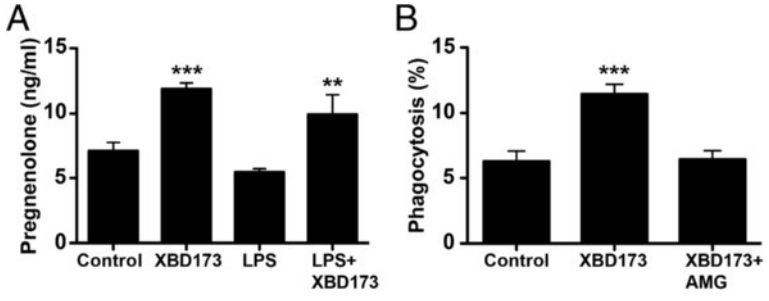

Figure 7 The TSPO ligand XBD173 increases pregnenolone levels and CYP11A1 inhibition prevents XBD173-induced phagocytosis. (A) Pregnenolone levels in cell culture supernatants of BV-2 cells treated with 20 μM XBD173, 50 ng/ml LPS, or 20 μM XBD173 + 50 ng/ml LPS for 24 hours. Data show mean ± SD (n = 3/group) ****P* <0.001 XBD173 versus vehicle-treated cells, ***P* <0.01 XBD173 + LPS versus LPS-treated cells. **(B)** Quantification of latex bead phagocytosis of BV-2 cells treated with 20 μM XBD173 or 20 μM XBD173 + 100 μM aminoglutethimide for 24 hours. Data show mean ± SEM (n = 30/group) ****P* <0.0001 XBD173 versus control cells. LPS, lipopolysaccharide; TSPO, translocator protein (18 kDa).

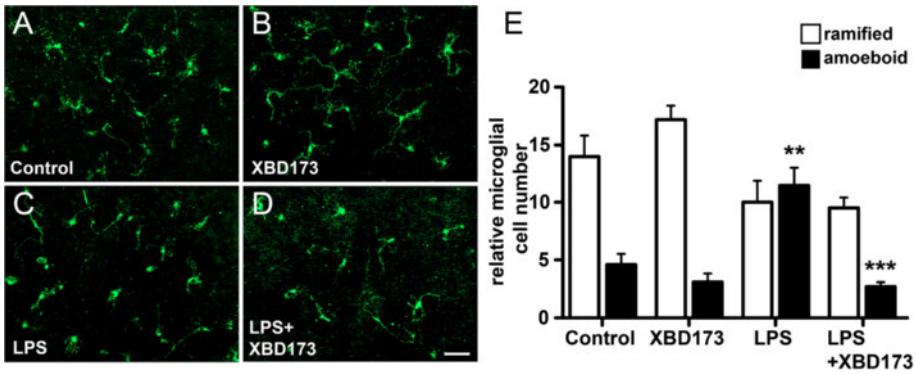

Figure 8 The TSPO ligand XBD173 reduces the number of alerted amoeboid retinal microglia *ex vivo*. (A-D) Representative GFP images of the retinal microglia network in explanted mouse retinas treated for 24 hours with vehicle **(A)**, 20 μM XBD173 **(B)**, 1 μg/ml LPS + vehicle **(C)** and 1 μg/ml LPS + 20 μM XBD173 **(D)**. **(E)** Quantification of ramified and amoeboid microglial cells in 10 independent image areas of two individual flat mounts (mean ± SEM). ***P* <0.01 for amoeboid cells in LPS versus control explants; ****P* <0.0001, for amoeboid cells in XBD173 + LPS versus LPS-treated explants. GFP, green fluorescent protein; LPS, lipopolysaccharide; TSPO, translocator protein (18 kDa).

production of the pro-inflammatory mediators CCL2, IL6 and iNOS. The TSPO ligand and mitochondrial effector PK11195 effectively inhibited LPS-induced microglial expression of COX-2 and TNF-alpha via modulation of $Ca2^{+}$-mediated signaling pathways [32]. The same compound reduced the expression of pro-inflammatory cytokines and neuronal apoptosis in quinolinic-acid-treated rat brain [33]. These findings together with our data on the global influence of XBD173 on gene expression revealed that targeting TSPO has a broad influence on inflammatory signaling in microglia. As we have shown in microglial cell culture, one potential mechanism of the effects of XBD173 could be the synthesis of pregnenolone, as has been previously shown for astrocytes [34]. These findings support the concept that microglia locally synthesize the anti-inflammatory neurosteroid precursor pregnenolone after activation of TSPO by respective ligands.

Our studies revealed that TSPO significantly influenced the f-actin cytoskeleton and fostered the formation of filopodia along with prominent effects on microglial migration and phagocytosis. A high phagocytic activity with a low migratory capacity is a typical hallmark of homeostatic microglia which constantly survey their environment with long protrusions [35]. Over the last years it has also become clear that microglial phagocytosis of apoptotic cells is largely anti-inflammatory [36]. Thus, we hypothesize that induction of TSPO signaling may shift alerted microglia to a more homeostatic and less inflammatory state. In line with this, TSPO ligands have been shown to influence chemotaxis and phagocytosis in peripheral blood cells [37-39]. TSPO overexpression also increased the proliferation and migratory capacity of rat C6 glioma cells whereas treatment with the TSPO ligand PK11195 had a strong anti-proliferative effect and exerted pro-apoptotic activity on these cells [40]. Treatment of LPS-challenged microglia with XBD173 could effectively reduce the number of amoeboid cells in the explanted mouse retina but did not significantly increase the fraction of ramified cells. This clearly indicates that TSPO signaling may serve to control microglia dynamics during the activation and/or resolution phase of retinal damage. In the native retina, endogenous ligands for TSPO may fulfill this function. Several endogenous molecules that bind TSPO have been identified in steroidogenic tissues, including the protein diazepam binding inhibitor (DBI) [41]. DBI can be cleaved into several active peptide fragments such as octadecaneuropeptide (ODN) and trikontatetraneuropeptide (TTN) which are released from astrocytes [10]. TTN then stimulates neurosynthesis in C6 glioma cells by acting on TSPO [8]. Thus, we hypothesize that either retinal astrocytes or Müller cells may express DBI and secrete active peptides to control microglial activity via targeting of TSPO.

Conclusions

We have shown that TSPO is highly expressed in reactive retinal microglia and BV-2 cells stimulated with LPS. The selective TSPO ligand XBD173 efficiently dampened pro-inflammatory gene expression in BV-2 microglial cells and reduced their neurotoxic potential on 661 W photoreceptor cells. XBD173 treatment of BV-2 cells and human iPS-derived microglial cells also promoted filopodia formation and phagocytic uptake. In the explanted mouse retina, XBD173 treatment blocked the LPS-dependent accumulation of amoeboid microglial cells. In conclusion, our data implicate that TSPO expression is connected to retinal microglia reactivity and that selective TSPO ligands may be a promising therapeutic approach to dampen microgliosis during retinal degeneration.

Abbreviations

CCL2: chemokine (C-C motif) ligand 2; CFSE: carboxyfluorescein diacetate succinimidyl ester; DBI: diazepam binding inhibitor; FACS: Fluorescence Activated Cell Sorting; FCS: fetal calf serum; GFAP: glial fibrillary acid protein; IL: interleukin; iNOS: inducible nitric oxide synthase; iPS: induced pluripotent stem cell; iPSdM: induced pluripotent stem cell-derived microglia; LPS: lipopolysaccharide; MAP2: microtubule-associated protein 2; NO: nitric oxide; TSPO: translocator protein (18 kDa).

Competing interests

RR has served as a consultant for Novartis developing TSPO ligands as anxiolytics and is a member of Novartis advisory boards. All other authors declare no competing financial interests.

Authors' contributions

TL, BW, HN and RR designed the research. MK, CN, AA, KM, FH, RS performed the research. MK, CN, HN and RS analyzed the data. TL and RR wrote the paper. All authors read and approved the final manuscript.

Acknowledgements

This work was funded by the Pro Retina Foundation and supported by the Hans- und Marlies Stock-Stiftung. The authors thank Prof. Muayyad Al Ubaidi for providing the 661 W photoreceptor cell line.

Author details

[1]Department of Ophthalmology, University of Cologne, D-50931 Cologne, Germany. [2]Department of Psychiatry and Psychotherapy, University of Regensburg, D-93053 Regensburg, Germany. [3]Institute of Reconstructive Neurobiology, University of Bonn, D-53127 Bonn, Germany. [4]Institute of Human Genetics, University of Regensburg, D-93053 Regensburg, Germany.

Received: 10 September 2013 Accepted: 23 December 2013
Published: 8 January 2014

References

1. Papadopoulos V, Baraldi M, Guilarte TR, Knudsen TB, Lacapere JJ, Lindemann P, Norenberg MD, Nutt D, Weizman A, Zhang MR, Gavish M: **Translocator protein (18 kDa): new nomenclature for the peripheral-type benzodiazepine receptor based on its structure and molecular function.** *Trends Pharmacol Sci* 2006, **27:**402–409.
2. McEnery MW, Snowman AM, Trifiletti RR, Snyder SH: **Isolation of the mitochondrial benzodiazepine receptor: association with the voltage-dependent anion channel and the adenine nucleotide carrier.** *Proc Natl Acad Sci U S A* 1992, **89:**3170–3174.
3. Papadopoulos V, Liu J, Culty M: **Is there a mitochondrial signaling complex facilitating cholesterol import?** *Mol Cell Endocrinol* 2007, **265–266:**59–64.
4. Rupprecht R, Papadopoulos V, Rammes G, Baghai TC, Fan J, Akula N, Groyer G, Adams D, Schumacher M: **Translocator protein (18 kDa) (TSPO) as a therapeutic target for neurological and psychiatric disorders.** *Nat Rev Drug Discov* 2010, **9:**971–988.
5. Kuhlmann AC, Guilarte TR: **Cellular and subcellular localization of peripheral benzodiazepine receptors after trimethyltin neurotoxicity.** *J Neurochem* 2000, **74:**1694–1704.
6. Maeda J, Higuchi M, Inaji M, Ji B, Haneda E, Okauchi T, Zhang MR, Suzuki K, Suhara T: **Phase-dependent roles of reactive microglia and astrocytes in nervous system injury as delineated by imaging of peripheral benzodiazepine receptor.** *Brain Res* 2007, **1157:**100–111.
7. Veiga S, Azcoitia I, Garcia-Segura LM: **Extragonadal synthesis of estradiol is protective against kainic acid excitotoxic damage to the hippocampus.** *Neuroreport* 2005, **16:**1599–1603.
8. Papadopoulos V, Berkovich A, Krueger KE, Costa E, Guidotti A: **Diazepam binding inhibitor and its processing products stimulate mitochondrial steroid biosynthesis via an interaction with mitochondrial benzodiazepine receptors.** *Endocrinology* 1991, **129:**1481–1488.
9. Girard C, Liu S, Adams D, Lacroix C, Sineus M, Boucher C, Papadopoulos V, Rupprecht R, Schumacher M, Groyer G: **Axonal regeneration and neuroinflammation: roles for the translocator protein 18 kDa.** *J Neuroendocrinol* 2012, **24:**71–81.
10. Chen MK, Guilarte TR: **Translocator protein 18 kDa (TSPO): molecular sensor of brain injury and repair.** *Pharmacol Ther* 2008, **118:**1–17.
11. Barron AM, Garcia-Segura LM, Caruso D, Jayaraman A, Lee JW, Melcangi RC, Pike CJ: **Ligand for translocator protein reverses pathology in a mouse model of Alzheimer's disease.** *J Neurosci* 2013, **33:**8891–8897.
12. Daugherty DJ, Selvaraj V, Chechneva OV, Liu XB, Pleasure DE, Deng W: **A TSPO ligand is protective in a mouse model of multiple sclerosis.** *EMBO Mol Med* 2013, **5:**891–903.
13. Wei XH, Wei X, Chen FY, Zang Y, Xin WJ, Pang RP, Chen Y, Wang J, Li YY, Shen KF, Zhou LJ, Liu XG: **The upregulation of translocator protein (18 kDa) promotes recovery from neuropathic pain in rats.** *J Neurosci* 2013, **33:**1540–1551.
14. Rupprecht R, Rammes G, Eser D, Baghai TC, Schule C, Nothdurfter C, Troxler T, Gentsch C, Kalkman HO, Chaperon F, Uzunov V, McAllister KH, Bertaina-Anglade V, La Rochelle CD, Tuerck D, Floesser A, Kiese B, Schumacher M, Landgraf R, Holsboer F, Kucher K: **Translocator protein (18 kD) as target for anxiolytics without benzodiazepine-like side effects.** *Science* 2009, **325:**490–493. Erratum in: *Science* 2009, **325**:1072. Dosage error in article text.
15. Nothdurfter C, Rammes G, Baghai TC, Schule C, Schumacher M, Papadopoulos V, Rupprecht R: **Translocator protein (18 kDa) as a target for novel anxiolytics with a favourable side-effect profile.** *J Neuroendocrinol* 2012, **24:**82–92.
16. Nothdurfter C, Baghai TC, Schule C, Rupprecht R: **Translocator protein (18 kDa) (TSPO) as a therapeutic target for anxiety and neurologic disorders.** *Eur Arch Psychiatry Clin Neurosci* 2012, **262**(Suppl 2):S107–S112.
17. Berger W, Kloeckener-Gruissem B, Neidhardt J: **The molecular basis of human retinal and vitreoretinal diseases.** *Prog Retin Eye Res* 2010, **29:**335–375.
18. Langmann T: **Microglia activation in retinal degeneration.** *J Leukoc Biol* 2007, **81:**1345–1351.
19. Weber BH, Schrewe H, Molday LL, Gehrig A, White KL, Seeliger MW, Jaissle GB, Friedburg C, Tamm E, Molday RS: **Inactivation of the murine X-linked juvenile retinoschisis gene, Rs1h, suggests a role of retinoschisin in retinal cell layer organization and synaptic structure.** *Proc Natl Acad Sci U S A* 2002, **99:**6222–6227.
20. Gehrig A, Langmann T, Horling F, Janssen A, Bonin M, Walter M, Poths S, Weber BH: **Genome-wide expression profiling of the retinoschisin-deficient retina in early postnatal mouse development.** *Invest Ophthalmol Vis Sci* 2007, **48:**891–900.
21. Ebert S, Weigelt K, Walczak Y, Drobnik W, Mauerer R, Hume DA, Weber BH, Langmann T: **Docosahexaenoic acid attenuates microglial activation and delays early retinal degeneration.** *J Neurochem* 2009, **110:**1863–1875.
22. Sasmono RT, Oceandy D, Pollard JW, Tong W, Pavli P, Wainwright BJ, Ostrowski MC, Himes SR, Hume DA: **A macrophage colony-stimulating factor receptor-green fluorescent protein transgene is expressed throughout the mononuclear phagocyte system of the mouse.** *Blood* 2003, **101:**1155–1163.
23. Ebert S, Schoeberl T, Walczak Y, Stoecker K, Stempfl T, Moehle C, Weber BH, Langmann T: **Chondroitin sulfate disaccharide stimulates microglia to adopt a novel regulatory phenotype.** *J Leukoc Biol* 2008, **84:**736–740.
24. Beutner C, Roy K, Linnartz B, Napoli I, Neumann H: **Generation of microglial cells from mouse embryonic stem cells.** *Nat Protoc* 2010, **5:**1481–1494.
25. Roy K, Beutner C, Neumann H: **Perspectives of stem cell-derived microglia for medicine**. In *Embryonic Stem Cells - Recent Advances in Pluripotent Stem Cell-Based Regenerative Medicine.* Edited by Atwook C, Atwook C. Rijeka, Croatia: InTech Europe; 2011:171–188.
26. Da Settimo F, Simorini F, Taliani S, La Motta C, Marini AM, Salerno S, Bellandi M, Novellino E, Greco G, Cosimelli B, Da Pozzo E, Costa B, Simola N, Morelli M, Martini C: **Anxiolytic-like effects of N, N-dialkyl-2-phenylindol-3-ylglyoxylamides by modulation of translocator protein promoting neurosteroid biosynthesis.** *J Med Chem* 2008, **51:**5798–5806.
27. Chauveau F, Boutin H, Van Camp N, Dollé F, Tavitian B: **Nuclear imaging of neuroinflammation: a comprehensive review of [11C]PK11195 challengers.** *Eur J Nucl Med Mol Imaging* 2008, **35:**2304–2319.
28. Venneti S, Lopresti BJ, Wiley CA: **Molecular imaging of microglia/macrophages in the brain.** *Glia* 2013, **61:**10–23.
29. Karlstetter M, Walczak Y, Weigelt K, Ebert S, Van den Brulle J, Schwer H, Fuchshofer R, Langmann T: **The novel activated microglia/macrophage WAP domain protein, AMWAP, acts as a counter-regulator of proinflammatory response.** *J Immunol* 2010, **185:**3379–3390.
30. Chen MK, Baidoo K, Verina T, Guilarte TR: **Peripheral benzodiazepine receptor imaging in CNS demyelination: functional implications of anatomical and cellular localization.** *Brain* 2004, **127:**1379–1392.

31. Chen MK, Guilarte TR: **Imaging the peripheral benzodiazepine receptor response in central nervous system demyelination and remyelination.** *Toxicol Sci* 2006, **91:**532–539.
32. Choi HB, Khoo C, Ryu JK, van Breemen E, Kim SU, McLarnon JG: **Inhibition of lipopolysaccharide-induced cyclooxygenase-2, tumor necrosis factor-alpha and [Ca2+]i responses in human microglia by the peripheral benzodiazepine receptor ligand PK11195.** *J Neurochem* 2002, **83:**546–555.
33. Ryu JK, Choi HB, McLarnon JG: **Peripheral benzodiazepine receptor ligand PK11195 reduces microglial activation and neuronal death in quinolinic acid-injected rat striatum.** *Neurobiol Dis* 2005, **20:**550–561.
34. Cascio C, Brown RC, Liu Y, Han Z, Hales DB, Papadopoulos V: **Pathways of dehydroepiandrosterone formation in rat brain glia.** *J Steroid Biochem Mol Biol* 2000, **75:**177–186.
35. Nimmerjahn A, Kirchhoff F, Helmchen F: **Resting microglial cells are highly dynamic surveillants of brain parenchyma *in vivo*.** *Science* 2005, **308:**1314–1318.
36. Sierra A, Abiega O, Shahraz A, Neumann H: **Janus-faced microglia: beneficial and detrimental consequences of microglial phagocytosis.** *Front Cell Neurosci* 2013, **7:**6.
37. Ruff MR, Pert CB, Weber RJ, Wahl LM, Wahl SM, Paul SM: **Benzodiazepine receptor-mediated chemotaxis of human monocytes.** *Science* 1985, **229:**1281–1283.
38. Cosentino M, Marino F, Cattaneo S, Di Grazia L, Francioli C, Fietta AM, Lecchini S, Frigo G: **Diazepam-binding inhibitor-derived peptides induce intracellular calcium changes and modulate human neutrophil function.** *J Leukoc Biol* 2000, **67:**637–643.
39. Marino F, Cattaneo S, Cosentino M, Rasini E, Di Grazia L, Fietta AM, Lecchini S, Frigo G: **Diazepam stimulates migration and phagocytosis of human neutrophils: possible contribution of peripheral-type benzodiazepine receptors and intracellular calcium.** *Pharmacology* 2001, **63:**42–49.
40. Rechichi M, Salvetti A, Chelli B, Costa B, Da Pozzo E, Spinetti F, Lena A, Evangelista M, Rainaldi G, Martini C, Gremigni V, Rossi L: **TSPO over-expression increases motility, transmigration and proliferation properties of C6 rat glioma cells.** *Biochim Biophys Acta* 2008, **1782:**118–125.
41. Guidotti A, Forchetti CM, Corda MG, Konkel D, Bennett CD, Costa E: **Isolation, characterization, and purification to homogeneity of an endogenous polypeptide with agonistic action on benzodiazepine receptors.** *Proc Natl Acad Sci U S A* 1983, **80:**3531–3535.

doi:10.1186/1742-2094-11-3
Cite this article as: Karlstetter *et al.*: Translocator protein (18 kDa) (TSPO) is expressed in reactive retinal microglia and modulates microglial inflammation and phagocytosis. *Journal of Neuroinflammation* 2014 **11**:3.

Scholz et al. Journal of Neuroinflammation (2015) 12:201
DOI 10.1186/s12974-015-0422-5

JOURNAL OF NEUROINFLAMMATION

RESEARCH Open Access

Targeting translocator protein (18 kDa) (TSPO) dampens pro-inflammatory microglia reactivity in the retina and protects from degeneration

Rebecca Scholz[1], Albert Caramoy[1], Mohajeet B. Bhuckory[2], Khalid Rashid[1], Mei Chen[2], Heping Xu[2], Christian Grimm[3] and Thomas Langmann[1*]

Abstract

Background: Reactive microglia are commonly seen in retinal degenerative diseases, and neurotoxic microglia responses can contribute to photoreceptor cell death. We and others have previously shown that translocator protein (18 kDa) (TSPO) is highly induced in retinal degenerations and that the selective TSPO ligand XBD173 (AC-5216, emapunil) exerts strong anti-inflammatory effects on microglia in vitro and ex vivo. Here, we investigated whether targeting TSPO with XBD173 has immuno-modulatory and neuroprotective functions in two mouse models of acute retinal degeneration using bright white light exposure.

Methods: BALB/cJ and *Cx3cr1*$^{GFP/+}$ mice received intraperitoneal injections of 10 mg/kg XBD173 or vehicle for five consecutive days, starting 1 day prior to exposure to either 15,000 lux white light for 1 h or 50,000 lux focal light for 10 min, respectively. The effects of XBD173 treatment on microglia and Müller cell reactivity were analyzed by immuno-stainings of retinal sections and flat mounts, fluorescence-activated cell sorting (FACS) analysis, and mRNA expression of microglia markers using quantitative real-time PCR (qRT-PCR). Optical coherence tomography (OCT), terminal deoxynucleotidyl transferase dUTP nick end labeling (TUNEL) stainings, and morphometric analyses were used to quantify the extent of retinal degeneration and photoreceptor apoptosis.

Results: Four days after the mice were challenged with bright white light, a large number of amoeboid-shaped alerted microglia appeared in the degenerating outer retina, which was nearly completely prevented by treatment with XBD173. This treatment also down-regulated the expression of TSPO protein in microglia but did not change the TSPO levels in the retinal pigment epithelium (RPE). RT-PCR analysis showed that the microglia/macrophage markers Cd68 and activated microglia/macrophage whey acidic protein (Amwap) as well as the pro-inflammatory genes *Ccl2* and *Il6* were reduced after XBD173 treatment. Light-induced degeneration of the outer retina was nearly fully blocked by XBD173 treatment. We further confirmed these findings in an independent mouse model of focal light damage. Retinas of animals receiving XBD173 therapy displayed significantly more ramified non-reactive microglia and more viable arrestin-positive cone photoreceptors than vehicle controls.

Conclusions: Targeting TSPO with XBD173 effectively counter-regulates microgliosis and ameliorates light-induced retinal damage, highlighting a new pharmacological concept for the treatment of retinal degenerations.

Keywords: Translocator protein (18 kDa) (TSPO), Microglia, Photoreceptors, Retinal degeneration, Light damage, Age-related macular degeneration

* Correspondence: thomas.langmann@uk-koeln.de
[1]Department of Ophthalmology, Laboratory for Experimental Immunology of the Eye, University of Cologne, 50931 Cologne, Germany
Full list of author information is available at the end of the article

Background

Microglial cells are the resident tissue macrophages of the central nervous system (CNS), including the retina. In the healthy retina, they are located in the plexiform layers from where they permanently scan the retinal environment with their motile protrusions [1]. Several receptors that are specific for the binding of chemokines, cytokines, complement factors, antibodies, or damage-associated molecular patterns enable these cells to recognize and immediately respond to pathological changes of their environment [2–4]. Beside their homeostatic function in the healthy retina, microglia reactivity and age-related changes of microglia physiology contribute to degenerative pathologies of the retina and the entire CNS [3, 5–14]. Together with monocytes and macrophages, microglial cells are major players in chronic immune processes including parainflammation [15]. Reactive microglia are detectable in the damaged photoreceptor layers of patients with degenerative retinal diseases such as retinitis pigmentosa and age-related macular degeneration (AMD) [6]. Microglia not only phagocytose dead cells but also take up living rods in a mouse model for retinitis pigmentosa [10]. Therefore, microglial activation cannot be just regarded as a bystander effect but rather actively contributes to photoreceptor cell death during retinal degeneration.

In attempts to better characterize retinal microglia reactivity and find novel markers, we and others have previously identified very high expression of translocator protein (18 kDa) in reactive retinal microglia [16, 17]. Translocator protein (TSPO), previously known as the peripheral benzodiazepine receptor, likely mediates the transport of cholesterol into the inner mitochondrial membrane, where it serves as a precursor for steroids and neurosteroids [18]. The protein is constitutively expressed in steroidogenic tissues and up-regulated in activated glial cells [19–21]. Glial up-regulation of TSPO is a major hallmark of neurodegenerative diseases [22], and various TSPO ligands have been developed as molecular markers to detect gliosis by means of PET imaging [23].

Specific TSPO ligands are also under investigation as treatment options for neurological disorders including Alzheimer's disease [24], multiple sclerosis [25], neuropathic pain [26], peripheral nerve injury [22], and anxiety disorders [27]. Classical synthetic TSPO ligands such as the benzodiazepine derivative 4′-chlorodiazepam (Ro5-4864) and the isoquinoline carboxamide PK11195 directly enhance GABAergic neurotransmission [28]. In contrast, structurally different synthetic TSPO ligands such as etifoxine (Stresam) and XBD173 (AC-5216, emapunil) also stimulate the synthesis of neurosteroids and exert potent anti-inflammatory and neuroprotective effects [29]. XBD173 is a very selective and high-affinity phenylpurine ligand for TSPO whereas the benzoxazine etifoxine additionally binds $GABA_A$ receptors [30]. Since XBD173 has a high and specific affinity for TSPO with a more beneficial side-effect profile than benzodiazepine derivatives, a precise and potentially long-term application to limit neuroinflammation seems feasible.

In a previous report, we have comprehensively characterized the anti-inflammatory effects of the TSPO ligand XBD173 using murine and human microglial cells as well as cultured mouse retinal explants [16]. XBD173 strongly suppressed pro-inflammatory gene expression in LPS-challenged microglia and diminished their neurotoxic potential on photoreceptor cell cultures, indicating that targeting TSPO with XBD173 is a promising approach to control microglial reactivity [16]. In this study, we addressed the questions whether XBD173 influences microglial reactivity in vitro and protects from acute white light-induced retinal degeneration in two different mouse models. We selected white light exposure as it is an environmental risk factor and mimics several features of human retinal degenerative diseases in rodents [31–33]. This model is also very useful for a quantitative correlation of microglial responses with processes of retinal degeneration [34–36].

Methods

Reagents

XBD173 (emapunil) was obtained by custom synthesis from APAC Pharmaceuticals, Ellicott City, MD21042. XBD173 was dissolved in DMSO.

RNA isolation and reverse transcription

Total RNA was extracted from murine retinas using the NucleoSpin® RNA Mini Kit (Macherey-Nagel, Dueren, Germany). RNA was quantified spectrophotometrically with a NanoDrop 2000 (Thermo Scientific). First-strand cDNA synthesis was carried out with the Revert Aid H Minus First-strand cDNA Synthesis Kit (Fermentas, K1632).

Quantitative RT-PCR

cDNA (25 ng) were amplified in 10 μl reaction mixture consisting of 5 μl Fast Start Universal Probe Master (Rox) (Roche), 2 μl of primers (10 μM), 0.375 μl purified water, and 0.125 μl of dual-labeled UPL probe (Roche Applied Science, Basel, Switzerland) with an Applied Biosystems 7900 HT Fast Real-Time PCR system (Applied Biosystems, Carlsbad, CA, USA). The following reaction parameters were used: 10 min 95 °C hold, followed by 40 cycles of 15 s 95 °C melt, and 1 min 60 °C anneal/extension. Primer sequences and UPL probe numbers were as follows: *Cd68*, forward primer 5′-ctctctaaggctacaggctgct-3′, reverse primer 5′-tcacggttgcaagagaaaca-3′, probe #27; *Amwap*, forward primer 5′-tttgatcactgtggggatga-3′, reverse primer 5′-acacttt ctggtgaaggcttg-3′, probe #1; *Tspo*, forward primer 5′-actgta ttcagccatggggta-3′, reverse primer 5′-accatagcgtcctctgtgaa

a-3′, probe #33; *Il6*, forward primer 5′-gatggatgctaccaaactg-gat-3′, reverse primer 5′-ccaggtagctatggtactccaga-3′, probe #6; *iNos*, forward primer 5′-ctttgccacggacgagac-3′, reverse primer 5′-tcattgtactctgagggctga-3′, probe #13; *Ccl2*, forward primer 5′-catccacgtgttggctca-3′, reverse primer 5′-gat catcttgctggtgaatgagt-3′, probe #62; *Casp8*, forward primer 5′-tgaacaatgagatccccaaat-3′, reverse primer 5′-caaaaatttca agcaggctca-3′, probe #11; and *Atp5b*, forward primer 5′-gg cacaatgcaggaaagg-3′, reverse primer 5′-tcagcaggcacatagata gcc-3′, probe #77. Measurements were performed in triplicates. *Atp5b* expression was used as reference gene, and results were analyzed with the ABI sequence detector software version 2.4 using the ΔΔCt method for relative quantification.

Animals

Experiments were performed with 10–14-week-old albino BALB/cJ mice and *Cx3cr1*$^{GFP/+}$ mice on C57BL/6J background of both sexes. Animals were housed in an air-conditioned environment with 12-h light-dark schedule and had free access to water and food. All experimental procedures complied with the German law on animal protection and the ARVO Statement for the Use of Animals in Ophthalmic and Vision Research. The animal protocols used in this study were reviewed and approved by the governmental body responsible for animal welfare in the state of Nordrhein-Westfalen (Landesamt für Natur, Umwelt und Verbraucherschutz Nordrhein-Westfalen, Germany) (reference number 84-02.04.2015-A039) and by the Animal Welfare and Ethical Review Board of Queen's University Belfast under the regulation of the UK Home Office Animal (Scientific Procedures) Act 1986.

XBD173 administration

The mice received intraperitoneal injections of XBD173 at a dose of 10 mg/kg body weight, dissolved in DMSO or DMSO vehicle control twice daily for the first 2 days, starting 1 day before the light exposure and once daily for the remaining 3 days.

Light exposure regimens

BALB/cJ and *Cx3cr1*$^{GFP/+}$ mice were dark-adapted for 16 h before light exposure. After pupil dilatation with 1 % phenylephrine and 2.5 % tropicamide under dim red light, the mice were exposed to bright white light with an intensity of 15,000 lux for 1 h or focal white light with an intensity of 50,000 lux delivered by an otoscope (1218AA, Karl Storz, Tuttlingen, Germany) for 10 min, respectively. After light exposure, the animals were housed in dark-reared conditions overnight and then maintained under normal light conditions for the remaining experimental period.

Immunohistochemistry

Eyes were harvested for immunohistochemical analysis 4 days after light exposure. After fixation with 4 % paraformaldehyde, eyes were embedded in optimal cutting temperature compound or dissected for retinal flat mount analysis. Sixteen-micrometer sections were rehydrated with phosphate-buffered saline (PBS) and blocked with 1 % dried milk solution containing 0.01 % Triton X-100. Flat mounts were incubated with 5 % Tween and 5 % Triton X-100 in PBS overnight, and non-specific binding was blocked by incubation with dried milk solution. Subsequently, retinal sections and flat mounts were incubated with primary antibodies at 4 °C overnight. Primary antibodies targeting the following proteins were used: rabbit anti-Iba1 antibody (dilution 1:500; Wako Chemicals, Neuss, Germany), rabbit anti-TSPO antibody (dilution 1:250; Abcam, Cambridge, UK), rabbit anti-glial fibrillary acidic protein (dilution 1:200; G9269, Sigma, USA), mouse anti-glutamine synthetase (dilution 1:200; MAB302, Millipore, Darmstadt, Germany), and rabbit anti-cone arrestin (Millipore, Darmstadt, Germany). After a washing step, the sections and flat mounts were incubated with a secondary antibody either conjugated to Alexa488 (green; dilution 1:1000) or Alexa594 (red; dilution 1:800) (Jackson Immuno-Research, West Grove, PA, USA) for 1 h. After counterstaining with 4′,6-Diamidin-2-phenylindol (DAPI) in some instances, the samples were mounted in DAKO fluorescent mounting medium (Dako Deutschland GmbH, Hamburg, Germany) and analyzed with an Axioskop2 MOT Plus Apotome microscope (Carl Zeiss) or an Eclipse TE200-U confocal microscope (Nikon).

Optical coherence tomography

Animals were anesthetized by intraperitoneal injection of Rompun (10 mg/kg body weight)-Ketavet (100 mg/kg body weight), and their pupils were dilated with phenylephrine HCl (0.25 %)-tropicamide (0.05 %) before image acquisition. Spectral domain optical coherence tomography (SD-OCT) was performed on both eyes with a Spectralis™ HRA + OCT device (Heidelberg Engineering) to investigate structural changes in the retina after light exposure and XBD173 administration. Thickness measurements were performed using the Heidelberg Eye Explorer Software using a circular ring scan (circle diameters 3 and 6 mm), centered on the optic nerve head, which represents the average retinal thickness (μm) in a certain field.

TUNEL assay and morphometric analyses

Retinal sections were labeled with an in situ cell death detection kit, fluorescein (Roche), to detect the amount of apoptotic cells 4 days after light exposure. For a better overview, the sections were also counterstained with DAPI for 10 min. After a washing procedure, sections were mounted in DAKO fluorescent mounting medium

(Dako Deutschland GmbH, Hamburg, Germany) and analyzed with an Axioskop2 MOT Plus Apotome microscope (Carl Zeiss). Quantitative morphometric analyses were performed by counting the number of rows of photoreceptor nuclei along the nasal/temporal axis.

Flow cytometry

Mouse retinas were dissected 4 days after light exposure and dissociated using the Neuronal Tissue Dissociation Kit-Postnatal Neurons (MACS, Miltenyi, Bergisch Gladbach, Germany). To identify microglia cells and macrophages, the single-cell suspension was stained with anti-mouse/human CD11b-APC antibody (MACS, Miltenyi, Bergisch Gladbach, Germany) at a dilution of 1:10 for 15 min in the dark at 4 °C. After a washing step, cells were fixed with FluoroFix Buffer (Biolegend, San Diego, CA, USA) in the dark for 30 min at room temperature. Afterwards, the cells were washed and resuspended in PBS solution (pH 7.2, 0.5 % containing bovine serum albumin (BSA), and 2 mM EDTA) until flow cytometric analyses with a fluorescence-activated cell sorting (FACS) Canto II (Becton Dickinson, Heidelberg, Germany). The number of CD11b+ cells was determined using FlowJo software (Treestar, Ashland, USA).

Statistical analysis

The differences between control mice and animals after light exposure that either received sham injections or XBD173 injections were analyzed using a one-way ANOVA and Dunnett's multiple comparison test. $p < 0.05$ was considered statistically significant.

Results

The TSPO ligand XBD173 prevents microglia reactivity and gliosis in murine retinas exposed to acute white light

We have previously identified that *Tspo* mRNA and protein are highly induced in genetic models of retinal degeneration and that its specific ligand XBD173 has potent anti-inflammatory activity on microglia in vitro [16]. Based on these data, we hypothesized that XBD173 could also modulate microglial responses in the damaged retina in vivo. We have chosen acute light-induced degeneration as it is a fast and reproducible mouse model that mimics several features of human retinal degenerative diseases including innate immune activation and selective cell death of photoreceptor cells [33].

Dark-adapted BALB/cJ mice were exposed to white light with an intensity of 15,000 lux for 1 h. The animals received daily intraperitoneal injections of 10 mg/kg XBD173 or vehicle, starting 1 day before the light exposure for five consecutive days (Fig. 1a). Four days after light exposure, the effects of XBD173 treatment on microgliosis were analyzed by staining of retinal sections and flat mounts. In healthy controls, immunolabeling of retinal sections with the marker IBA1 showed ramified microglia exclusively in the plexiform layers and inner retina (Fig. 1b). Light exposure and vehicle administration induced strong microglia reactivity resulting in the migration and appearance of amoeboid-shaped microglia in the degenerating photoreceptor layer and the subretinal area (Fig. 1c). This severe thinning of the outer retina and accumulation of microglia in and around the outer nuclear layer was not detectable in mice treated with XBD173 (Fig. 1d). We next analyzed changes in the microglial network in retinal flat mounts stained with Iba1. In contrast to controls, where microglial cells are highly ramified in the outer plexiform layer (OPL) (Fig. 1e), light-exposed retinas showed clear signs of microglia reactivity in the OPL (Fig. 1f), which was reverted in conditions of XBD173 therapy (Fig. 1g). Furthermore, the appearance of many amoeboid-shaped microglia in the subretinal area triggered by light exposure was strongly reduced in the XBD173 treatment group (Fig. 1h–j). This finding that XBD173 very likely prevented migration of many microglia from the inner to the outer retina was corroborated by a quantitative analysis counting the number of microglial cells in the outer nuclear layer (ONL) and subretinal area (Fig. 1k, l). We then determined the number of CD11b-positive cells in the retina using flow cytometry. These data also showed that XBD173 administration strongly reduced the percentage of CD11b-positive cells in the light-exposed retina compared to vehicle controls (Fig. 1m–p).

We then wanted to better characterize the reactive gliosis and its relation to the expression of TSPO itself. Exposure to light in the vehicle control triggered strong expression of TSPO that was mainly confined to outer retinal microglia and some astrocytes in the ganglion cell layer (Fig. 2a, b). This cellular expression pattern is in agreement with previous immunohistochemical data from genetic mouse models of retinal degeneration [16, 37] and highlights the induced expression of TSPO in microglia upon activation. Administration of XBD173 strongly diminished TSPO expression (Fig. 2c), indicating a much less reactive microgliosis and confirming our stainings with Iba1 (Fig. 1). Interestingly, we also identified specific expression of TSPO in the retinal pigment epithelium (RPE) network that was visualized by co-staining with phalloidin (Fig. 2d). However, this RPE-specific expression pattern of TSPO was not obviously influenced by light exposure or XBD173 therapy (Fig. 2e, f), indicating a constitutive role of TSPO in the RPE that is unrelated to gliosis. We then analyzed the expression of glutamine synthetase (GS), a constitutively expressed Müller cell protein and glial fibrillary acid protein (GFAP), a marker für Müller cell and astrocyte reactivity. GS staining was not significantly changed by light exposure and XBD173 treatment (Fig. 2g–i, m), whereas XBD173 significantly reduced the light-dependent induction of GFAP expression (Fig. 2j–l, n). These findings

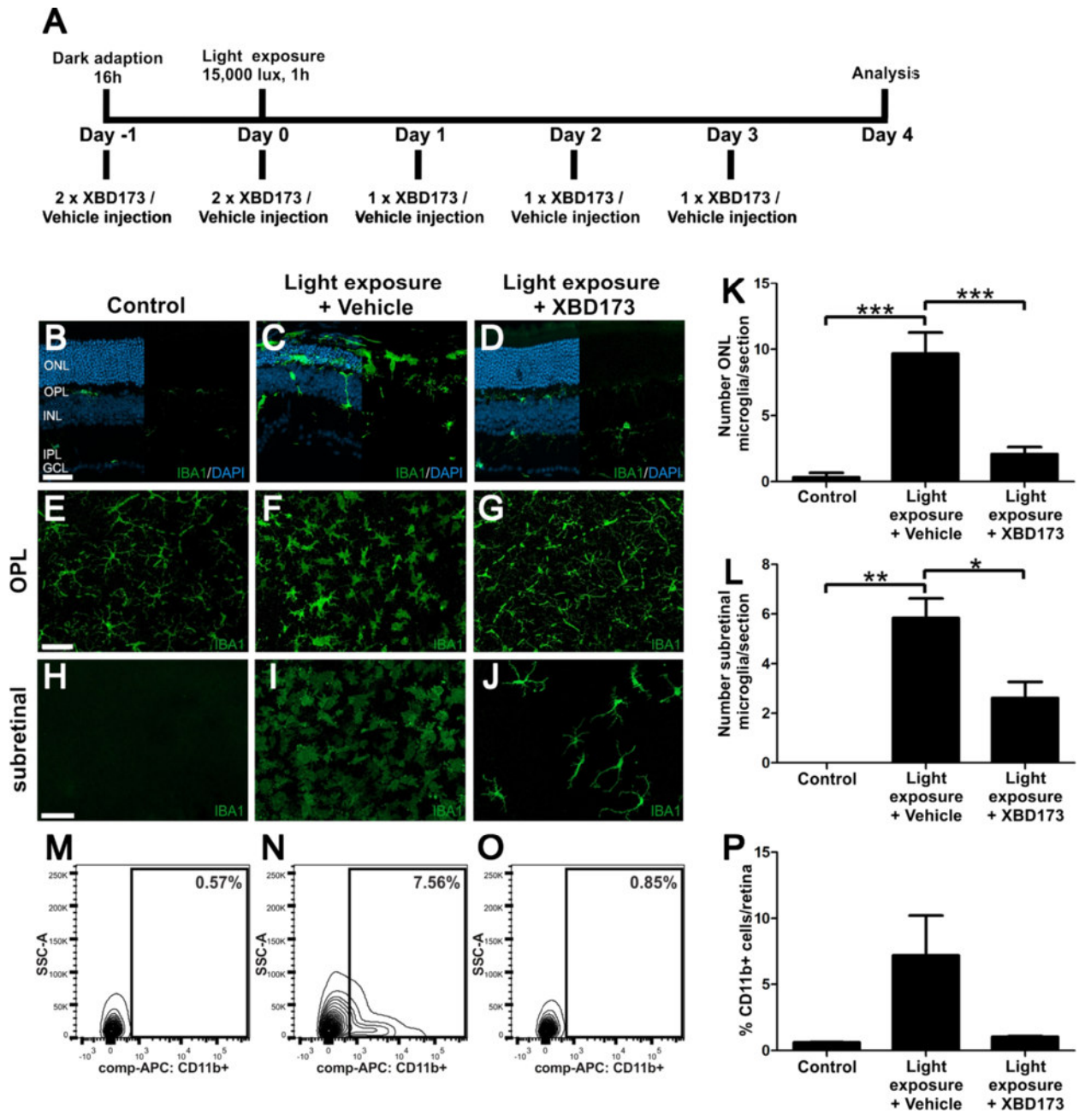

Fig. 1 XBD173 treatment of light-exposed mice prevents microglia reactivity. **a** Light exposure regimen and mode of XBD173 administration. Representative photomicrographs show retinal sections (**b**–**d**) and flat mounts (**e**–**j**) stained with IBA1 (*green*) and DAPI (*blue*). In control retinas, microglial cells were located in the OPL, IPL, and GCL (**b**, **e**, **h**). Light-exposed retinas injected with vehicle control showed a massive thinning of the ONL and many amoeboid-shaped, reactive microglia in the ONL and the subretinal space (**c**, **f**, **i**). Compared to vehicle controls, the ONL of XBD173-treated retinas appeared markedly preserved and less amoeboid microglia were detectable in the ONL and the subretinal space (**d**, **g**, **j**). The total number of Iba1-positive microglial cells in the ONL (**k**) and the subretinal area (**l**) after light damage was significantly reduced in the XBD173 therapy group. Data show mean ± SEM (control $n = 3$, light exposure and vehicle treatment $n = 6$, light exposure and XBD173 treatment $n = 12$ sections). The percentage of CD11b-positive cells in the retina as determined by flow cytometry was strongly reduced by XBD173 treatment in representative FACS plots (**m**–**o**) and quantitative analyses of $n = 3$–4 retinas (**p**). *ONL* outer nuclear layer, *OPL* outer plexiform layer, *INL* inner nuclear layer, *IPL* inner plexiform layer, *GCL* ganglion cell layer. *$p < 0.05$; **$p < 0.01$; ***$p < 0.001$. Scale bar 50 μm

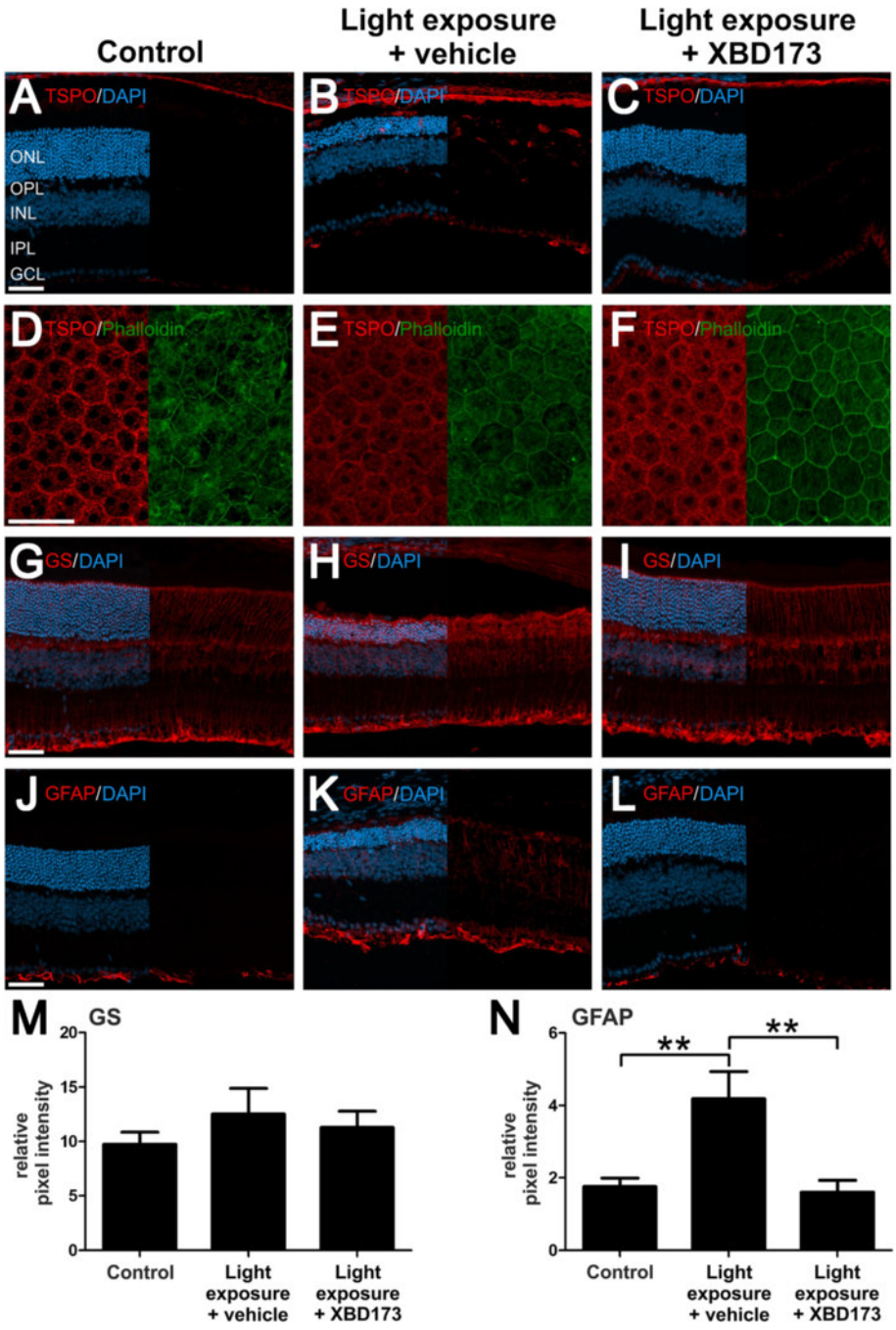

Fig. 2 XBD173 treatment of light-exposed mice down-regulates TSPO in microglia and prevents gliosis. Representative photomicrographs of retinal sections and flat mounts from mice 4 days after light exposure. Control retinas show weak TSPO labeling (**a**), and strong up-regulation of TSPO expression confined to microglia was present upon light exposure and vehicle treatment (**b**). XBD173-treated mice displayed only constitutive expression of TSPO in the RPE, but no strong signal in the retina was found (**c**). Number of analyzed photomicrographs: control $n = 5$ sections from two individual mice, light exposure and vehicle treatment $n = 7$ sections from five individual mice, light exposure and XBD173 treatment $n = 11$ sections from five individual mice. The expression of TSPO in the RPE was relatively unaffected in the different conditions as shown in flat mount images stained with anti-TSPO antibody and phalloidin (**d**–**f**). Glutamine synthetase (*GS*), a constitutive Müller cell protein, and glial fibrillary acidic protein (*GFAP*) as markers for gliosis were analyzed (**g**–**n**). GS expression did not differ in the various treatment groups (**g**–**i**, **m**) whereas GFAP expression was changed significantly (**j**–**l**, **n**). Data show mean ± SEM (control $n = 5$ sections from five individual mice, light exposure and vehicle treatment $n = 5$ sections from three individual mice, light exposure and XBD173 treatment $n = 5$ sections from four individual mice). $^{**}p < 0.01$. *ONL* outer nuclear layer, *OPL* outer plexiform layer, *INL* inner nuclear layer, *IPL* inner plexiform layer, *GCL* ganglion cell layer. Scale bar 50 μm

indicate that gliosis triggered by light damage can be prevented by targeting TSPO.

XBD173 reduces pro-inflammatory gene expression in retinal degeneration

In addition to these cellular analyses of retinal microglia, we investigated whether mRNA levels of pro-inflammatory transcripts were influenced by XBD173 administration in vivo. CD68, activated microglia/macrophage whey acidic protein (AMWAP), and TSPO itself are molecules that are connected with microglia proliferation and reactivity [16, 38, 39]. Four days after light exposure, all three genes were induced in the retina, with especially high levels of *Amwap* (Fig. 3a–c). In light-exposed mice treated with XBD173, the expression of *Cd68* (Fig. 3a, $p = 0.0342$), *Amwap* (Fig. 3b, $p = 0.0182$), and *Tspo* (Fig. 3c, $p = 0.0338$) were significantly suppressed. Furthermore, transcripts that reflect the activation of key microglial pathways including chemotaxis, pro-inflammatory cytokines, and radical production were analyzed. mRNA levels of the chemotactic molecule *Ccl2* and the cytokine *Il6* were strongly up-regulated in the retinas of sham-injected light-exposed mice, and XBD173 administration diminished their expression (Fig. 3d, e). Notably, the expression of *iNos* was not significantly altered by light exposure or XBD173 treatment (Fig. 3f) potentially indicating different time kinetics of chemokine/cytokine levels and oxygen radical responses. These data suggest that XBD173 has potent microglia-related immuno-modulatory effects in vivo in the mouse retina.

XBD173 treatment prevents light-induced retinal degeneration

We next asked whether targeting TSPO with XBD173 also improves the outcome of disease progression. We first performed in vivo optical coherence tomography (OCT) to detect the retinal damage after light exposure and under conditions of XBD173 treatment. The OCT images showed clear changes especially in ONL reflectance in the retinas of sham-treated light-exposed mice, indicating a severe degeneration of the photoreceptor layer (Fig. 4a, b). In contrast, XBD173-treated animals displayed nearly normal retinal layers similar to that of healthy controls (Fig. 4c). Volume scans revealed a significant thinning of the retinal tissue, especially in the central area around the optic nerve head after light exposure, which was much less pronounced in the XBD173-treated groups (Fig. 4d–f). Quantification of the retinal thickness in all analyzed animals demonstrates a significant reduction in the 3- and 6-mm central areas, respectively, after light exposure ($p < 0.0001$),

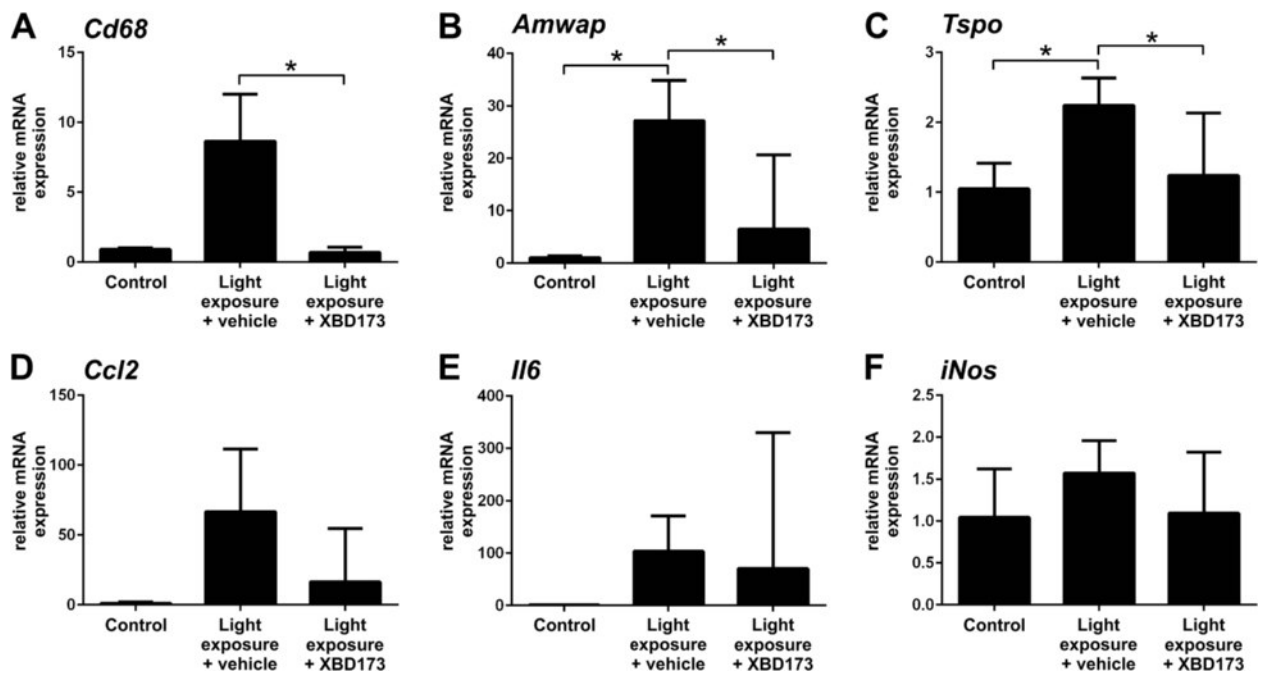

Fig. 3 XBD173 treatment dampens microglia-related pro-inflammatory marker expression after light exposure. To determine the mRNA expression of inflammation-associated genes in the retina, qRT-PCR analysis was performed 4 days after light exposure. **a**–**c** The microglia markers *Cd68* and *Amwap* were up-regulated after light exposure, and TSPO levels were also increased. In contrast, the retinas from XBD173-treated mice expressed significantly less *Cd68*, *Amwap*, and *Tspo* transcripts after light exposure. **d**, **e** XBD173 treatment reduced the expression of *Ccl2* and *Il6* that were elevated by light exposure. **f** iNOS expression was not altered. Data show mean ± SEM out of three independent experiments (control $n = 4$–8, light exposure plus vehicle treatment $n = 8$–15, light exposure plus XBD173 treatment $n = 8$–15 per group, measured in duplicates) with $^{*}p < 0.05$; $^{**}p < 0.01$; $^{***}p < 0.001$

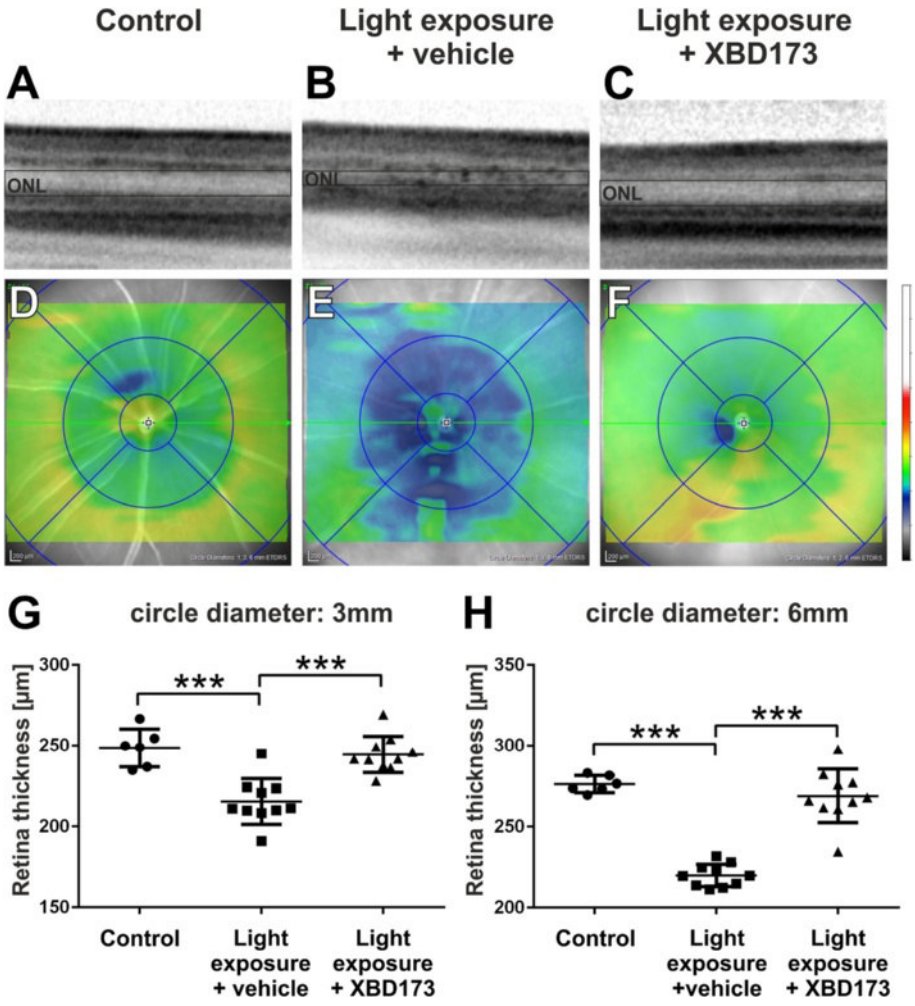

Fig. 4 XBD173 preserves retinal thickness in light-exposed mice. SD-OCT was performed 4 days after light exposure to analyze changes in retinal structures. **a**–**c** Light-exposed mice show an altered reflectance in the ONL, which was not present in XBD173-treated mice. **d**–**f** Representative heat maps show the average retinal thickness of control and light-exposed mice after vehicle or XBD173 treatment, respectively. Light-exposed mice show a significant thinning of the retina, in the central (**g**) and more peripheral area (**h**), which was preserved by XBD173 treatment. **g**, **h** One data point represents the average thickness of the central retina, calculated from four different areas around the optic nerve head in circle diameters of 3 mm (**g**) and 6 mm (**h**), respectively. Data show mean ± SEM out of two independent experiments (control $n = 6$, light exposure plus vehicle treatment $n = 10$, light exposure plus XBD173 treatment $n = 10$/group) with $^{***}p < 0.001$

that could be rescued by administration of XBD173 ($p < 0.0001$) (Fig. 4g, h).

To confirm these findings on the histological level, panorama images of retinal sections proceeding through the optic nerve head obtained 4 days after light exposure were stained with DAPI (Fig. 5a–c). The photoreceptor layer showed a clear thinning in sham-injected mice exposed to light, which was not evident in mice after XBD173 administration (Fig. 5a–c). In accordance with these data, the number of terminal deoxynucleotidyl transferase dUTP nick end labeling (TUNEL)-positive cells as indicators of cell death was also increased with light and strongly reduced by XBD173 injection (Fig. 5d, e). Further quantitative morphometric analyses along the nasal/temporal axis revealed that light exposure especially reduced the central retinal thickness and that this decline was significantly less in the XBD173-treated group of mice (Fig. 5g). Moreover, molecular analyses using quantitative real-time PCR (qRT-PCR) of total retinal RNA detected a clear counter-regulatory effect of XBD173 on caspase 8 mRNA levels (Fig. 5h, $p = 0.0007$). These data together clearly point towards a strong neuroprotective effect of XBD173 in conditions of light damage.

XBD173 prevents focal light-induced retinal damage

We were finally interested to validate our findings in an independent model using focal light-induced retinal damage. *Cx3cr1*$^{GFP/+}$ reporter mouse eyes, which facilitate label-free microglia visualization, were exposed to 50,000 lux cold light delivered by an otoscope for 10 min in the

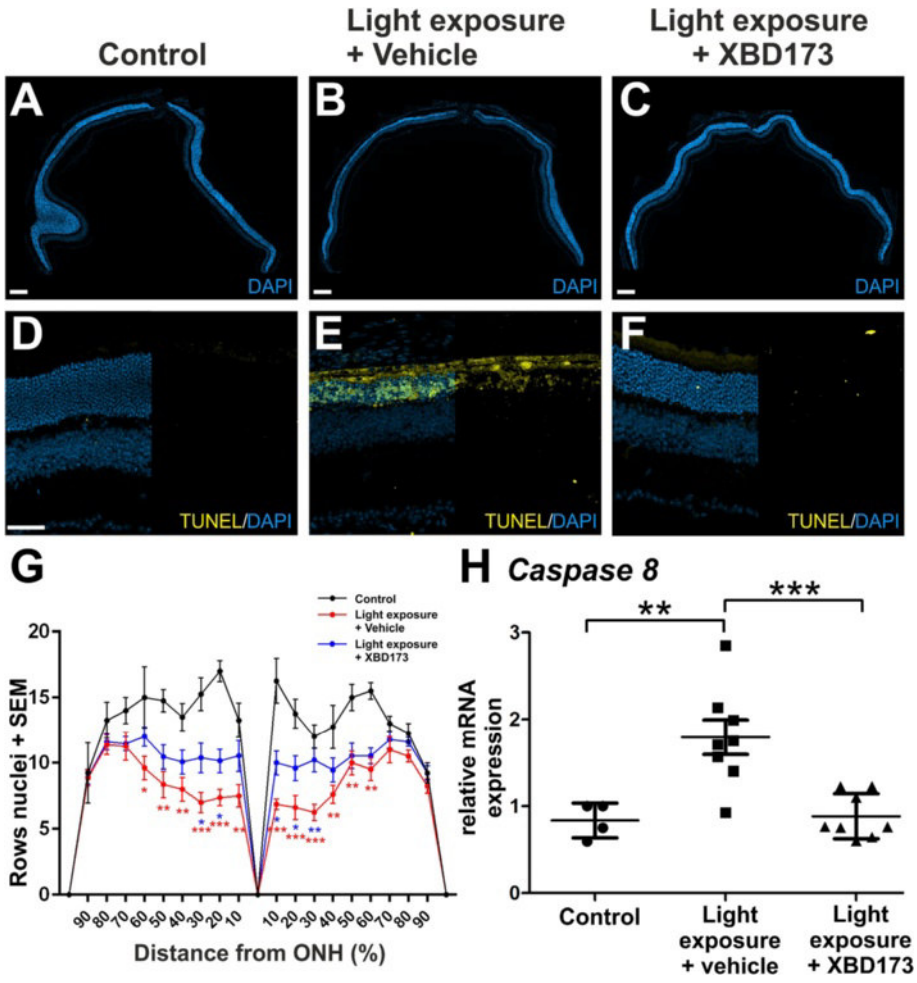

Fig. 5 XBD173 protects the light-exposed retina from cell death. **a**–**c** Representative panorama sections of the retina were stained with DAPI to further characterize structural changes. Light exposure caused severe degeneration particularly of the ONL. XBD173 administration reduced degeneration, represented by a clearly thicker photoreceptor layer, scale bar 200 μM. **d**–**f** Representative photomicrographs of TUNEL-stained retinal sections show the amount of apoptotic cells 4 days after light exposure. Light exposure caused a strong increase of apoptotic cells, especially in the ONL. Only very few TUNEL-positive cells were visible after XBD173 administration. Scale bar 50 μm (**g**). For quantification of retinal thickness, anterior and posterior areas were divided into ten sections with the optic nerve as reference and rows of photoreceptor nuclei were counted. Data show mean ± SEM (control $n = 4$, light exposure plus vehicle treatment $n = 8$, light exposure plus XBD173 treatment $n = 10$/group) with $^{*}p < 0.05$; $^{**}p < 0.01$; $^{***}p < 0.001$ light exposed + vehicle versus control (*red color*) and light exposed + XBD173 versus light exposed + vehicle (*blue color*). **h** mRNA analyses revealed a significantly lower expression of caspase 8 in light-exposed XBD173-treated mice compared to controls and vehicle-injected retinas. Data show mean ± SEM out of two independent experiments (control $n = 4$, light exposure plus vehicle treatment $n = 8$, light exposure plus XBD173 treatment $n = 8$/group, measured in triplicates) with $^{**}p < 0.01$; $^{***}p < 0.001$

same experimental design as described above for complete light exposure (Fig. 6a). Fundus imaging showed a clear focal light-induced retinal damage with a central area of atrophy (Fig. 6b). Confocal imaging of GFP-positive ONL microglia within the retinal lesion area of sham-treated mice clearly indicated a reactive phenotype compared to controls and XBD173-injected animals, respectively (Fig. 6c–e). As short cellular processes and enlargement of soma are characteristic for microglial activation, we quantified this morphological change using a grid system by counting the points of all cells that crossed the grid as described previously [40]. This analysis showed a significant reduction of grid cross points in focal light-exposed retinas, and this was fully reverted in the XBD173-treated group of animals (Fig. 6f).

In the last set of experiments, we determined the number of cone photoreceptors in the focal light damage model using confocal microscopy of retinal flat mounts that were stained with anti-cone arrestin antibodies. The areas of focal light damage showed a much weaker arrestin staining compared to controls and compared to the retinas of XBD173-treated animals, respectively (Fig. 6g–i). The quantitative analysis of 6–8 independent retinas revealed a more than 8-fold reduction in the number of cone

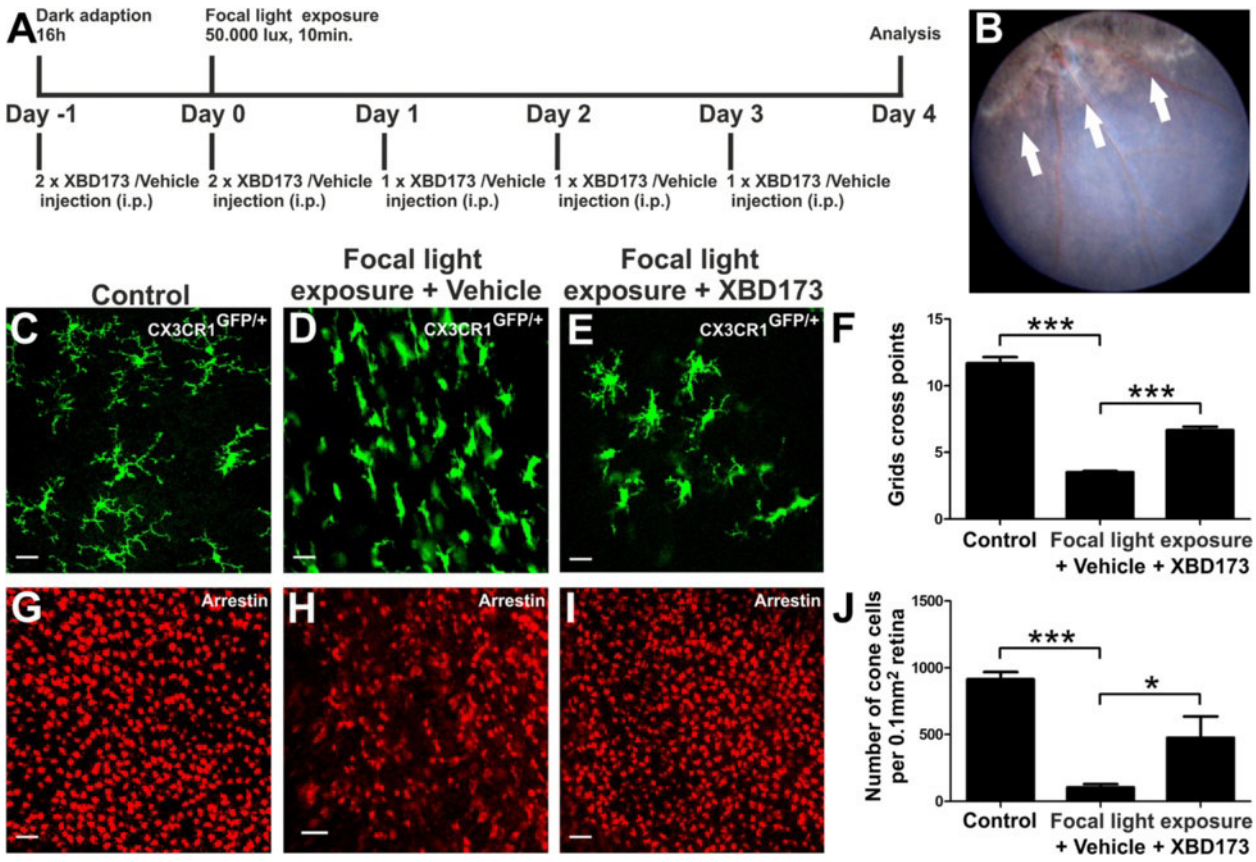

Fig. 6 XBD173 treatment prevents microglia reactivity and rescues cone photoreceptors in focal light-induced damage. **a** Light exposure regimen and mode of XBD173 administration. **b** Representative fundus image showing the focal light lesion 4 days after *Cx3cr1*$^{GFP/+}$ mice were exposed to 50,000 lux for 10 min. **c**–**e** Representative confocal images of GFP-positive retinal microglia in flat mounts from control mice (**c**) and lesion areas of light-exposed mice (**d**, **e**). The average size of microglial cells was assessed using the grid cross point system (**f**). Data show mean ± SEM ($n = 40$–180 cells per group) with ***$p < 0.001$. **g**–**i** Retinal flat mounts were processed for cone arrestin staining and examined by confocal microscopy. Representative confocal images of cone arrestin-positive cells in flat mounts from control mice (**g**) and lesion areas of light-exposed mice (**h**, **i**). **j** Average density of cone photoreceptor cells. Data show mean ± SEM ($n = 6$–8 retinas per group) with *$p < 0.05$; ***$p < 0.001$. Scale bar 50 μm

photoreceptors upon light damage and a 4.8-fold increase in the XBD173 therapy group, indicating a prominent effect on photoreceptor survival (Fig. 6j).

Discussion

Due to its high expression in activated glia, TSPO is a marker for brain gliosis and TSPO ligands are commonly used for in vivo imaging in humans and mice [41, 42]. We have previously identified high TSPO levels in retinal microglia of murine models of inherited retinal degeneration [16, 37]. In the present study, we now show that TSPO is also strongly induced in retinal microglia after light exposure and that the TSPO ligand XBD173 has potent microglia-modulatory and neuroprotective functions in the retina in vivo. To our knowledge, this is the first report of TSPO-directed pharmacological targeting of the diseased retina.

To mimic exposure to bright daylight, which is a well-known environmental risk factor for retinal degenerations, we exposed the mice to 15,000 lux UV-free white light for 1 h in the first set of experiments and to 50,000 lux focal cold white light for 10 min in the validation studies. White light has an emission spectrum relatively similar to that of daylight, and it is less artificial than the light of a particular wavelength [43, 44]. Furthermore, white light contains a significant fraction of short-wavelength blue light (403 nm) which is thought to have a higher damaging potential than the light of longer wavelength including green light (490–580 nm), which was used in some studies to mimic retinal degeneration [45]. The higher damaging potential of blue light is due to a process called photoreversal, the regeneration of rhodopsin from bleaching intermediates that results in a higher number of photon absorption in a certain time span [46].

Very early microglial activation was observed already 1 day after light challenge in both models (data not shown), indicating that microglia sense subtle disturbances in the light-damaged retina before overt cell death occurs. TSPO

expression was present in these reactive microglia, and our analyses towards the phenotype and behavior of microglia together with previous in vitro data [16] suggest that XBD173 exerts its neuroprotective function at least partially via modulation of microglia. Likewise, another specific TSPO ligand, etifoxine, also potently diminished inflammatory pathology and thereby attenuated the clinical score of experimental autoimmune encephalomyelitis, an experimental mouse model for multiple sclerosis [25]. The tight correlation of microglia reactivity with TSPO expression was also identified in the genetic mouse model of myosin VII deficiency that mimics both features of retinal dystrophies and glaucoma [47]. Therefore, TSPO induction in retinal microglia may be an early and reliable marker for changes in the microglia phenotype in different types of retinal degenerative diseases [37].

Our mRNA expression data of XBD173-treated retinas showed not only decreased transcript levels of *Cd68*, *Amwap*, and *Tspo* but also reduced *Ccl2* and *Il6* expression. The CCL2/CCR2 axis is crucial in subretinal macrophage and microglia accumulation in retinal degeneration models and human AMD, and these findings implicate that CCL2/CCR2 inhibition may be a novel tool to limit inflammation and neurodegeneration in the retina [48, 49]. Similarly, human reactive microglia express IL6, which in turn prevents retinal regeneration and promotes subretinal immune cell survival [50, 51]. Thus, the XBD173/TSPO axis seems to target two key pathways of chronic microglia reactivity in the retina.

As we have shown previously in microglial cell cultures [16], one potential mechanism of the anti-inflammatory effects of XBD173 could be the local synthesis of pregnenolone, as has been also demonstrated for brain astrocytes [52]. Pregnenolone can be further metabolized to progesterone and allopregnanolone that are both potent neuroprotective and anti-inflammatory molecules [53–55]. When orally applied to *rd1* mice with inherited retinal degeneration, progesterone potently reduced oxidative stress levels, diminished gliosis, and provided a temporal improvement in photoreceptor function [56].

We have demonstrated constitutive mitochondrial TSPO expression in the RPE that was unaffected by light exposure or XBD173 therapy. Therefore, TSPO in RPE mitochondria could potentially fulfill a housekeeping function. Of note, increased damage of mitochondrial DNA specifically in the RPE has been recently implicated as a risk factor for AMD and mutations of electron transport chain components could potentially limit energy production [57]. Thus, in addition to its anti-inflammatory effects on microglia, TSPO may sustain mitochondrial homeostasis and integrity by regulating the oxygen consumption rate. However, this function and the previously identified physiological roles of TSPO remain to be characterized with novel cell-type specific knockout mouse models [58, 59].

Conclusions

We have shown that modulation of microglia with the synthetic TSPO ligand XBD173 preserved the retinal structure by counter-regulation of microglial pro-inflammatory responses during light exposure. Our data suggest that targeting TSPO in the retina may be a novel promising approach for anti-inflammatory and neuroprotective therapies in retinal degenerative disorders.

Competing interests

All authors declare no competing financial interests.

Authors' contributions

RS designed the research, performed the research, and analyzed the data. AC, MB, KR, and MC performed the research and analyzed the data. HX and CG designed the research and wrote the paper. TL designed the research, analyzed the data, obtained the funding, and wrote the manuscript. All authors read and approved the final manuscript.

Acknowledgements

This work was supported by the DFG (LA1203/6-2, LA1203/9-1, LA1203/10-1, and FOR2240), the Velux Foundation, the Hans und Marlies Stock-Foundation, the Pro Retina Foundation, the Bayer Graduate Program in Pharmacology, and Fight for Sight (1425/1426). We thank the members of the Brachvogel Laboratory, Institute of Biochemistry, University of Cologne, for their help with the FACS analyses.

Author details

[1]Department of Ophthalmology, Laboratory for Experimental Immunology of the Eye, University of Cologne, 50931 Cologne, Germany. [2]Centre for Experimental Medicine, School of Medicine, Dentistry and Biomedical Sciences, Queen's University Belfast, Belfast BT12 6BA, UK. [3]Department of Ophthalmology, Lab for Retinal Cell Biology, University of Zürich, 8057 Zürich, Switzerland.

Received: 23 September 2015 Accepted: 26 October 2015
Published online: 02 November 2015

References

1. Hume DA, Perry VH, Gordon S. Immunohistochemical localization of a macrophage-specific antigen in developing mouse retina: phagocytosis of dying neurons and differentiation of microglial cells to form a regular array in the plexiform layers. J Cell Biol. 1983;97:253–7.
2. Kettenmann H, Hanisch UK, Noda M, Verkhratsky A. Physiology of microglia. Physiol Rev. 2011;91:461–553.
3. Damani MR, Zhao L, Fontainhas AM, Amaral J, Fariss RN, Wong WT. Age-related alterations in the dynamic behavior of microglia. Aging Cell. 2011;10:263–76.
4. Nimmerjahn A, Kirchhoff F, Helmchen F. Resting microglial cells are highly dynamic surveillants of brain parenchyma in vivo. Science. 2005;308:1314–8.
5. Aloisi F. Immune function of microglia. Glia. 2001;36:165–79.
6. Gupta N, Brown KE, Milam AH. Activated microglia in human retinitis pigmentosa, late-onset retinal degeneration, and age-related macular degeneration. Exp Eye Res. 2003;76:463–71.
7. Langmann T. Microglia activation in retinal degeneration. J Leukoc Biol. 2007;81:1345–51.
8. Karlstetter M, Langmann T. Microglia in the aging retina. Adv Exp Med Biol. 2014;801:207–12.
9. Xu H, Chen M, Forrester JV. Para-inflammation in the aging retina. Prog Retin Eye Res. 2009;28:348–68.
10. Zhao L, Zabel MK, Wang X, Ma W, Shah P, Fariss RN, et al. Microglial phagocytosis of living photoreceptors contributes to inherited retinal degeneration. EMBO Mol Med. 2015;7(9):1179–97.
11. Sierra A, Gottfried-Blackmore AC, McEwen BS, Bulloch K. Microglia derived from aging mice exhibit an altered inflammatory profile. Glia. 2007;55:412–24.
12. Roque RS, Rosales AA, Jingjing L, Agarwal N, Al-Ubaidi MR. Retina-derived microglial cells induce photoreceptor cell death in vitro. Brain Res. 1999;836:110–9.
13. Wu DC, Jackson-Lewis V, Vila M, Tieu K, Teismann P, Vadseth C, et al. Blockade of microglial activation is neuroprotective in the 1-methyl-4-

phenyl-1,2,3,6-tetrahydropyridine mouse model of Parkinson disease. J Neurosci. 2002;22:1763–71.
14. Amor S, Puentes F, Baker D, van der Valk P. Inflammation in neurodegenerative diseases. Immunology. 2010;129:154–69.
15. Chen M, Xu H. Parainflammation, chronic inflammation, and age-related macular degeneration. J Leukoc Biol. 2015.
16. Karlstetter M, Nothdurfter C, Aslanidis A, Moeller K, Horn F, Scholz R, et al. Translocator protein (18 kDa) (TSPO) is expressed in reactive retinal microglia and modulates microglial inflammation and phagocytosis. J Neuroinflammation. 2014;11:3.
17. Wang M, Wang X, Zhao L, Ma W, Rodriguez IR, Fariss RN, et al. Macroglia-microglia interactions via TSPO signaling regulates microglial activation in the mouse retina. J Neurosci. 2014;34:3793–806.
18. Papadopoulos V, Liu J, Culty M. Is there a mitochondrial signaling complex facilitating cholesterol import? Mol Cell Endocrinol. 2007;265–266:59–64.
19. Kuhlmann AC, Guilarte TR. Cellular and subcellular localization of peripheral benzodiazepine receptors after trimethyltin neurotoxicity. J Neurochem. 2000;74:1694–704.
20. Maeda J, Higuchi M, Inaji M, Ji B, Haneda E, Okauchi T, et al. Phase-dependent roles of reactive microglia and astrocytes in nervous system injury as delineated by imaging of peripheral benzodiazepine receptor. Brain Res. 2007;1157:100–11.
21. Veiga S, Azcoitia I, Garcia-Segura LM. Extragonadal synthesis of estradiol is protective against kainic acid excitotoxic damage to the hippocampus. Neuroreport. 2005;16:1599–603.
22. Girard C, Liu S, Adams D, Lacroix C, Sineus M, Boucher C, et al. Axonal regeneration and neuroinflammation: roles for the translocator protein 18 kDa. J Neuroendocrinol. 2012;24:71–81.
23. Chen MK, Guilarte TR. Translocator protein 18 kDa (TSPO): molecular sensor of brain injury and repair. Pharmacol Ther. 2008;118:1–17.
24. Barron AM, Garcia-Segura LM, Caruso D, Jayaraman A, Lee JW, Melcangi RC, et al. Ligand for translocator protein reverses pathology in a mouse model of Alzheimer's disease. J Neurosci. 2013;33:8891–7.
25. Daugherty DJ, Selvaraj V, Chechneva OV, Liu XB, Pleasure DE, Deng W. A TSPO ligand is protective in a mouse model of multiple sclerosis. EMBO Mol Med. 2013;5:891–903.
26. Wei XH, Wei X, Chen FY, Zang Y, Xin WJ, Pang RP, et al. The upregulation of translocator protein (18 kDa) promotes recovery from neuropathic pain in rats. J Neurosci. 2013;33:1540–51.
27. Rupprecht R, Rammes G, Eser D, Baghai TC, Schule C, Nothdurfter C, et al. Translocator protein (18 kD) as target for anxiolytics without benzodiazepine-like side effects. Science. 2009;325:490–3.
28. Nothdurfter C, Rammes G, Baghai TC, Schule C, Schumacher M, Papadopoulos V, et al. Translocator protein (18 kDa) as a target for novel anxiolytics with a favourable side-effect profile. J Neuroendocrinol. 2012;24:82–92.
29. Nothdurfter C, Baghai TC, Schule C, Rupprecht R. Translocator protein (18 kDa) (TSPO) as a therapeutic target for anxiety and neurologic disorders. Eur Arch Psychiatry Clin Neurosci. 2012;262 Suppl 2:S107–12.
30. Rupprecht R, Papadopoulos V, Rammes G, Baghai TC, Fan J, Akula N, et al. Translocator protein (18 kDa) (TSPO) as a therapeutic target for neurological and psychiatric disorders. Nat Rev Drug Discov. 2010;9:971–88.
31. Cruickshanks KJ, Klein R, Klein BE. Sunlight and age-related macular degeneration. The beaver dam eye study. Arch Ophthalmol. 1993;111:514–8.
32. Swaroop A, Chew EY, Rickman CB, Abecasis GR. Unraveling a multifactorial late-onset disease: from genetic susceptibility to disease mechanisms for age-related macular degeneration. Annu Rev Genomics Hum Genet. 2009;10:19–43.
33. Grimm C, Reme CE. Light damage as a model of retinal degeneration. Methods Mol Biol. 2013;935:87–97.
34. Marc RE, Jones BW, Watt CB, Vazquez-Chona F, Vaughan DK, Organisciak DT. Extreme retinal remodeling triggered by light damage: implications for age related macular degeneration. Mol Vis. 2008;14:782–806.
35. Narimatsu T, Ozawa Y, Miyake S, Kubota S, Hirasawa M, Nagai N, et al. Disruption of cell-cell junctions and induction of pathological cytokines in the retinal pigment epithelium of light-exposed mice. Invest Ophthalmol Vis Sci. 2013;54:4555–62.
36. Pennesi ME, Neuringer M, Courtney RJ. Animal models of age related macular degeneration. Mol Aspects Med. 2012;33:487–509.
37. Karlstetter M, Scholz R, Rutar M, Wong WT, Provis JM, Langmann T. Retinal microglia: just bystander or target for therapy? Prog Retin Eye Res. 2015;45:30–57.
38. Karlstetter M, Walczak Y, Weigelt K, Ebert S, Van den Brulle J, Schwer H, et al. The novel activated microglia/macrophage WAP domain protein, AMWAP, acts as a counter-regulator of proinflammatory response. J Immunol. 2010;185:3379–90.
39. Aslanidis A, Karlstetter M, Scholz R, Fauser S, Neumann H, Fried C, et al. Activated microglia/macrophage whey acidic protein (AMWAP) inhibits NFkappaB signaling and induces a neuroprotective phenotype in microglia. J Neuroinflammation. 2015;12:77.
40. Chen M, Zhao J, Luo C, Pandi SP, Penalva RG, Fitzgerald DC, et al. Para-inflammation-mediated retinal recruitment of bone marrow-derived myeloid cells following whole-body irradiation is CCL2 dependent. Glia. 2012;60:833–42.
41. Chauveau F, Boutin H, Van Camp N, Dolle F, Tavitian B. Nuclear imaging of neuroinflammation: a comprehensive review of [11C]PK11195 challengers. Eur J Nucl Med Mol Imaging. 2008;35:2304–19.
42. Venneti S, Lopresti BJ, Wiley CA. Molecular imaging of microglia/macrophages in the brain. Glia. 2013;61:10–23.
43. Wenzel A, Grimm C, Samardzija M, Reme CE. Molecular mechanisms of light-induced photoreceptor apoptosis and neuroprotection for retinal degeneration. Prog Retin Eye Res. 2005;24:275–306.
44. Youssef PN, Sheibani N, Albert DM. Retinal light toxicity. Eye (Lond). 2011;25:1–14.
45. Zhang C, Lei B, Lam TT, Yang F, Sinha D, Tso MO. Neuroprotection of photoreceptors by minocycline in light-induced retinal degeneration. Invest Ophthalmol Vis Sci. 2004;45:2753–9.
46. Grimm C, Wenzel A, Williams T, Rol P, Hafezi F, Reme C. Rhodopsin-mediated blue-light damage to the rat retina: effect of photoreversal of bleaching. Invest Ophthalmol Vis Sci. 2001;42:497–505.
47. Schubert T, Gleiser C, Heiduschka P, Franz C, Nagel-Wolfrum K, Sahaboglu A, et al. Deletion of myosin VI causes slow retinal optic neuropathy and age-related macular degeneration (AMD)-relevant retinal phenotype. Cell Mol Life Sci. 2015;72(20):3953–69.
48. Raoul W, Auvynet C, Camelo S, Guillonneau X, Feumi C, Combadiere C, et al. CCL2/CCR2 and CX3CL1/CX3CR1 chemokine axes and their possible involvement in age-related macular degeneration. J Neuroinflammation. 2010;7:87.
49. Sennlaub F, Auvynet C, Calippe B, Lavalette S, Poupel L, Hu SJ, et al. CCR2(+) monocytes infiltrate atrophic lesions in age-related macular disease and mediate photoreceptor degeneration in experimental subretinal inflammation in Cx3cr1 deficient mice. EMBO Mol Med. 2013;5:1775–93.
50. Balasubramaniam B, Carter DA, Mayer EJ, Dick AD. Microglia derived IL-6 suppresses neurosphere generation from adult human retinal cell suspensions. Exp Eye Res. 2009;89:757–66.
51. Levy O, Calippe B, Lavalette S, Hu SJ, Raoul W, Dominguez E, et al. Apolipoprotein E promotes subretinal mononuclear phagocyte survival and chronic inflammation in age-related macular degeneration. EMBO Mol Med. 2015;7:211–26.
52. Cascio C, Brown RC, Liu Y, Han Z, Hales DB, Papadopoulos V. Pathways of dehydroepiandrosterone formation in rat brain glia. J Steroid Biochem Mol Biol. 2000;75:177–86.
53. Yao XL, Liu J, Lee E, Ling GS, McCabe JT. Progesterone differentially regulates pro- and anti-apoptotic gene expression in cerebral cortex following traumatic brain injury in rats. J Neurotrauma. 2005;22:656–68.
54. Djebaili M, Guo Q, Pettus EH, Hoffman SW, Stein DG. The neurosteroids progesterone and allopregnanolone reduce cell death, gliosis, and functional deficits after traumatic brain injury in rats. J Neurotrauma. 2005;22:106–18.
55. Djebaili M, Hoffman SW, Stein DG. Allopregnanolone and progesterone decrease cell death and cognitive deficits after a contusion of the rat pre-frontal cortex. Neuroscience. 2004;123:349–59.
56. Sanchez-Vallejo V, Benlloch-Navarro S, Lopez-Pedrajas R, Romero FJ, Miranda M. Neuroprotective actions of progesterone in an in vivo model of retinitis pigmentosa. Pharmacol Res. 2015;99:276–88.
57. Terluk MR, Kapphahn RJ, Soukup LM, Gong H, Gallardo C, Montezuma SR, et al. Investigating mitochondria as a target for treating age-related macular degeneration. J Neurosci. 2015;35:7304–11.
58. Selvaraj V, Stocco DM. The changing landscape in translocator protein (TSPO) function. Trends Endocrinol Metab. 2015;26:341–8.
59. Gut P, Zweckstetter M, Banati RB. Lost in translocation: the functions of the 18-kD translocator protein. Trends Endocrinol Metab. 2015;26:349–56.

Scholz et al. Journal of Neuroinflammation (2015) 12:209
DOI 10.1186/s12974-015-0431-4

JOURNAL OF NEUROINFLAMMATION

RESEARCH Open Access

Minocycline counter-regulates pro-inflammatory microglia responses in the retina and protects from degeneration

Rebecca Scholz[1], Markus Sobotka[1], Albert Caramoy[1], Thomas Stempfl[2], Christoph Moehle[2] and Thomas Langmann[1*]

Abstract

Background: Microglia reactivity is a hallmark of retinal degenerations and overwhelming microglial responses contribute to photoreceptor death. Minocycline, a semi-synthetic tetracycline analog, has potent anti-inflammatory and neuroprotective effects. Here, we investigated how minocycline affects microglia in vitro and studied its immuno-modulatory properties in a mouse model of acute retinal degeneration using bright white light exposure.

Methods: LPS-treated BV-2 microglia were stimulated with 50 μg/ml minocycline for 6 or 24 h, respectively. Pro-inflammatory gene transcription was determined by real-time RT-PCR and nitric oxide (NO) secretion was assessed using the Griess reagent. Caspase 3/7 levels were determined in 661W photoreceptors cultured with microglia-conditioned medium in the absence or presence of minocycline supplementation. BALB/cJ mice received daily intraperitoneal injections of 45 mg/kg minocycline, starting 1 day before exposure to 15.000 lux white light for 1 hour. The effect of minocycline treatment on microglial reactivity was analyzed by immunohistochemical stainings of retinal sections and flat-mounts, and messenger RNA (mRNA) expression of microglia markers was determined using real-time RT-PCR and RNA-sequencing. Optical coherence tomography (OCT) and terminal deoxynucleotidyl transferase dUTP nick end labeling (TUNEL) stainings were used to measure the extent of retinal degeneration and photoreceptor apoptosis.

Results: Stimulation of LPS-activated BV-2 microglia with minocycline significantly diminished the transcription of the pro-inflammatory markers CCL2, IL6, and inducible nitric oxide synthase (iNOS). Minocycline also reduced the production of NO and dampened microglial neurotoxicity on 661W photoreceptors. Furthermore, minocycline had direct protective effects on 661W photoreceptors by decreasing caspase 3/7 activity. In mice challenged with white light, injections of minocycline strongly decreased the number of amoeboid alerted microglia in the outer retina and down-regulated the expression of the microglial activation marker translocator protein (18 kDa) (TSPO), CD68, and activated microglia/macrophage whey acidic protein (AMWAP) already 1 day after light exposure. Furthermore, RNA-seq analyses revealed the potential of minocycline to globally counter-regulate pro-inflammatory gene transcription in the light-damaged retina. The severe thinning of the outer retina and the strong induction of photoreceptor apoptosis induced by light challenge were nearly completely prevented by minocycline treatment as indicated by a preserved retinal structure and a low number of apoptotic cells.

Conclusions: Minocycline potently counter-regulates microgliosis and light-induced retinal damage, indicating a promising concept for the treatment of retinal pathologies.

Keywords: Minocycline, Microglia, Photoreceptors, Retinal degeneration, Light damage, Age-related macular degeneration

* Correspondence: thomas.langmann@uk-koeln.de
[1]Laboratory for Experimental Immunology of the Eye, Department of Ophthalmology, University of Cologne, 50931 Cologne, Germany
Full list of author information is available at the end of the article

Background

Age-related macular degeneration (AMD) is a leading cause of severe visual impairment in the elderly, and the number of affected persons steadily increases as a consequence of demographic changes [1]. Late stage AMD can be classified in a dry and a wet form, representing atrophic and neovascular processes, respectively. Wet AMD can be treated with intravitreal injections of anti-vascular endothelial growth factor (VEGF) medication, while no established treatment options exist for the dry form [2]. The pathogenesis of AMD is characterized by the early presence of drusen, damage of the retinal pigment epithelium (RPE) and photoreceptor layer primarily affecting the macular region and a chronic inflammatory response in the retina leading to the expression of pro-inflammatory and pro-angiogenic factors [2]. This immunological response in the retina can be regarded as para-inflammation and involves the reactivity of microglial cells [3–5].

Microglial cells are the tissue macrophages of the central nervous system (CNS), including the retina. In the healthy adult retina, they are located in the plexiform layers from where they permanently scan the retinal environment with their motile protrusions [6]. The expression of several receptors that are specific for the binding of chemokines, cytokines, complement factors, antibodies, or damage-associated molecular patterns enables these cells to recognize and immediately respond to pathological changes of their environment [7–9]. Besides their supportive function in the healthy retina, microglia reactivity and age-related changes of microglia physiology contribute to degenerative pathologies of the retina and the entire CNS [3, 4, 8, 10–17]. A large number of amoeboid shaped reactive microglia are detectable in the degenerating photoreceptor layer of AMD and retinitis pigmentosa retinas [4]. These cells contain phagocytosed rhodopsin-positive particles [4], and a recent report demonstrated that microglia do not only phagocytose dead cells but also take up living rods in a mouse model for retinitis pigmentosa [13]. Therefore, microglial activation cannot be just regarded as a bystander effect but rather actively contributes to photoreceptor cell death during retinal degeneration.

Because of these findings, substances that modulate microglial reactivity such as minocycline are good candidates to prevent inflammation and dampen degenerative processes in the retina. Minocycline is a second-generation semi-synthetic tetracycline analog, which is used against Gram-positive and Gram-negative bacteria for over 30 years. Besides its bacteriostatic capacity, minocycline exerts anti-inflammatory, anti-apoptotic, and neuroprotective effects in experimental models of Parkinson's disease [18], multiple sclerosis [19–22], neuropathic pain [16], Alzheimer's disease [23, 24], and in a genetic mouse model of retinitis pigmentosa [25].

In this study, we addressed the questions how minocycline modulates microglial reactivity in vitro and whether it protects from acute white light-induced retinal degeneration in the mouse. We selected white light exposure as it is an environmental risk factor that mimics several features of AMD in rodents including degeneration of photoreceptors and the retinal pigment epithelium [26–28]. This model is also very useful for a temporal correlation of microglial responses with processes of retinal degeneration and RPE dysfunction [29–31].

Methods

Reagents

Minocycline hydrochloride (M9511), *Escherichia coli* 0111:B4 lipopolysaccharide (LPS), and Z-Leu-Leu-Leu-al (MG-132) were purchased from Sigma-Aldrich (St. Louis, MO, USA).

Cell culture

BV-2 microglia were cultured in RPMI1640 with 5 % fetal calf serum (FCS) supplemented with 2 mM L-glutamine, 1 % penicillin/streptomycin, and 195 nM β-mercaptoethanol at 37 °C in a humidified atmosphere of 5 % CO_2, as described previously [32, 33]. BV-2 cells were pre-incubated for 30 min with 50 μg/ml minocycline or NaCl as vehicle control. Afterwards, the cells were stimulated with 50 ng/ml LPS, 50 μg/ml minocycline, or 50 ng/ml LPS plus 50 μg/ml minocycline for 24 h. After stimulation, cells or supernatant were harvested for further analysis. 661W photoreceptor-like cells were a kind gift from Prof. Muayyad Al-Ubaidi (Department of Cell Biology, University of Oklahoma Health Sciences Center, Oklahoma City, OK, USA). 661W photoreceptor cells were cultured with Dulbecco's modified Eagle's medium (DMEM), high glucose with L-glutamine, supplemented with 10 % FCS and 1 % penicillin/streptomycin. Cultures were maintained in a sterile humidified environment at 37 °C and 5 % CO_2 as described elsewhere [34].

RNA isolation and reverse transcription

Total RNA was extracted from cultured BV-2 microglia or murine retinas using the NucleoSpin® RNA Mini Kit (Macherey-Nagel, Dueren, Germany). RNA was quantified spectrophotometrically with a NanoDrop 2000 (Thermo Scientific). First-strand complementary DNA (cDNA) synthesis was carried out with the Revert Aid H Minus First-strand cDNA Synthesis Kit (Fermentas, K1632).

Real-time RT-PCR

cDNA (25 ng) were amplified in a 10-μl reaction mixture consisting of 5 μl Fast Start Universal Probe Master (Rox) (Roche), 2 μl of primers (10 μM), 0.375 μl purified water, and 0.125 μl of dual-labeled Universal ProbeLibrary (UPL)

probe (Roche Applied Science, Basel, Switzerland) with an Applied Biosystems 7900 HT Fast Real-time PCR system (Applied Biosystems, Carlsbad, CA, USA). The following reaction parameters were used: 10 min 95 °C hold, followed by 40 cycles of 15 s 95 °C melt, and 1 min 60 °C anneal/extension. Primer sequences and UPL probe numbers were as follows: CD68, forward primer 5′-ctctctaaggctacaggctgct-3′, reverse primer 5′-tcacggttgcaag agaaaca-3′, probe #27; activated microglia/macrophage whey acidic protein (AMWAP), forward primer 5′-tttgatc actgtggggatga-3′, reverse primer 5′-acactttctggtgaaggcttg-3′, probe #1; translocator protein (TSPO), forward primer 5′-actgtattcagccatggggta-3′, reverse primer 5′-accatagcgt cctctgtgaaa-3′, probe #33; IL6, forward primer 5′-gatgg atgctaccaaactggat-3′, reverse primer 5′-ccaggtagctatggta ctccaga-3′, probe #6; inducible nitric oxide synthase (iNOS), forward primer 5′-ctttgccacggacgagac-3′, reverse primer 5′-tcattgtactctgagggctga-3′, probe #13; CCL2, forward primer 5′-catccacgtgttggctca-3′, reverse primer 5′-gatcatcttgctggtgaatgagt-3′, probe #62; CASP8, forward primer 5′-tgaacaatgagatccccaaat-3′, reverse primer 5′-caaaaatttcaagcaggctca-3′, probe #11; and ATP5B, forward primer 5′-ggcacaatgcaggaaagg-3′, reverse primer 5′-tcagc aggcacatagatagcc-3′, probe #77. Measurements were performed in triplicates. ATP5B expression was used as reference gene and results were analyzed with the ABI sequence detector software version 2.4 using the ΔΔCt method for relative quantification.

RNA-sequencing and bioinformatic data analysis

Library preparation and RNA-seq were carried out as described in the Illumina TruSeq Stranded mRNA Sample Preparation Guide, the Illumina HiSeq 1000 System User Guide (Illumina, Inc., San Diego, CA, USA), and the KAPA Library Quantification Kit—Illumina/ABI Prism User Guide (Kapa Biosystems, Inc., Woburn, MA, USA). In brief, 300 ng of total RNA was used for purifying the poly-A containing messenger RNA (mRNA) molecules using poly-T oligo-attached magnetic beads. Following purification, the mRNA was fragmented to an average insert size of 200–400 bases using divalent cations under elevated temperature (94 °C for 4 min). The cleaved RNA fragments were copied into first-strand cDNA using reverse transcriptase and random primers. Strand specificity was achieved by replacing dTTP with dUTP in the Second Strand Marking Mix (SMM), followed by second-strand cDNA synthesis using DNA Polymerase I and RNase H. The incorporation of dUTP in second-strand synthesis quenches the second strand during amplification, because the polymerase used in the assay is not incorporated past this nucleotide. The addition of Actinomycin D to First Stand Synthesis Act D mix (FSA) prevents spurious DNA-dependent synthesis, while allowing RNA-dependent synthesis, improving strand specificity. These cDNA fragments then had the addition of a single "A" base and subsequent ligation of the adapter. The products were purified and enriched with PCR to create the final cDNA library. The libraries were quantified using the KAPA SYBR FAST ABI Prism Library Quantification Kit. Equimolar amounts of each library were used for cluster generation on the cBot (TruSeq SR Cluster Kit v3). The sequencing run was performed on a HiSeq 1000 instrument using the indexed, 50 cycles single read (SR) protocol and the TruSeq SBS v3 Kit. Image analysis and base calling resulted in .bcl files, which were converted into .fastq files by the CASAVA1.8.2 software. Library preparation and RNA-seq were performed at the service facility "KFB—Center of Excellence for Fluorescent Bioanalytics" (Regensburg, Germany).

The RNA express workflow on Illumina BaseSpace was used to determine differential gene expression in two biological replicates of control retinas, light-exposed retinas, and light-exposed retinas treated with minocycline, respectively. In brief, alignment of RNA-seq reads to the mouse UCSC mm10 genome and mapping to genes was performed with STAR aligner [35]. Differential gene expression between the two biological replicates each was calculated with DESeq2 [36]. The cutoff of genes considered to be differentially expressed was a log2 fold change of ≥2 or ≤−2.

Integrative analysis of genome-wide expression activities was performed with the Gene Expression Dynamics Inspector (GEDI), a Matlab (Mathworks, Natick, MA) freeware program which uses self-organizing maps (SOMs) to translate high-dimensional data into a 2D mosaic [37]. Each tile of the mosaic represents an individual SOM cluster and is color-coded to represent high or low expression of the cluster's genes, thus identifying the underlying pattern.

The RNA-seq raw data and normalized DESeq2 counts of this study are publicly available at the National Center for Biotechnology Information Gene Expression Omnibus (http://www.ncbi.nlm.nih.gov/geo/) as series record GSE71025.

Nitrite measurement

Nitric oxide concentrations were determined by measurement of nitrite released into BV-2 culture supernatants using the Griess reagent system (Promega). Fifty-microliter cell culture supernatants from differentially stimulated BV-2 cells were incubated with 100 μl Griess reagent in each well of a translucent 96-well plate. After incubation for 30 min at room temperature, absorbance was measured at 540 nm on an Infinite F200 Pro plate reader (Tecan). Nitrite concentrations were calculated on the basis of a sodium nitrite reference curve.

661 W photoreceptor apoptosis assay

To investigate microglial neurotoxicity and to assess whether minocycline also has direct effect on photoreceptors, 661W cells were incubated for 48 h with culture supernatants from differentially stimulated BV-2 cells or culture supernatants supplemented with minocycline. Apoptotic cell death was determined using the Caspase-Glo® 3/7 Assay (Promega). Cells were lysed and incubated with a luminogenic caspase-3/7 substrate, which contains the tetrapeptide sequence DEVD. After incubation at room temperature for 1 h, the generated luminescence was measured on an Infinite F200 Pro plate reader (Tecan). A blank reaction without cells was used to determine background luminescence associated with the cell culture system and Caspase-Glo® 3/7 reagent. The values of the blank reactions were subtracted from all experimental values. Negative control reactions were performed to determine the basal caspase activity of 661 W cells. Relative luciferase units (RLU) reflect the level of apoptotic cell death.

Animals

All experiments were performed with 10–14-weeks-old albino BALB/cJ mice of both sexes. Animals were housed in an air-conditioned environment with 12-h light-dark schedule and had free access to water and food. All experimental procedures complied with the German law on animal protection and the ARVO Statement for the Use of Animals in Ophthalmic and Vision Research. The animal protocols used in this study were reviewed and approved by the governmental body responsible for animal welfare in the state of Nordrhein-Westfalen (Landesamt für Natur, Umwelt und Verbraucherschutz Nordrhein-Westfalen, Germany) (reference number 84-02.04.2015-A039).

Minocycline administration

The mice received intraperitoneal injections of minocycline at a dose of 45 mg/kg or NaCl as solvent control where indicated twice daily for the first two days, starting one day before the light exposure and once daily for the remaining days.

Light exposure regimen

BALB/cJ mice were dark-adapted for 16 h before light exposure. After pupil dilatation with 1 % Phenylephrin and 2.5 % Tropicamid under dim red light, the mice were exposed to bright white light with an intensity of 15.000 lx for 1 h. After light exposure, the animals were housed in dark-reared conditions overnight and then maintained under normal light conditions for the remaining experimental period.

Immunohistochemistry

Eyes were harvested for immunohistochemical analysis 4 days after light exposure. After fixation with 4 % paraformaldehyde, eyes were embedded in optimal cutting temperature (OCT) compound or dissected for retinal flat mount analysis. Sixteen-micrometer sections were rehydrated with PBS and blocked with dried milk solution. Flat mounts were incubated with 5 % Tween, 5 % Triton-X100 in PBS overnight and non-specific binding was blocked by incubation with dried milk solution. Subsequently, retinal sections and flat mounts were incubated with primary antibodies at 4 °C overnight. Primary antibodies targeting the following molecules were used: rabbit anti-Iba1 antibody (Wako Chemicals, Neuss, Germany), rabbit anti-TSPO antibody (Abcam, Cambridge, UK), and rabbit anti-Glial Fibrillary Acidic Protein (G9269, Sigma). After a washing step, the sections and flat mounts were incubated with a secondary antibody either conjugated to Alexa488 (green) or Alexa594 (red) (Jackson Immuno-Research, West Grove, PA, USA) for 1 h. After counterstaining with 4',6-diamidino-2-phenylindole (DAPI), the samples were mounted in DAKO fluorescent mounting medium (Dako Deutschland GmbH, Hamburg, Germany) and analyzed with an Axioskop2 MOT Plus Apotome microscope (Carl Zeiss).

Optical coherence tomography (OCT)

Animals were anesthetized by intraperitoneal injection of Rompun (10 mg/kg body weight)-Ketavet (100 mg/kg body weight), and their pupils were dilated with Phenylephrine HCl (0.25 %)-Tropicamide (0.05 %) before image acquisition. Spectral-domain OCT (SD-OCT) was performed on both eyes with a Spectralis™ HRA + OCT device (Heidelberg Engineering) to investigate structural changes in the retina after light exposure and minocycline administration. Thickness measurements were performed with a circular ring scan (circle diameter 1, 3, 6 ETDRS), centered on the optic nerve head, which represents the average retinal thickness [μm] in a certain field. Central retinal thickness was calculated from four fields around the optic nerve head using the Heidelberg Eye Explorer Software.

Terminal deoxynucleotidyl transferase dUTP nick end labeling (TUNEL) assay

Retinal sections were labeled with an in situ cell death detection kit, Fluorescein (Roche) to detect the amount of apoptotic cells 4 days after light exposure. For a better overview, the sections were also counterstained with DAPI for 10 min. After a washing procedure, sections were mounted in DAKO fluorescent mounting medium (Dako Deutschland GmbH, Hamburg, Germany) and analyzed with an Axioskop2 MOT Plus Apotome microscope (Carl Zeiss).

Statistical analysis

Nitrite secretion, caspase 3/7 activities, and real-time RT-PCR data from BV-2 cells were analyzed with one-way ANOVA and Bonferroni's multiple comparison tests. Real-time RT-PCR data of murine retinas and OCT measurements of retinal thickness were analyzed using a one-way ANOVA and Dunnett's multiple comparison tests. $p < 0.05$ was considered statistically significant.

Results

Minocycline dampens the pro-inflammatory response and neurotoxic potential of microglia and promotes photoreceptor survival in vitro

We first investigated whether minocycline treatment affects reactivity and neurotoxicity of BV-2 microglial cells. Gene expression of the chemoattractant protein CCL2, the pro-inflammatory cytokine IL6, and iNOS, which catalyzes the generation of toxic nitric oxide (NO), were analyzed in LPS-activated BV-2 cells that were treated with minocycline for 6 and 24 h, respectively. Minocycline significantly dampened LPS-induced gene expression of CCL2 (Fig. 1a, $p < 0.0001$ for LPS versus minocycline + LPS treatment), IL6 (Fig. 1b, $p = 0.002$ for LPS versus minocycline + LPS treatment), and iNOS (Fig. 1c, $p < 0.0001$ for LPS versus minocycline + LPS treatment) in a short-term setting of 6-h incubation. Minocycline also decreased mRNA expression of these three genes after a 24-h treatment period (Fig. 1d–f), but the level of significance was only reached for iNOS (Fig. 1f, $p < 0.0001$ for LPS versus minocycline + LPS treatment). These findings indicate that minocycline action on microglia is a relatively rapid process and very likely interferes with immediate/early mechanisms of pro-inflammatory activation.

Since iNOS levels were also significantly inhibited by minocycline in the longer incubation experiment, we determined the amount of nitric oxide produced by BV-2 cells after stimulation with LPS, minocycline, and both compounds together after 24 h. LPS-treated microglial cells stimulated with minocycline released significantly less nitric oxide compared to cells that were stimulated with LPS alone (Fig. 2a, $p < 0.0001$), indicating that minocycline may reduce microglial neurotoxicity.

Using an apoptosis assay of 661W photoreceptor-like cells treated with microglia-conditioned medium with or without additional minocycline supplementation, we tested whether minocycline can reduce microglial neurotoxicity and possibly exert direct beneficial effects on photoreceptor survival. The supernatant from LPS-stimulated microglia significantly increased caspase 3/7 activity in 661 W cells as a biomarker of cell death (Fig. 2b, $p < 0.0001$ for LPS versus control treatment). In contrast, conditioned medium from LPS-treated BV-2 cells that were co-stimulated with minocycline induced significantly lower caspase 3/7 levels in 661 W cells (Fig. 2b, left part, $p < 0.0001$ for LPS versus minocycline + LPS supernatant treatment). Furthermore, treatment of 661W photoreceptors with supernatant from LPS-treated BV-2 cells that was supplemented with

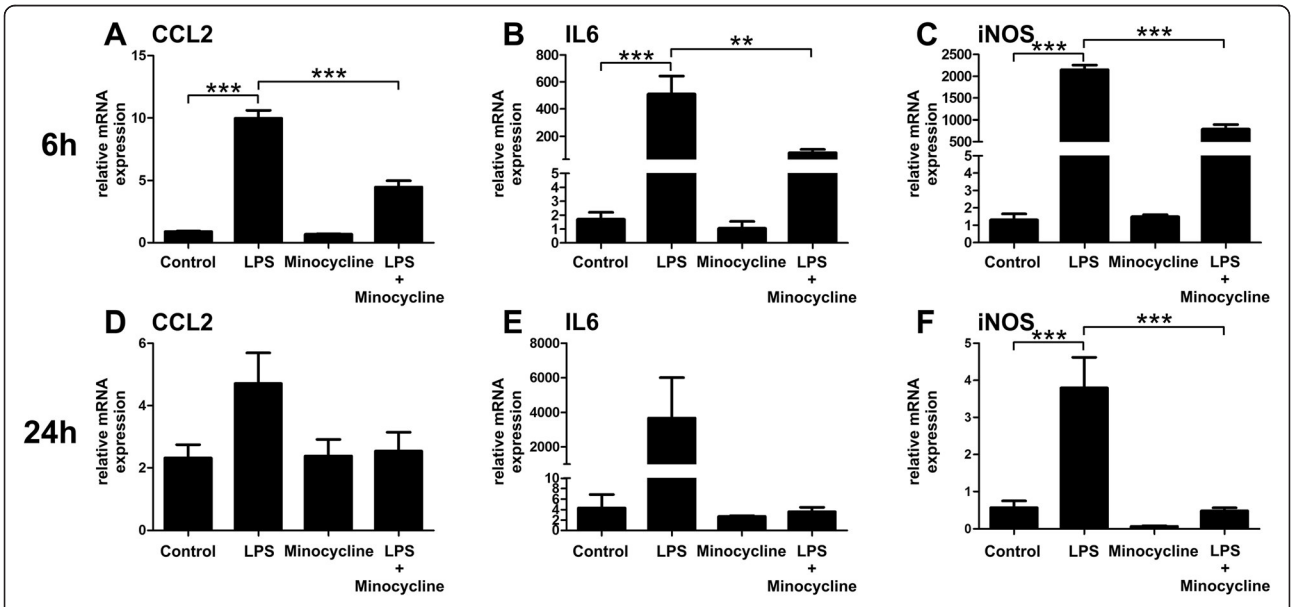

Fig. 1 Minocycline dampens pro-inflammatory gene transcription in microglia. BV-2 microglial cells were pre-treated with 50 μg/ml minocycline or NaCl as a vehicle control for 30 min. The cells were then further stimulated with either 50 μg/ml minocycline, 50 ng/ml LPS, or a combination of both. Six hours (**a**–**c**) and 24 h (**d**–**f**) later transcript levels of the pro-inflammatory marker genes CCL2 (**a**, **d**), IL6 (**b**, **e**), and iNOS (**c**, **f**) were determined by quantitative real-time PCR. Data show mean ± SEM out of three independent experiments ($n = 5$/group, measured in triplicates) with $^{*}p < 0.05$, $^{**}p < 0.01$, $^{***}p < 0.001$

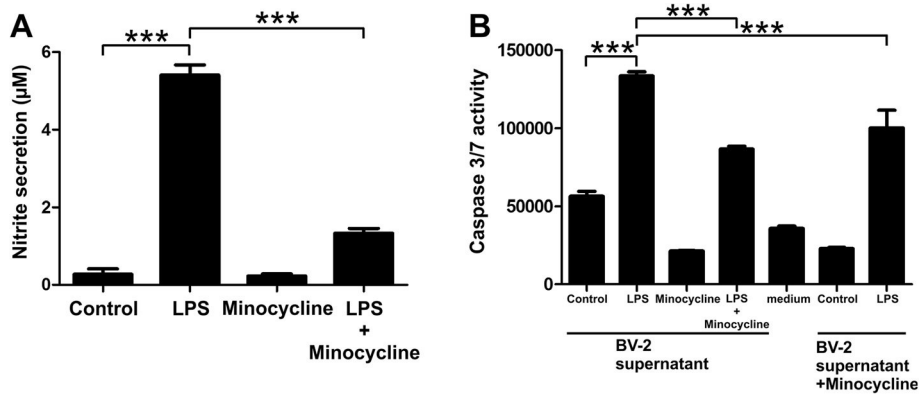

Fig. 2 Minocycline stimulation dampens microglial NO production and reduces their neurotoxic potential on 661W photoreceptors. BV-2 cells were pre-treated with 50 µg/ml minocycline or NaCl for 30 min. The cells were then further stimulated with either 50 µg/ml minocycline, 50 ng/ml LPS, or a combination of both. **a** Twenty-four hours later, the nitric oxide production was determined by Griess reaction which detects the amount of nitrite in the cell culture supernatant. Data show mean ± SEM ($n = 3$/group, measured in triplicates). **b** To determine the neurotoxic potential of microglia, the cell culture supernatant of the differentially treated microglial cells was transferred to 661W photoreceptor cells. Furthermore, cell culture supernatant of untreated and LPS-stimulated BV-2 cells supplemented with minocycline was transferred to 661W photoreceptor cells to test whether minocycline may have a direct neuroprotective effect. After 48 h of incubation with microglia conditioned-medium, apoptotic cell death was analyzed by caspase 3/7 activity measurements. Data show mean ± SEM ($n = 3$/group, measured in duplicates) with $^{*}p < 0.05$, $^{**}p < 0.01$, $^{***}p < 0.001$

minocycline also reduced caspase 3/7 levels (Fig. 2b, right part, $p < 0.001$ for LPS versus LPS supernatant + minocycline supplement). Thus, minocycline reduced the levels of secreted neurotoxic and pro-apoptotic molecules from microglia but also exerted direct survival-promoting effects on photoreceptors that were challenged with reactive microglia-supernatants.

Minocycline prevents microglia reactivity in retinas exposed to acute white light

To test the effects of minocycline on microglial responses in the damaged retina in vivo, we selected the murine model of acute light-induced degeneration. This model mimics several features of AMD including immune activation and apoptosis of photoreceptor cells. After 16 h of dark adaptation, BALB/cJ mice were exposed to white light with an intensity of 15.000 lux for 1 h. The mice received daily intraperitoneal injections of 45 mg/kg minocycline, starting 1 day before the light exposure for five consecutive days. The first 2 days, the mice received two injections per day and then once daily for the remaining 3 days (Fig. 3, top, schematic drawing). Four days after light exposure, the effect of minocycline administration was analyzed by staining of retinal sections and flat mounts with markers for reactive gliosis. In control animals, retinal immunolabeling with the marker Iba1 showed ramified microglia in the plexiform layers as expected (Fig. 3a). Light exposure caused a severe thinning of the outer nuclear layer and many amoeboid shaped microglia appeared in the degenerating photoreceptor layer and the subretinal area (Fig. 3b). This prominent degeneration of photoreceptors and accumulation of microglia in the outer retina was not detectable in retinas of mice treated with minocycline (Fig. 3c). To better analyze the microglial network and localization, retinal flat mounts were stained with Iba1. In contrast to healthy controls, where microglial cells are absent in the outer retina, retinal flat mounts from light-exposed mice showed high numbers of amoeboid shaped microglia in the subretinal area (Fig. 3d, e). Treatment with minocycline clearly prevented migration of many microglia to the subretinal area, and the cells in this region had a more ramified morphology (Fig. 3f).

To better characterize the reactive phenotype of glia cells, the expression of the activation markers TSPO for microglia and glial fibrillary acid protein (GFAP) for Müller cells and astrocytes were analyzed. Exposure to light initiated a strong increase in TSPO expression, especially confined to outer retinal microglia (Fig. 3h). In contrast, administration of minocycline strongly reduced TSPO expression, indicating a less reactive microglia phenotype (Fig. 3i). Expression of GFAP in Müller cells and astrocytes of retinas exposed to light was also increased compared to controls (Fig. 3j, k), whereas minocycline-treated animals displayed only weak GFAP staining (Fig. 3l). These findings indicate that the reactive gliosis elicited by acute light damage can be significantly suppressed by minocycline treatment.

Minocycline counter-regulates pro-inflammatory gene expression in retinal degeneration

In addition to these in situ analyses of retinas, we investigated whether mRNA levels of microglia-related pro-inflammatory marker genes were influenced by minocycline

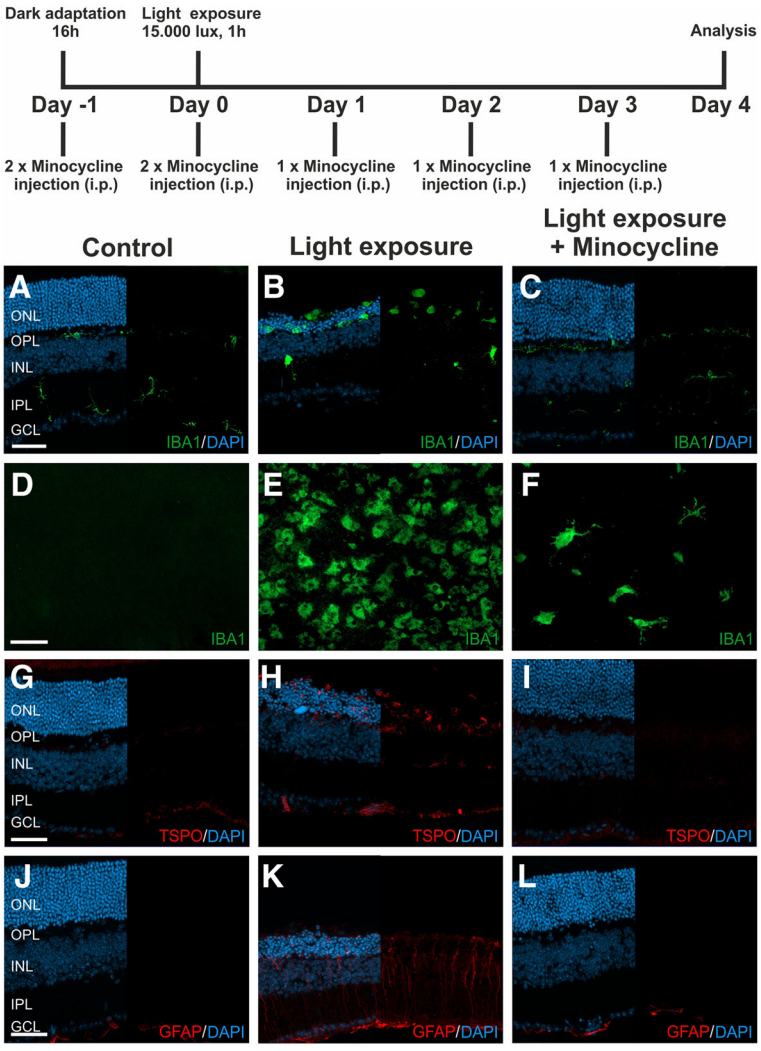

Fig. 3 Treatment of light-exposed mice with minocycline blocks microglia reactivity and Müller cell gliosis. Of both sexes, 10- to 14-week-old BALB/c mice were dark-adapted for 16 h. After pupil dilatation, the mice were exposed to bright white light with an intensity of 15.000 lux for 1 hour. The mice received intraperitoneal injections of minocycline at a dose of 45 mg/kg body weight twice daily for the first 2 days, starting 1 day before the light exposure and once daily for the remaining 3 days. Four days after the light exposure OCT, immunohistochemical stainings, real-time RT-PCR analysis, and RNA sequencing were performed to determine the in vivo effects of minocycline treatment (schematic drawing). Representative photomicrographs show retinal sections (**a**–**c**) and flat mounts (**d**–**f**) stained with Iba1 (*green*), TSPO (*red*) (**g**–**i**), and GFAP (*red*) (**j**–**l**). In control retinas, microglial cells were located in the OPL, IPL, and GCL (**a**, **d**); low levels of TSPO were only observable in the GCL (**g**); and signs for Müller cell gliosis were not detectable (**j**). **b**, **e**, **h**, and **k** Photomicrographs of light-exposed mice showed a massive thinning of the ONL and an increased number of amoeboid shaped, reactive microglia in the ONL, and the subretinal space (**b**, **e**). **h** A strong up-regulation of TSPO expression was detectable in microglia. **k** Up-regulation of GFAP indicates Müller cell gliosis. **c**, **f**, **i**, and **l** Representative photomicrographs of minocycline-treated mice 4 days after light exposure. Compared to untreated controls, the ONL of minocycline-treated mice appeared markedly preserved and less microglia were detectable in the ONL and the subretinal space (**c**, **f**). **i** Microglial cells were negative for TSPO expression. **l** GFAP expression was only detectable in astrocytes, indicating a lack of reactive Müller cells. *TSPO* translocator protein, *GFAP* glial fibrillary acid protein, *ONL* outer nuclear layer, *OPL* outer plexiform layer, *INL* inner nuclear layer, *IPL* inner plexiform layer, *GCL* ganglion cell layer. Scale bar 50 μm

administration in vivo. CD68, AMWAP, and TSPO are markers that are associated with microglia proliferation and reactivity [38–41]. Four days after light exposure all three markers were clearly up-regulated in the retina, with especially high induction levels of CD68 and AMWAP (Fig. 4a–c). In mice treated with minocycline, the expression of CD68 (Fig. 4a, $p = 0.0002$) and AMWAP (Fig. 4b, $p = 0.007$) were significantly suppressed and mRNA levels of TSPO were reduced (Fig. 4c, $p = 0.057$). Furthermore, transcripts that reflect the activation of key microglial pathways including chemotaxis, pro-inflammatory cytokines, and radical production were analyzed. In retinas of light exposed mice that were treated with minocycline, mRNA levels of the chemotactic molecule CCL2 were

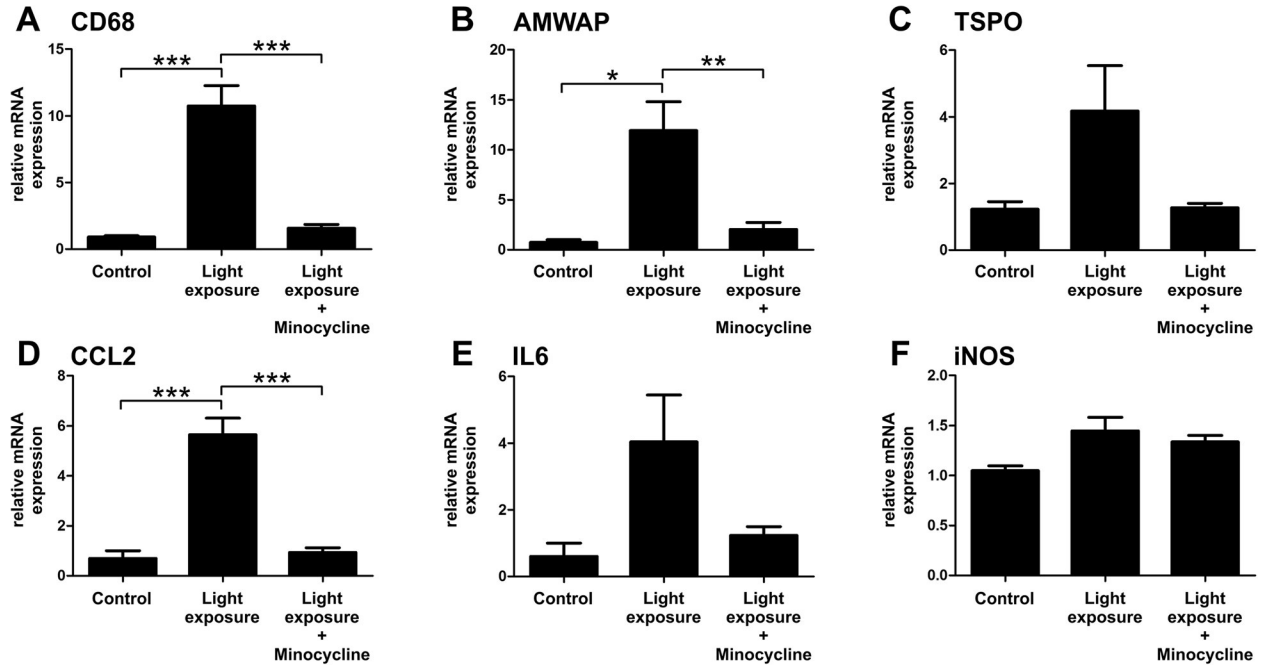

Fig. 4 Minocycline treatment dampens microglia-related pro-inflammatory marker expression after light exposure. To determine the mRNA expression of inflammation associated genes in the retina, qRT-PCR analysis were performed 4 days after light exposure. **a**–**c** The microglia activation markers CD68 and AMWAP were significantly up-regulated after light exposure, and TSPO levels were also increased. In contrast, retinas from minocycline-treated mice expressed significantly less CD68 and AMWAP transcripts and also reduced mRNA levels of TSPO. **d** Minocycline treatment reduced the expression of CCL2 that was significantly elevated by light exposure. **e** IL6 was enhanced by light exposure, which was reversed in the minocycline administration group. **f** iNOS expression was not significantly altered. Data show mean ± SEM (control $n = 4$, light exposure $n = 4$, light exposure and minocycline treatment $n = 5$/group, measured in triplicates) with $^{*}p < 0.05$, $^{**}p < 0.01$, $^{***}p < 0.001$

significantly decreased compared to untreated animals (Fig. 4d, $p < 0.0001$). The expression of IL6 was also elevated after exposure to light and returned to baseline in the minocycline administration group (Fig. 4e). In contrast to our in vitro data, no significant differences in iNOS expression were detectable after light exposure or minocycline treatment after the 4-day period (Fig. 4f). This suggests that minocycline also exerts microglia-related anti-inflammatory effects in vivo in the retina.

Minocycline dampens early microglia responses to acute white light

Analysis 4 days after light exposure revealed that minocycline reduced the number of activated microglial cells and impaired their pro-inflammatory gene transcription. We next studied whether minocycline also affects early microglia responses at time points that lack overt cell death as trigger for migration and reactivity. Furthermore, we included a vehicle-treated control group in these experiments to exclude potentially protective stress-related effects. One day after light exposure retinal sections from control, vehicle- or minocycline-treated mice were stained with Iba1. Ramified microglia were present in the plexiform layers and the ganglion cell layer of control animals (Fig. 5a). In contrast, retinas from light-exposed and vehicle-treated mice revealed many amoeboid shaped microglia in the outer nuclear layer (ONL), which did not show structural changes at this early time point after light challenge (Fig. 5b). Minocycline treatment completely prevented this early microglia migration into the ONL (Fig. 5c).

We next also analyzed the mRNA expression of microglia-associated markers in a time kinetic experiment. Light exposure enhanced the expression of the CD68, AMWAP, and TSPO in vehicle-treated mice already 1 day after exposure to white light (Fig. 5d–f). Minocycline administration dampened the expression of these genes at every analyzed time point and reached statistical significance for CD68 (Fig. 5d, vehicle versus control $p < 0.0001$, vehicle versus minocycline $p = 0.0001$ 1 day after light exposure) and TSPO (Fig. 5f, vehicle versus control $p = < 0.0001$, vehicle versus minocycline $p = 0.0018$ 1 day after light exposure, and vehicle versus minocycline $p = 0.0113$ 2 days after light exposure). The migration marker CCL2 was strongly up-regulated in light-exposed vehicle controls, reaching statistical significance 1 day after light exposure (control versus vehicle $p = 0.0046$). Minocycline-treated mice expressed lower CCL2 at every analyzed time point. Furthermore, minocycline also significantly reduced the expression of IL6,

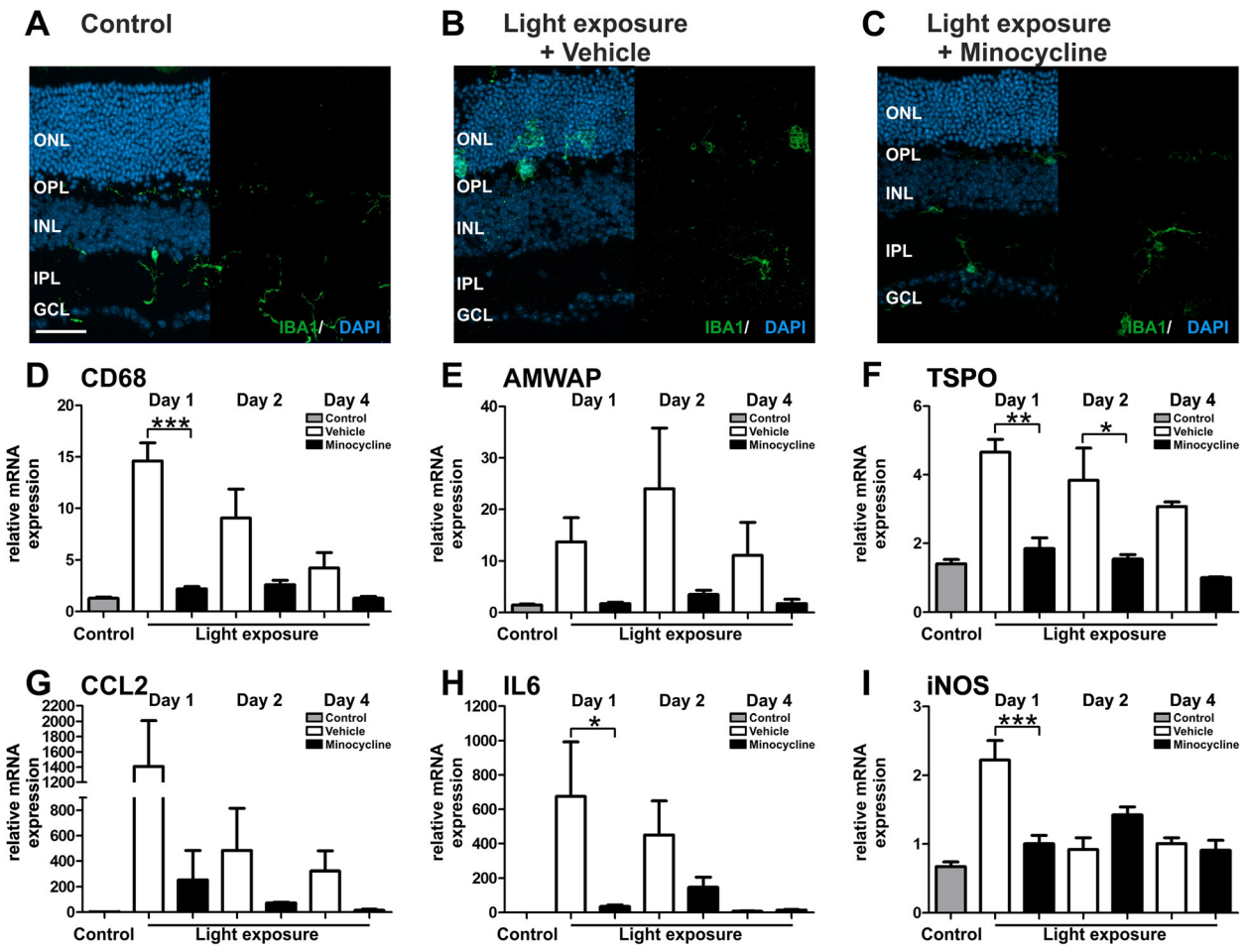

Fig. 5 Minocycline suppresses early microglial activation after exposure to bright white light. Representative photomicrographs show retinal sections (**a**–**c**) stained with Iba1 (*green*) of control, vehicle- or minocycline-treated mice 1 day after light exposure. In healthy controls, microglial cells are only located in the plexiform layers and GCL (**a**). Images of light-exposed vehicle-treated mice show amoeboid microglia located in the ONL, whereas retinal structures appear unaffected 1 day after light exposure (**b**). Compared to vehicle-treated mice, amoeboid, reactive microglia are absent in the ONL of mice treated with minocycline (**c**). *ONL* outer nuclear layer, *OPL* outer plexiform layer, *INL* inner nuclear layer, *IPL* inner plexiform layer, *GCL* ganglion cell layer. Scale bar 50 μm. Data show representative photomicrographs (control $n = 6$, light exposure and vehicle treatment $n = 3$, light exposure and minocycline treatment $n = 3$/group). Retinal mRNA expression of microglia and inflammation-associated genes were determined by real-time RT-PCR at 1, 2, or 4 days after light exposure (**d**–**i**). Compared to controls, the microglial-associated markers CD68, AMWAP, and TSPO were markedly increased in vehicle-treated mice peaking 1 day after light exposure. Expression levels in minocycline-treated mice were lower at every analyzed time point (**d**–**f**). CCL2 was induced in light-exposed vehicle-treated mice, which was suppressed in the minocycline-treated group (**g**). Minocycline treatment also significantly reduced the expression of IL6 and iNOS, which was strongly upregulated in the vehicle-treated group (**h**, **i**). Data show mean ± SEM (control $n = 6$, light exposure and vehicle treatment $n = 3$, light exposure and minocycline treatment $n = 3$/group, measured in triplicates) with $^{*}p < 0.05$, $^{**}p < 0.01$, $^{***}p < 0.001$

which was strongly upregulated in the vehicle-treated group (Fig. 5h, control versus vehicle $p = 0.0082$, vehicle versus minocycline $p = 0.0371$ 1 day after light exposure). In contrast to our previous analysis after 4 days (Fig. 4f), iNOS was induced 1 day after light exposure in vehicle controls and was significantly reduced in the minocycline administration group (Fig. 5i, control versus vehicle $p < 0.0001$, vehicle versus minocycline $p = 0.0004$ 1 day after light exposure).

In a small pilot experiment, we further explored whether microglia may be even earlier alarmed in the light damage condition. Indeed, ramified microglia projected their long protrusions reaching through the ONL already 4 h after light exposure (Additional file 1: Figure S1A, B). mRNA analysis in these retinas clearly showed increased expression of CCL2, IL6, and CD68 in the absence of changes in caspase 8 levels (Additional file 1: Figure S1C–F). Therefore, we conclude that microglial activation is an early event after light exposure that is not only triggered by dead cells and that minocycline is very effective in attenuating this process.

Minocycline exerts global anti-inflammatory effects on the retinal transcriptome

We then asked whether minocycline treatment has a global effect on gene expression in the light exposure model of retinal degeneration. RNA-sequencing analysis with two biological replicates was performed on total retinal RNA isolated from control mice, from animals after light exposure, and from light-exposed animals that received minocycline. We first used the Gene Expression Dynamics Inspector (GEDI) to determine the global patterns of gene expression in the three different conditions. GEDI is based on self-organizing maps to identify genome-wide transcriptome activity via "gestalt" recognition [37]. GEDI is sample-oriented rather than gene-oriented, which allows the identification of genome-wide patterns. Each mosaic tile in the GEDI map represents a gene cluster that is expressed at similar levels, with blue color indicating a low level and red corresponding to high expression. The three GEDI maps show a highly dynamic regulation of gene expression in light-exposed and minocycline-treated retinas compared to control (Fig. 6a). Light exposure initiated the formation of a prominent red cluster band that was nearly reversed by minocycline treatment (Fig. 6a). In the next step, we performed DESeq2 analysis to determine differential gene expression between the groups using a log2 fold change cutoff of ≥2. The MA-plots demonstrate that light exposure caused a significant induction of 217 genes with no down-regulated transcripts (Fig. 6b). In contrast, the light-exposed versus light-exposed plus minocycline treatment analysis identified 113 down-regulated and 38 up-regulated transcripts (Fig. 6c). A closer look at the differentially expressed genes showed that most of the transcripts induced under light damage conditions belong to immune-related biological pathways including markers directly related to microglia reactivity such as macrophage scavenger receptor 1 (MSR1), AMWAP (alias WFDC17), CD68, and complement factor C3 (Additional file 2: Table S1). The vast majority of transcripts down-regulated by minocycline treatment was induced by light exposure alone, and hence, their expression was reversed (Additional file 3: Table S2). These results demonstrate that both light damage and minocycline have a major impact on the global pattern of gene expression in the retina and that minocycline administration effectively counterbalances most of the pro-inflammatory signaling events in the degenerating retina.

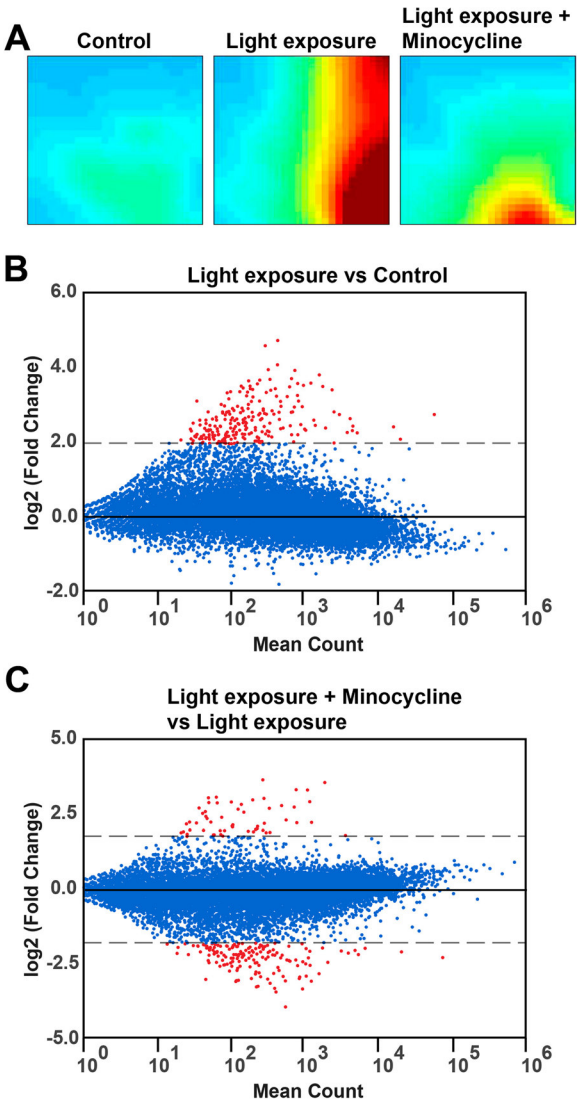

Fig. 6 Light exposure and minocycline exert global effects on the retinal transcriptome. **a** Gene Expression Dynamics Inspector (GEDI) analysis of the complete RNA-seq dataset (Gene Expression Omnibus Series Nr. GSE71025) from control retinas and light-exposed retinas in the absence or presence of minocycline. Biological duplicates were analyzed for each condition and the pseudo-color scale indicates high (*red*) or low (*blue*) expression levels. **b**, **c** DESeq2 analysis to determine differential gene expression between the indicated groups using a log2 fold change cutoff of ≥2 and ≤−2. The MA-plots demonstrate that light exposure caused a global induction of 217 genes (**b**), whereas light exposure plus minocycline administration reversed this effect with many counter-regulated transcripts (**c**)

Minocycline treatment protects the retina from light-induced degeneration

We finally asked whether targeting retinal microglia with minocycline also improves the outcome of disease progression. We first performed in vivo optical coherence tomography (OCT) of mice to detect structural changes of the retina after light exposure and under conditions of minocycline treatment. The OCT images showed clear changes in ONL reflectance in retinas of light-exposed animals, indicating a strong degeneration of the photoreceptor layer (Fig. 7a, b). In contrast, minocycline-treated mice displayed a normal hyperreflective photoreceptor layer similar to that of controls (Fig. 7c). Volume scans revealed

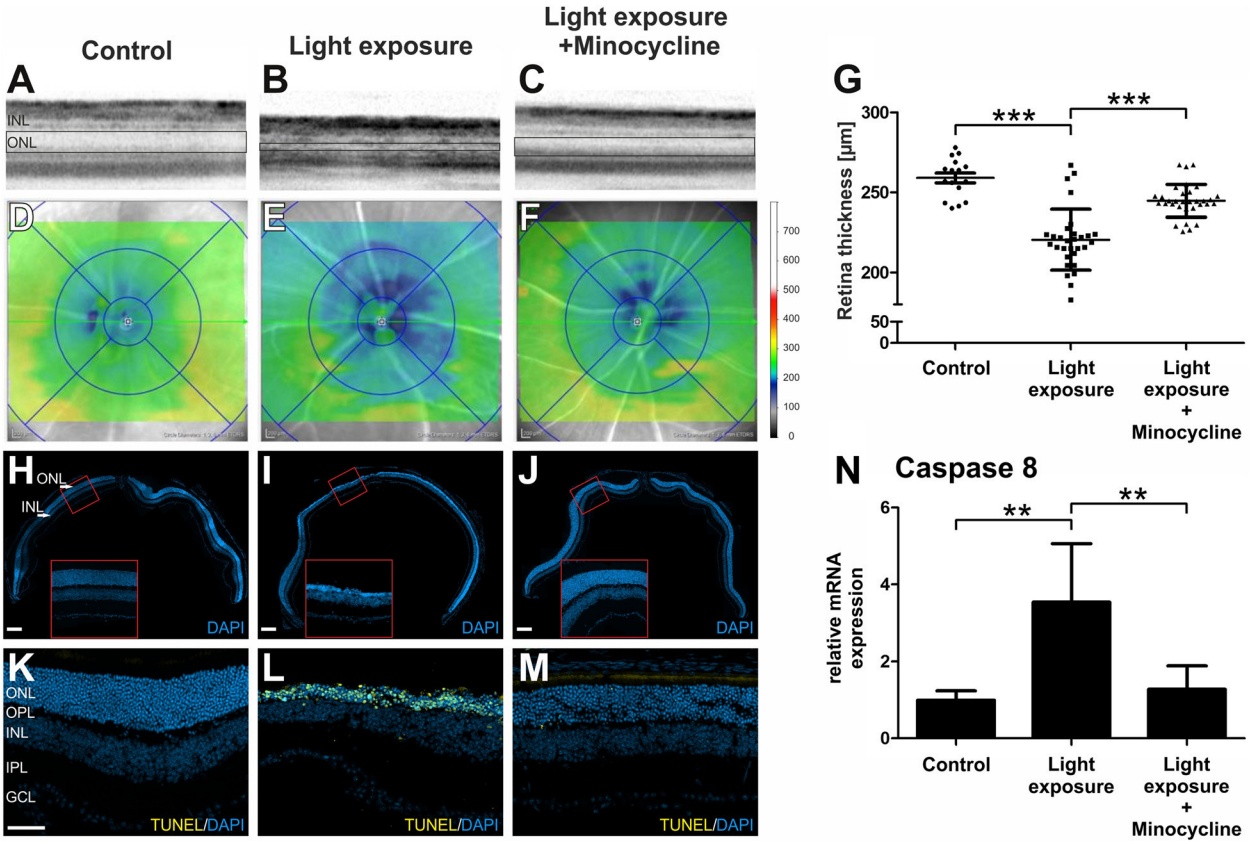

Fig. 7 Minocycline prevents light-induced retinal degeneration. **a**–**g** SD-OCT was performed 4 days after light exposure to analyze changes in retinal structures. **a**–**c** Light-exposed mice show an altered reflectance in the ONL, which was not present in minocycline-treated mice. **d**–**f** Representative heat maps show the average retinal thickness of control, light-exposed minocycline-treated and untreated mice. Light-exposed mice show a significant thinning of the retina, especially in the central area, which was preserved by minocycline treatment. **g** One data point represents the average thickness of the central retina [µm], calculated from four different areas around the optic nerve head. Data show mean ± SEM (control $n = 16$ eyes, light exposure $n = 30$ eyes, light exposure and minocycline treatment $n = 32$ eyes). **h**–**j** Representative panorama sections of the retina were stained with DAPI to further characterize structural changes in the retina. Light exposure caused severe degeneration particularly of the ONL. Minocycline administration reduced degeneration, represented by a clearly thicker photoreceptor layer, scale bar, 200 µM. **k**–**m** Representative photomicrographs of TUNEL-stained retinal sections show the amount of apoptotic cells 4 days after light exposure. Light exposure caused a strong increase of apoptotic cells, especially in the ONL. Less TUNEL-positive cells were visible after minocycline administration. **n** RNA analyses revealed a significantly higher expression of caspase 8 in light-exposed retinas, compared to retinas of minocycline-treated mice, indicating a higher amount of apoptotic cells. Scale bar, 50 µm. Data show mean ± SEM (control $n = 4$ retinas, light exposure $n = 4$ retinas, light exposure and minocycline treatment $n = 5$ retinas, measured in triplicates) *$p < 0.05$, **$p < 0.01$, ***$p < 0.001$

a severe thinning of the retina, especially in the central area around the optic nerve head after light exposure, which was not observed in the minocycline-treated groups (Fig. 7d–f). Quantification of the retinal thickness in all analyzed animals demonstrate a significant reduction in the central area after light exposure ($p < 0.0001$), which could be rescued by treatment with minocycline ($p < 0.0001$) (Fig. 7g). To confirm these findings, panorama images of retinal sections proceeding through the optic nerve head were stained with DAPI. The photoreceptor layer showed a clear thinning in the group of mice exposed to light, which was not evident in mice after minocycline treatment (Fig. 7h–j, Fig. 3a–c). TUNEL stainings and mRNA analyses of caspase 8 levels also revealed that light exposure significantly induced cell death in mouse retinas, which was prevented in minocycline-treated animals (Fig. 7k–n). These data clearly point toward a strong neuroprotective effect of minocycline in conditions of acute light damage.

Discussion

Several studies revealed that minocycline exerts antimicrobial, anti-inflammatory, anti-apoptotic, and neuroprotective properties in different animal models of neuronal degenerative diseases, including Parkinson's disease, multiple sclerosis, Alzheimer's disease, Huntington's disease, amyotrophic lateral sclerosis, and retinitis pigmentosa [16, 18–20, 23, 25, 42–44]. Here, we report for

the first time that minocycline administration preserves the retinal structure in a white light-induced degeneration model, which mimics several features of dry AMD and monogenic retinal dystrophies. The main questions discussed in this study were if and how minocycline stimulation modulates the neurotoxic potential of microglia and whether minocycline administration could be a suitable immuno-modulatory strategy to treat retinal degeneration.

Our in vitro studies in LPS-activated BV-2 microglia demonstrated that minocycline was capable to diminish gene expression of the pro-inflammatory markers CCL2, IL6, and iNOS in a rapid temporal response. This is consistent with earlier reports with microglia isolated from rat retinas where minocycline dampened mRNA expression and secretion of IL1β, TNFα, and iNOS [45]. In line with this, Henry et al. reported that minocycline reduced mRNA levels of TLR 2, MHC-II, IL1β, and IL6 in BV-2 cells [46]. These results together with our data suggest that minocycline is highly effective in reducing pro-inflammatory gene transcription in microglia.

The production of toxic nitric oxide by phagocytes plays an important role in degenerative processes [47–49]. Here, we demonstrated that minocycline effectively dampened nitric oxide production of LPS-stimulated microglia. Furthermore, minocycline reduced the general neurotoxic potential of reactive microglia on 661W photoreceptor cells. Supernatants from microglia that were stimulated with both LPS and minocycline were less toxic to photoreceptors than those of cells that were treated with LPS only. Investigations in RAW264.7 macrophages and spinal cord microglia also confirmed that minocycline blocks the production of toxic nitric oxide [50, 51]. Hence, others have found an association of reduced iNOS levels and NO itself with delayed neurodegeneration [19, 47, 52]. In the 1-methyl-4-phenyl-1,2,3,6-tetrahydropyridine (MPTP) mouse model of Parkinson's disease, minocycline reduced MPP+ induced glial iNOS expression, which was most likely due to an inhibition of p38 MAPK phosphorylation [19].

Besides the reduction of NO production, several other mechanisms of action are discussed for the beneficial effects of minocycline. Indeed, we here also showed that minocycline administration directly protected photoreceptors from microglia mediated death. In a model of Huntington's disease, minocycline delayed disease progression and mortality by inhibition of caspase-1 and caspase-3 up-regulation, enzymes which play an important role in the induction of necrosis and apoptosis [43]. Studies in R6/2 mice confirmed that minocycline can inhibit both caspase-independent (apoptosis inducing factor) and caspase-dependent (Smac/Diablo and cytochrome c) mitochondrial cell death pathways [53]. However, despite its ability to reduce pro-inflammatory markers in a mouse model for age-related neuron loss, minocycline failed to inhibit apoptosis and neuron loss [54].

A further mechanism how minocycline exerts its protective functions is the inhibition of matrix metalloproteases (MMPs). MMPs are a family of zinc- and calcium-dependent proteolytic enzymes that are responsible for the degradation of structural proteins in the extracellular matrix and their activation is associated with neurological disorders. Thus, blockage of MMPs by minocycline decreased the cerebral infarct size in a mouse model of focal cerebral ischemia. This effect was most likely due to the inhibition of CCL2, TNFα, and indoleamine 2,3-dioxygenase (IDO) expression [55, 56].

Our OCT images and immunohistochemical analysis showed that the treatment with minocycline preserved retinal structure and reduced the amount of apoptotic cells after exposure to bright white light. The protection of photoreceptors was associated with a reduced number of reactive, amoeboid-shaped, TSPO-positive microglia in the outer retina. Accordingly, our mRNA analyses of retinas revealed suppression of microglial activation markers including AMWAP and CD68 after administration of minocycline [38–40]. Analysis at different time points after light exposure revealed that microglial activation is an early event that precedes photoreceptor death. Moreover, our RNA-sequencing data revealed a global transcriptomic effect of minocycline with a complete cluster of light-damage-induced pro-inflammatory genes that was counter-regulated by minocycline. Of note, the RNA-seq dataset also detected up-regulation of structural retinal genes such as keratins and adhesion molecules by minocycline. These results strongly indicate that modulation of microglia reactivity is a key mechanism in minocycline's mode of action in the retina. This notion is supported by studies demonstrating that inhibition of microglia with minocycline protects from neuronal degenerative diseases including Alzheimer disease or Parkinson disease [16, 18]. In the eye, minocycline could also reduce microglial activation and improve neuronal function [13, 25, 57, 58]. In a model of green light exposure, preservation of retinal structure and ERG amplitudes by minocycline was associated with reduced numbers of CD11b+ cells in the outer retina [58]. To mimic exposure to bright daylight, which is discussed as a contributing factor for retinal degenerations, we used 15.000 lux UV-free white light in our studies. White light has an emission spectrum similar to that of daylight, and it is less artificial than light of a particular wavelength [59, 60]. Furthermore, white light contains also short wavelength blue light (403 nm) which is thought to have a higher damaging potential than light of longer wavelength including green light (490–580 nm), which was used in earlier studies [58]. The higher damaging potential of blue light is due to a process

called photo-reversal, the regeneration of rhodopsin from bleaching intermediates that results in a higher number of photon absorption in a certain time span. Because of different light exposure settings in our study and the work of Zhang et al. [58], different underlying damage mechanisms cannot be ruled out [28, 59, 61, 62].

In the *rd10* mouse model for retinitis pigmentosa, minocycline inhibited microglial activation and down-regulated the expression of pro-inflammatory molecules including TNFα, COX1, and COX2. Moreover, pro-apoptotic molecules such as BAX and Caspase 3 were suppressed by minocycline, and the retinal structure and function were preserved [25]. Of note, minocycline could also diminish photoreceptor death in *rds* mice by a microglia-independent mechanism as depletion of microglia by clodronate prevented their recruitment but failed to inhibit photoreceptor apoptosis [63].

Conclusions

We have shown that microglia activity is an early event in retinal degeneration induced by bright white light. Minocycline administration preserved the retinal structure by a global counter-regulation of microglial pro-inflammatory responses and direct effects on photoreceptors during light exposure. Our data suggest that treatment strategies that modulate microglial reactivity and support photoreceptor survival provide a potential therapeutic option for retinal degenerative diseases.

Additional files

Additional file 1: Figure S1. Early microglial activation after exposure to bright white light. Representative photomicrographs show retinal sections (A–B) stained with Iba1 (green) of control mice and animals 4 h after light exposure. In healthy controls, microglial cells are only located in the plexiform layers and GCL (A). Images of light exposed mice show microglia with protrusions in the ONL (B). ONL, outer nuclear layer; OPL, outer plexiform layer; INL, inner nuclear layer; IPL, inner plexiform layer; GCL, ganglion cell layer. Scale bar 50 μm. Data show representative photomicrographs (control $n = 5$, light exposure $n = 4$). Retinal mRNA expression of microglia-associated genes and caspase 8 were determined by real-time RT-PCR (C-F). Data show mean ± SEM (control $n = 5$ retinas, light exposure $n = 4$ retinas measured in triplicates) with $^{*}p < 0.05$. (JPG 684 kb)

Additional file 2: Table S1. Differentially expressed transcripts comparing light exposure versus control. (DOCX 85 kb)

Additional file 3: Table S2. Differentially expressed transcripts comparing light exposure versus light exposed plus minocycline treatment. (DOCX 80 kb)

Competing interests

All authors declare no competing financial interests.

Authors' contributions

RS designed the research, performed the research, analyzed the data, and wrote the manuscript. MS, AC, TS, and CM performed the research and analyzed the data. TL analyzed the data, obtained the funding, designed the study, and wrote the manuscript. All authors read and approved the final manuscript.

Acknowledgements

This work was supported by the DFG (LA1203/6-2, LA1203/9-1, and FOR2240), the Hans und Marlies Stock-Foundation, the Pro Retina Foundation, and the Bayer Graduate Program in Pharmacology. The authors thank Prof. Muayyad Al Ubaidi for providing the 661W photoreceptor cell line.

Author details

[1]Laboratory for Experimental Immunology of the Eye, Department of Ophthalmology, University of Cologne, 50931 Cologne, Germany. [2]Center of Excellence for Fluorescent Bioanalytics, University of Regensburg, 93053 Regensburg, Germany.

Received: 31 July 2015 Accepted: 12 November 2015
Published online: 17 November 2015

References

1. Wong WL, Su X, Li X, Cheung CM, Klein R, Cheng CY, et al. Global prevalence of age-related macular degeneration and disease burden projection for 2020 and 2040: a systematic review and meta-analysis. Lancet Glob Health. 2014;2:e106–116.
2. Jager RD, Mieler WF, Miller JW. Age-related macular degeneration. N Engl J Med. 2008;358:2606–17.
3. Xu H, Chen M, Forrester JV. Para-inflammation in the aging retina. Prog Retin Eye Res. 2009;28:348–68.
4. Gupta N, Brown KE, Milam AH. Activated microglia in human retinitis pigmentosa, late-onset retinal degeneration, and age-related macular degeneration. Exp Eye Res. 2003;76:463–71.
5. Karlstetter M, Scholz R, Rutar M, Wong WT, Provis JM, Langmann T. Retinal microglia: just bystander or target for therapy? Prog Retin Eye Res. 2015;45:30–57.
6. Hume DA, Perry VH, Gordon S. Immunohistochemical localization of a macrophage-specific antigen in developing mouse retina: phagocytosis of dying neurons and differentiation of microglial cells to form a regular array in the plexiform layers. J Cell Biol. 1983;97:253–7.
7. Kettenmann H, Hanisch UK, Noda M, Verkhratsky A. Physiology of microglia. Physiol Rev. 2011;91:461–553.
8. Damani MR, Zhao L, Fontainhas AM, Amaral J, Fariss RN, Wong WT. Age-related alterations in the dynamic behavior of microglia. Aging Cell. 2011;10:263–76.
9. Nimmerjahn A, Kirchhoff F, Helmchen F. Resting microglial cells are highly dynamic surveillants of brain parenchyma in vivo. Science. 2005;308:1314–8.
10. Aloisi F. Immune function of microglia. Glia. 2001;36:165–79.
11. Langmann T. Microglia activation in retinal degeneration. J Leukoc Biol. 2007;81:1345–51.
12. Karlstetter M, Langmann T. Microglia in the aging retina. Adv Exp Med Biol. 2014;801:207–12.
13. Zhao L, Zabel MK, Wang X, Ma W, Shah P, Fariss RN, et al. Microglial phagocytosis of living photoreceptors contributes to inherited retinal degeneration. EMBO Mol Med. 2015;7(9):1179–97.
14. Sierra A, Gottfried-Blackmore AC, McEwen BS, Bulloch K. Microglia derived from aging mice exhibit an altered inflammatory profile. Glia. 2007;55:412–24.
15. Roque RS, Rosales AA, Jingjing L, Agarwal N, Al-Ubaidi MR. Retina-derived microglial cells induce photoreceptor cell death in vitro. Brain Res. 1999;836:110–9.
16. Wu DC, Jackson-Lewis V, Vila M, Tieu K, Teismann P, Vadseth C, et al. Blockade of microglial activation is neuroprotective in the 1-methyl-4-phenyl-1,2,3,6-tetrahydropyridine mouse model of Parkinson disease. J Neurosci. 2002;22:1763–71.
17. Amor S, Puentes F, Baker D, van der Valk P. Inflammation in neurodegenerative diseases. Immunology. 2010;129:154–69.
18. Biscaro B, Lindvall O, Tesco G, Ekdahl CT, Nitsch RM. Inhibition of microglial activation protects hippocampal neurogenesis and improves cognitive deficits in a transgenic mouse model for Alzheimer's disease. Neurodegener Dis. 2012;9:187–98.
19. Du Y, Ma Z, Lin S, Dodel RC, Gao F, Bales KR, et al. Minocycline prevents nigrostriatal dopaminergic neurodegeneration in the MPTP model of Parkinson's disease. Proc Natl Acad Sci U S A. 2001;98:14669–74.
20. Popovic N, Schubart A, Goetz BD, Zhang SC, Linington C, Duncan ID. Inhibition of autoimmune encephalomyelitis by a tetracycline. Ann Neurol. 2002;51:215–23.

21. Owolabi SA, Saab CY. Fractalkine and minocycline alter neuronal activity in the spinal cord dorsal horn. FEBS Lett. 2006;580:4306–10.
22. Mika J, Osikowicz M, Makuch W, Przewlocka B. Minocycline and pentoxifylline attenuate allodynia and hyperalgesia and potentiate the effects of morphine in rat and mouse models of neuropathic pain. Eur J Pharmacol. 2007;560:142–9.
23. Garrido-Mesa N, Zarzuelo A, Galvez J. Minocycline: far beyond an antibiotic. Br J Pharmacol. 2013;169:337–52.
24. Niimi N, Kohyama K, Matsumoto Y. Minocycline suppresses experimental autoimmune encephalomyelitis by increasing tissue inhibitors of metalloproteinases. Neuropathology. 2013;33:612–20.
25. Peng B, Xiao J, Wang K, So KF, Tipoe GL, Lin B. Suppression of microglial activation is neuroprotective in a mouse model of human retinitis pigmentosa. J Neurosci. 2014;34:8139–50.
26. Cruickshanks KJ, Klein R, Klein BE. Sunlight and age-related macular degeneration: the beaver dam eye study. Arch Ophthalmol. 1993;111:514–8.
27. Swaroop A, Chew EY, Rickman CB, Abecasis GR. Unraveling a multifactorial late-onset disease: from genetic susceptibility to disease mechanisms for age-related macular degeneration. Annu Rev Genomics Hum Genet. 2009;10:19–43.
28. Grimm C, Reme CE. Light damage as a model of retinal degeneration. Methods Mol Biol. 2013;935:87–97.
29. Marc RE, Jones BW, Watt CB, Vazquez-Chona F, Vaughan DK, Organisciak DT. Extreme retinal remodeling triggered by light damage: implications for age related macular degeneration. Mol Vis. 2008;14:782–806.
30. Narimatsu T, Ozawa Y, Miyake S, Kubota S, Hirasawa M, Nagai N, et al. Disruption of cell-cell junctions and induction of pathological cytokines in the retinal pigment epithelium of light-exposed mice. Invest Ophthalmol Vis Sci. 2013;54:4555–62.
31. Pennesi ME, Neuringer M, Courtney RJ. Animal models of age related macular degeneration. Mol Aspects Med. 2012;33:487–509.
32. Blasi E, Barluzzi R, Bocchini V, Mazzolla R, Bistoni F. Immortalization of murine microglial cells by a v-raf/v-myc carrying retrovirus. J Neuroimmunol. 1990;27:229–37.
33. Ebert S, Weigelt K, Walczak Y, Drobnik W, Mauerer R, Hume DA, et al. Docosahexaenoic acid attenuates microglial activation and delays early retinal degeneration. J Neurochem. 2009;110:1863–75.
34. Ebert S, Schoeberl T, Walczak Y, Stoecker K, Stempfl T, Moehle C, et al. Chondroitin sulfate disaccharide stimulates microglia to adopt a novel regulatory phenotype. J Leukoc Biol. 2008;84:736–40.
35. Dobin A, Davis CA, Schlesinger F, Drenkow J, Zaleski C, Jha S, et al. STAR: ultrafast universal RNA-seq aligner. Bioinformatics. 2013;29:15–21.
36. Anders S, Huber W. Differential expression analysis for sequence count data. Genome Biol. 2010;11:R106.
37. Eichler GS, Huang S, Ingber DE. Gene expression dynamics inspector (GEDI): for integrative analysis of expression profiles. Bioinformatics. 2003;19:2321–2.
38. Karlstetter M, Walczak Y, Weigelt K, Ebert S, Van den Brulle J, Schwer H, et al. The novel activated microglia/macrophage WAP domain protein, AMWAP, acts as a counter-regulator of proinflammatory response. J Immunol. 2010;185:3379–90.
39. Karlstetter M, Nothdurfter C, Aslanidis A, Moeller K, Horn F, Scholz R, et al. Translocator protein (18 kDa) (TSPO) is expressed in reactive retinal microglia and modulates microglial inflammation and phagocytosis. J Neuroinflammation. 2014;11:3. doi:10.1186/1742-2094-11-3.
40. Aslanidis A, Karlstetter M, Scholz R, Fauser S, Neumann H, Fried C, et al. Activated microglia/macrophage whey acidic protein (AMWAP) inhibits NFkappaB signaling and induces a neuroprotective phenotype in microglia. J Neuroinflammation. 2015;12:77.
41. Scholz R, Caramoy A, Bhuckory MB, Rashid K, Chen M, Xu H, et al. Targeting translocator protein (18 kDa) (TSPO) dampens pro-inflammatory microglia reactivity in the retina and protects from degeneration. J Neuroinflammation. 2015;12:201.
42. Nikodemova M, Watters JJ, Jackson SJ, Yang SK, Duncan ID. Minocycline down-regulates MHC II expression in microglia and macrophages through inhibition of IRF-1 and protein kinase C (PKC)alpha/betaII. J Biol Chem. 2007;282:15208–16.
43. Chen M, Ona VO, Li M, Ferrante RJ, Fink KB, Zhu S, et al. Minocycline inhibits caspase-1 and caspase-3 expression and delays mortality in a transgenic mouse model of huntington disease. Nat Med. 2000;6:797–801.
44. Tikka TM, Vartiainen NE, Goldsteins G, Oja SS, Andersen PM, Marklund SL, et al. Minocycline prevents neurotoxicity induced by cerebrospinal fluid from patients with motor neurone disease. Brain. 2002;125:722–31.
45. Tso MO, Zhu X, Wang AL, Yu AC, Lau LT, Lee C, et al. Minocycline inhibits LPS-induced retinal microglia activation. Neurochem Int. 2005;47:152–8.
46. Henry CJ, Huang Y, Wynne A, Hanke M, Himler J, Bailey MT, et al. Minocycline attenuates lipopolysaccharide (LPS)-induced neuroinflammation, sickness behavior, and anhedonia. J Neuroinflammation. 2008;5:15.
47. Yang L-p, Li Y, Zhu X-a, Tso MOM. Minocycline delayed photoreceptor death in the rds mice through iNOS-dependent mechanism. Mol Vis. 2007;13:1073–82.
48. Yrjanheikki J, Tikka T, Keinanen R, Goldsteins G, Chan PH, Koistinaho J. A tetracycline derivative, minocycline, reduces inflammation and protects against focal cerebral ischemia with a wide therapeutic window. Proc Natl Acad Sci U S A. 1999;96:13496–500.
49. Hoey S, Grabowski PS, Ralston SH, Forrester JV, Liversidge J. Nitric oxide accelerates the onset and increases the severity of experimental autoimmune uveoretinitis through an IFN-gamma-dependent mechanism. J Immunol. 1997;159:5132–42.
50. Amin AR, Patel RN, Thakker GD, Lowenstein CJ, Attur MG, Abramson SB. Post-transcriptional regulation of inducible nitric oxide synthase mRNA in murine macrophages by doxycycline and chemically modified tetracyclines. FEBS Lett. 1997;410:259–64.
51. Matsui T, Svensson CI, Hirata Y, Mizobata K, Hua XY, Yaksh TL. Release of prostaglandin E(2) and nitric oxide from spinal microglia is dependent on activation of p38 mitogen-activated protein kinase. Anesth Analg. 2010;111:554–60.
52. Beattie MS. Inflammation and apoptosis: linked therapeutic targets in spinal cord injury. Trends Mol Med. 2004;10:580–3.
53. Wang X, Zhu S, Drozda M, Zhang W, Stavrovskaya IG, Cattaneo E, et al. Minocycline inhibits caspase-independent and -dependent mitochondrial cell death pathways in models of huntington's disease. Proc Natl Acad Sci U S A. 2003;100:10483–7.
54. Cheng S, Hou J, Zhang C, Xu C, Wang L, Zou X, et al. Minocycline reduces neuroinflammation but does not ameliorate neuron loss in a mouse model of neurodegeneration. Sci Rep. 2015;5:10535.
55. Park CH, Shin TK, Lee HY, Kim SJ, Lee WS. Matrix metalloproteinase inhibitors attenuate neuroinflammation following focal cerebral ischemia in mice. Korean J Physiol Pharmacol. 2011;15:115–22.
56. Koistinaho M, Malm TM, Kettunen MI, Goldsteins G, Starckx S, Kauppinen RA, et al. Minocycline protects against permanent cerebral ischemia in wild type but not in matrix metalloprotease-9-deficient mice. J Cereb Blood Flow Metab. 2005;25:460–7.
57. Bosco A, Inman DM, Steele MR, Wu G, Soto I, Marsh-Armstrong N, et al. Reduced retina microglial activation and improved optic nerve integrity with minocycline treatment in the DBA/2 J mouse model of glaucoma. Invest Ophthalmol Vis Sci. 2008;49:1437–46.
58. Zhang C, Lei B, Lam TT, Yang F, Sinha D, Tso MO. Neuroprotection of photoreceptors by minocycline in light-induced retinal degeneration. Invest Ophthalmol Vis Sci. 2004;45:2753–9.
59. Wenzel A, Grimm C, Samardzija M, Reme CE. Molecular mechanisms of light-induced photoreceptor apoptosis and neuroprotection for retinal degeneration. Prog Retin Eye Res. 2005;24:275–306.
60. Youssef PN, Sheibani N, Albert DM. Retinal light toxicity. Eye (Lond). 2011;25:1–14.
61. Grimm C, Wenzel A, Williams T, Rol P, Hafezi F, Reme C. Rhodopsin-mediated blue-light damage to the rat retina: effect of photoreversal of bleaching. Invest Ophthalmol Vis Sci. 2001;42:497–505.
62. Grimm C, Reme CE, Rol PO, Williams TP. Blue light's effects on rhodopsin: photoreversal of bleaching in living rat eyes. Invest Ophthalmol Vis Sci. 2000;41:3984–90.
63. Hughes EH, Schlichtenbrede FC, Murphy CC, Broderick C, van Rooijen N, Ali RR, et al. Minocycline delays photoreceptor death in the rds mouse through a microglia-independent mechanism. Exp Eye Res. 2004;78:1077–84.

Additional File 1: Supplementary Figure 1 - Early microglial activation after exposure to bright white light.

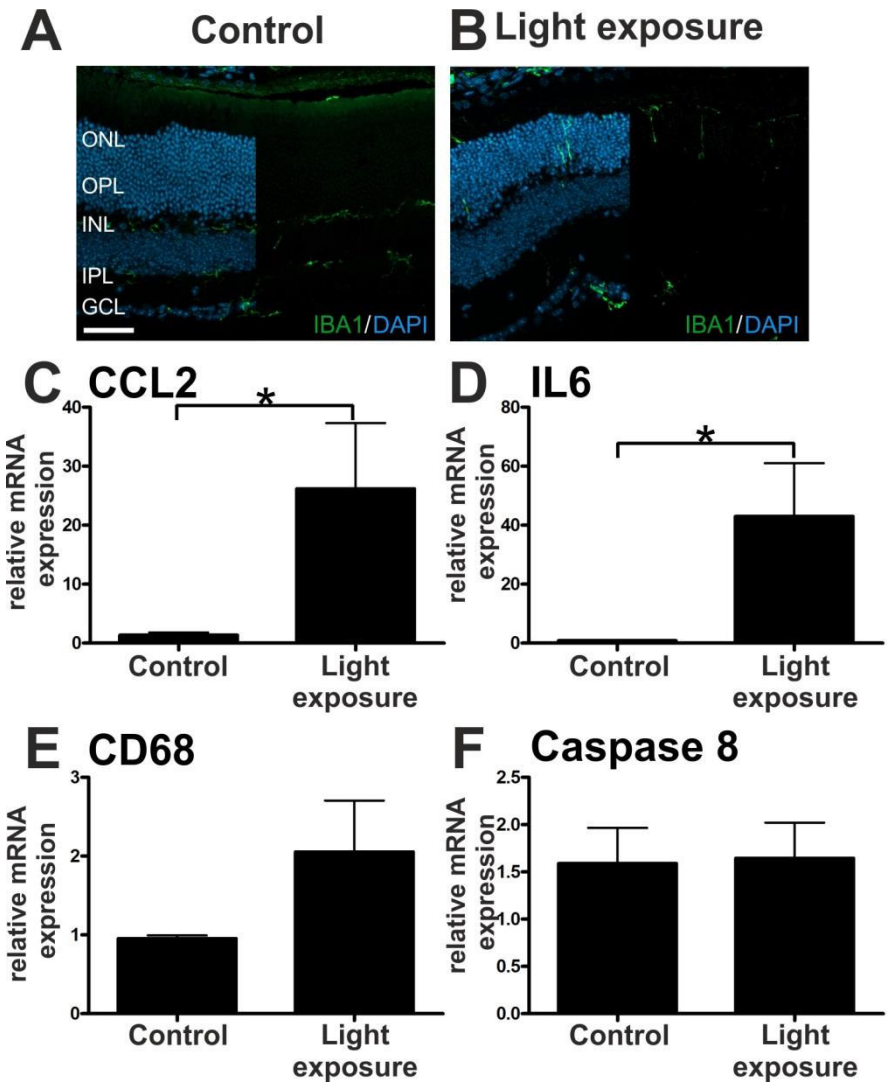

Additional file 1: Figure S1. Early microglial activation after exposureto bright white light. Representative photomicrographs show retinalsections (A–B) stained with Iba1 (green) of control mice and animals 4 hafter light exposure. In healthy controls, microglial cells are only locatedin the plexiform layers and GCL (A). Images of light exposed mice show microglia with protrusions in the ONL (B). ONL, outer nuclear layer; OPL, outer plexiform layer; INL, inner nuclear layer; IPL, inner plexiform layer; GCL, ganglion cell layer. Scale bar 50 μm. Data show representative photomicrographs (control n = 5, light exposure n = 4). Retinal mRNA expression of microglia-associated genes and caspase 8 were determined by real-time RT-PCR (C-F). Data show mean ± SEM (control n = 5 retinas, lightexposure n = 4 retinas measured in triplicates) with *p < 0.05. (JPG 684 kb

Additional File 2: Supplementary Table 1 - Differentially expressed transcripts comparing light exposure versus control

Nr	Gene	Mean count	log2 FC
1	Msr1	281	4.74
2	Ms4a6d	213	3.96
3	Clec7a	464	3.94
4	Steap4	195	4.6
5	Slc15a3	125	3.52
6	Timp1	63.9	3.34
7	Cd68	597	3.54
8	C3ar1	279	4.09
9	Ctse	67.1	3.18
10	Hal	70.7	3.37
11	Mmp12	26.3	3.12
12	Cd84	166	3.68
13	Emr1	421	3.72
14	Mki67	102	3.47
15	Lcn2	434	2.83
16	Lcp1	262	3.45
17	Tlr13	120	2.7
18	Tyrobp	741	3.6
19	Apobec1	202	2.77
20	Siglec1	130	3.11
21	Cybb	116	3.36
22	Top2a	53.7	3.03
23	Fcer1g	229	3.41
24	Ly9	69	2.77
25	Cd300a	70.5	2.52
26	C3	224	3.7

27	Cd22	59.1	2.99
28	Wfdc17	41.6	2.64
29	Nlrc5	76.9	2.21
30	Trem2	398	3.5
31	Cxcr4	126	3.45
32	Gatm	576	2.97
33	1300002K09Rik	46.9	2.61
34	Csf2rb2	50.2	2.04
35	Wdfy4	52.2	2.45
36	Laptm5	501	3.27
37	Myo1f	113	3.26
38	Klhl6	56	2.8
39	Cebpa	119	3.03
40	C1qc	949	3.82
41	Glipr1	36.6	2.83
42	Plin2	457	2.96
43	Arl11	60.1	2.63
44	Cx3cr1	309	2.98
45	Cdk1	28.9	2.48
46	AF251705	86.7	2.98
47	Arhgap25	44.8	2.45
48	Cd53	371	3.24
49	Nckap1l	295	2.63
50	Irf8	113	2.4
51	Tlr7	155	3.58
52	Ms4a6b	67.3	2.84
53	P2ry13	55.9	2.83
54	Arhgap30	94.5	2.81
55	Unc93b1	238	2.86

56	Gusb	552	2.49
57	Ctsd	27500	2.76
58	Tnfrsf1b	136	3.23
59	Syk	77.9	2.87
60	Itgb2	165	3.12
61	Bcl3	46.4	2.69
62	Vav1	79.7	2.6
63	Tbxas1	38.6	2.47
64	Apoc1	70.9	2.4
65	Fcgr2b	103	2.62
66	Fcgr3	201	3.35
67	Itgam	251	2.77
68	Parvg	83.1	2.23
69	Sash3	30	2.17
70	Oasl2	184	2.91
71	Ms4a7	64.9	2.83
72	Hexb	2340	2.65
73	Irf5	61.9	2.25
74	Rrm2	16.5	2.08
75	Hpgds	118	2.92
76	Tnfaip8l2	34.9	2.33
77	Rac2	74.8	2.92
78	Dock2	81.5	2.44
79	Ctsz	1710	2.76
80	Gpr34	218	2.3
81	Pik3cg	43.5	2.1
82	Anpep	92.6	3.37
83	Havcr2	170	2.62
84	Btk	37.2	2.35

85	Galnt6	36.9	2.32
86	Ptprc	108	2.66
87	P2ry6	34.3	2.61
88	Xdh	132	2.61
89	Spp1	8340	2.43
90	Casp1	22.4	2.32
91	Cd33	75.8	2.31
92	Rasal3	38	2.1
93	Serpina3n	504	3.59
94	Ly86	178	2.3
95	Crym	1460	2
96	Lyn	102	2.54
97	Fyb	84.8	2.64
98	Grn	2150	2.28
99	Htr2b	34.4	2.14
100	Arpc1b	189	2.44
101	Lilrb4	120	3.66
102	Cd180	96.5	3.52
103	C1qb	1050	3.51
104	Abcc3	135	3.43
105	C1qa	1380	3.42
106	Plau	271	3.25
107	Stab1	517	3.12
108	Colec12	305	3.11
109	Capg	98.8	2.93
110	Plin4	184	2.87
111	Ifi44	102	2.86
112	B2m	1460	2.83
113	Blnk	62.8	2.82

114	Cyth4	133	2.82
115	Lgals3	418	2.82
116	Rnase4	292	2.82
117	Lgals9	167	2.79
118	Serping1	191	2.79
119	Gp49a	60.5	2.75
120	Ncf1	161	2.75
121	Pld4	137	2.7
122	Ifi27l2a	74.6	2.67
123	Bst2	177	2.65
124	Fam46c	102	2.62
125	Csf1r	808	2.61
126	Fcgr1	71.6	2.61
127	Igsf6	28.7	2.61
128	Dab2	109	2.56
129	4632428N05Rik	223	2.53
130	Psmb8	112	2.53
131	Serpina3f	23.6	2.53
132	Ifi202b	88	2.52
133	Tifab	34.4	2.52
134	Anxa3	90.4	2.5
135	Sepp1	844	2.47
136	Lgals3bp	406	2.46
137	Spsb1	109	2.46
138	Mt2	2540	2.45
139	Ctla2b	52.6	2.44
140	Hmha1	146	2.41
141	Ctss	1140	2.4
142	Olfml3	329	2.4

143	Lcp2	33.1	2.39
144	Ifi44l	47.8	2.38
145	Ifit1	78.3	2.38
146	Serpine2	306	2.38
147	Lgals1	618	2.37
148	Pycard	21.8	2.37
149	Arhgdib	110	2.36
150	Tlr4	39.2	2.35
151	Hpse	146	2.34
152	Hvcn1	92.2	2.34
153	Mpeg1	2500	2.33
154	Cyba	208	2.32
155	P2rx7	48.4	2.31
156	Sla	64.2	2.29
157	Naip2	41.6	2.28
158	Psmb9	83.8	2.28
159	Irgm1	130	2.27
160	Lyz2	2880	2.27
161	H2-Q4	197	2.24
162	Itpripl2	99.8	2.24
163	Nupr1	122	2.24
164	Oas1b	26.4	2.23
165	Sfpi1	49.8	2.23
166	Chi3l1	506	2.22
167	Lipa	422	2.22
168	Slfn2	37.8	2.22
169	Tubb6	49.4	2.22
170	Clec5a	25.9	2.21
171	Grap	32.2	2.21

172	Plcg2	61	2.21
173	Ptplad2	42	2.21
174	AI607873	44.5	2.2
175	Litaf	215	2.19
176	Gna15	24.8	2.18
177	Plscr2	64.6	2.18
178	Serpine1	66.9	2.18
179	Apbb1ip	37.6	2.16
180	Fabp5	154	2.16
181	Hk3	61.5	2.16
182	S100a6	236	2.16
183	Serpina3m	25.6	2.16
184	Evi2a	42.4	2.15
185	Gbp3	155	2.15
186	Rassf2	102	2.15
187	Csf3r	80.6	2.13
188	H2-T23	161	2.13
189	Adap2	59.5	2.12
190	Fcgr4	30.7	2.12
191	Kcnk6	34	2.12
192	Slc7a7	58.8	2.12
193	Clec2d	107	2.11
194	Cst7	22.2	2.11
195	Fcrls	28.6	2.11
196	Apoe	10200	2.1
197	Trim30a	71.8	2.1
198	Slc11a1	56.1	2.08
199	Adcy7	153	2.05
200	Anxa4	145	2.05

201	Gbp1	163	2.05
202	Gbp2	150	2.05
203	H2-T24	59.9	2.05
204	Eif2ak2	166	2.04
205	Tgfbr2	163	2.04
206	Tnfrsf1a	177	2.04
207	Axl	448	2.03
208	Isg15	53.6	2.03
209	Amz1	31.4	2.02
210	5430435G22Rik	85.9	2.01
211	Ifitm3	169	2.01
212	Rsad2	58.7	2.01
213	Cmklr1	30.9	2
214	Ucp2	638	2.34
215	Emp1	107	2.23
216	Emilin2	23.6	2.06
217	Parp14	163	2.02

Additional File 3: Supplementary Table 2 - Differentially expressed transcripts comparing light exposure versus light exposed plus minocyline treatment

Nr	Gene	Mean count	log2 FC
1	Dsp	176	3.66
2	Krt12	1080	3.57
3	Aldh3a1	467	3.33
4	Krt5	651	3.32
5	Tmprss11a	45.1	3.08
6	Dsc3	35.8	3.06
7	Fbln1	182	3.04
8	Calml3	131	2.99
9	Myh11	695	2.93
10	Lypd2	70	2.92
11	Dsg1a	36.2	2.9
12	Aqp3	46.3	2.89
13	Prb1	93.9	2.84
14	Tyr	305	2.8
15	Dcn	441	2.75
16	Lypd3	27.2	2.72
17	Edn3	213	2.71
18	Sdc1	85.3	2.68
19	Tacstd2	32.7	2.6
20	Krt6a	101	2.58
21	Anxa8	30.2	2.54
22	Slurp1	33.2	2.44
23	Krt6b	52.8	2.41
24	Trim29	34.4	2.37
25	Fam129a	348	2.32
26	1600029D21Rik	38.4	2.25

27	Cldn4	20.6	2.25
28	Gja1	733	2.24
29	Tagln	476	2.23
30	Fam83a	25.2	2.22
31	Islr	184	2.21
32	Gjb2	18.8	2.19
33	Prpmp5	73.2	2.16
34	Muc4	71.6	2.12
35	Mlana	151	2.11
36	Lum	72.6	2.09
37	Tspan10	149	2.04
38	Bace2	143	2.01
39	Arpc1b	239	-2.01
40	Htr2b	40.9	-2.02
41	Naip5	37	-2.02
42	Fyb	107	-2.03
43	Grn	2620	-2.03
44	Lyn	129	-2.04
45	Crym	1750	-2.05
46	Ly86	216	-2.06
47	Serpina3n	697	-2.06
48	Cd33	92	-2.07
49	Rasal3	46.2	-2.07
50	Casp1	28.3	-2.08
51	Spp1	10200	-2.08
52	Xdh	165	-2.08
53	P2ry6	42.8	-2.09
54	Ptprc	133	-2.09
55	Anpep	118	-2.1

56	Btk	45.8	-2.1
57	Galnt6	45.5	-2.1
58	Havcr2	206	-2.1
59	Gpr34	266	-2.11
60	Pik3cg	52.2	-2.11
61	Ctsz	2150	-2.12
62	Pbk	14.3	-2.13
63	Dock2	99.2	-2.14
64	Rac2	93	-2.14
65	Hpgds	148	-2.15
66	Tnfaip8l2	42.3	-2.15
67	Fcgr1	86.8	-2.17
68	Hexb	2890	-2.17
69	Irf5	75.1	-2.17
70	Ms4a7	80.2	-2.17
71	Rrm2	19.9	-2.17
72	Oasl2	235	-2.18
73	Fcgr3	250	-2.19
74	Itgam	310	-2.19
75	Parvg	101	-2.19
76	Pik3ap1	56.4	-2.19
77	Sash3	36.4	-2.19
78	Fcgr2b	126	-2.21
79	Apoc1	85.4	-2.22
80	Tbxas1	47.6	-2.22
81	Vav1	98.5	-2.22
82	Bcl3	59.4	-2.25
83	Itgb2	205	-2.25
84	Syk	96.4	-2.26

85	Tnfrsf1b	175	-2.26
86	Ctsd	34100	-2.27
87	Gusb	668	-2.28
88	Unc93b1	297	-2.28
89	Arhgap30	117	-2.29
90	Gp49a	73.6	-2.29
91	P2ry13	69.8	-2.29
92	Ms4a6b	83.3	-2.3
93	Tlr7	192	-2.32
94	Cd53	462	-2.35
95	Irf8	135	-2.35
96	Nckap1l	356	-2.35
97	AF251705	107	-2.36
98	Arhgap25	54.1	-2.36
99	Cdk1	35.6	-2.37
100	Cx3cr1	378	-2.37
101	Kif4	390	-2.39
102	Arl11	72.7	-2.4
103	Csf2rb	88	-2.4
104	Plin2	567	-2.41
105	C1qc	1180	-2.43
106	Glipr1	45.3	-2.43
107	Cebpa	148	-2.44
108	Gm8221	36.4	-2.44
109	Klhl6	68.6	-2.45
110	Myo1f	141	-2.45
111	Laptm5	618	-2.48
112	Wdfy4	62	-2.49
113	Csf2rb2	57.7	-2.51

114	1300002K09Rik	56.2	-2.52
115	Cxcr4	157	-2.53
116	Gatm	702	-2.53
117	Trem2	487	-2.54
118	Cd22	71	-2.56
119	Nlrc5	90.4	-2.56
120	Wfdc17	50.1	-2.56
121	Fam46c	121	-2.58
122	C3	274	-2.6
123	Cd300a	84.2	-2.63
124	Fcer1g	283	-2.7
125	Ly9	82.7	-2.7
126	Top2a	66.3	-2.72
127	Cybb	144	-2.75
128	Siglec1	158	-2.78
129	Apobec1	242	-2.8
130	Tyrobp	913	-2.81
131	Tlr13	142	-2.82
132	Stab1	627	-2.89
133	Lcp1	319	-2.9
134	Abcc3	165	-2.91
135	Lcn2	519	-2.92
136	Emr1	512	-2.97
137	Mki67	126	-2.97
138	Cd84	203	-2.99
139	Mmp12	33.1	-3
140	Hal	86.1	-3.03
141	Ctse	81.4	-3.04
142	C3ar1	341	-3.05

143	Cd68	728	-3.06
144	Timp1	79.8	-3.07
145	Ms4a6c	218	-3.13
146	Slc15a3	153	-3.23
147	Lilrb4	146	-3.25
148	Steap4	249	-3.3
149	Clec7a	563	-3.32
150	Ms4a6d	259	-3.42
151	Msr1	342	-3.92

Lebenslauf

This page only appears in the printed version of the thesis.

Danksagung

This page only appears in the printed version of the thesis.

Erklärung

Ich versichere, dass ich die von mir vorgelegte Dissertation selbständig angefertigt, die benutzten Quellen und Hilfsmittel vollständig angegeben und die Stellen der Arbeit – einschließlich Tabellen, Karten, und Abbildungen - , die anderen Werken im Wortlaut oder dem Sinn nach entnommen sind, in jedem Einzelfall als Entlehnung kenntlich gemacht habe; dass diese Dissertation noch keiner anderen Fakultät oder Universität zur Prüfung vorgelegen hat; dass sie – abgesehen von unten angegebenen Teilpublikationen – noch nicht veröffentlicht worden ist sowie, dass ich eine solche Veröffentlichung vor Abschluss des Promotionsverfahrens nicht vornehmen werde. Die Bestimmungen dieser Promotionsordnung sind mir bekannt. Die von mir vorgelegte Dissertation ist von Prof. Dr. rer. nat. Thomas Langmann betreut worden.

Publikationen:

Targeting translocator protein (18 kDa) (TSPO) dampens pro-inflammatory microglia reactivity in the retina and protects from degeneration
Scholz R, Caramoy A, Mohajeet B, Rashid K, Chen M, Xu H, Grimm C, Thomas Langmann T*, Journal of Neuroinflammation (2015) 12:201 DOI 10.1186/s12974-015-0422-5

Translocator protein (18 kDa) (TSPO) is expressed in reactive retinal microglia and modulates microglial inflammation and phagocytosis
Karlstetter M †, Nothdurfter C †, Aslanidis A, Moeller K, Horn F, **Scholz R**, Neumann H, Weber B, Rupprecht R † *, Langmann T † *, Journal of Neuroinflammation 2014, 11:3

Minocycline counter-regulates proinflammatory microglia responses in the retina and protects from degeneration
Scholz R, Sobotka M, Caramoy A, Stempfl T, Moehle C, Langmann T*, Journal of Neuroinflammation (2015) 12:209 DOI 10.1186/s12974-015-0431-4

Ich versichere, dass ich alle Angaben wahrheitsgemäß nach bestem Wissen und Gewissen gemacht habe und verpflichte mich, jedmögliche, die obigen Angaben betreffenden Veränderungen, dem Promotionsausschuss unverzüglich mitzuteilen.

Köln, den 14.05.2016

R Scholz

Rebecca Scholz